

ISTANBUL TECHNICAL UNIVERSITY ★ GRADUATE SCHOOL

**COMPUTATIONAL DESIGN OF RECIPROCAL FRAME STRUCTURES:
INCORPORATING FORCE VARIABLES INTO DESIGN PROCESS**



M.Sc. THESIS

Hanım Gülsüm KARAHAAN

Department of Informatics

Architectural Design Computing Programme

JUNE 2024

ISTANBUL TECHNICAL UNIVERSITY ★ GRADUATE SCHOOL

**COMPUTATIONAL DESIGN OF RECIPROCAL FRAME STRUCTURES:
INCORPORATING FORCE VARIABLES INTO DESIGN PROCESS**



M.Sc. THESIS

**Hanım Gülsüm KARAHAN
(523211009)**

Department of Informatics

Architectural Design Computing Programme

Thesis Advisor: Assoc. Prof. Dr. Sevil YAZICI

JUNE 2024

İSTANBUL TEKNİK ÜNİVERSİTESİ ★ LİSANSÜSTÜ EĞİTİM ENSTİTÜSÜ

**KUVVET DEĞİŞKENLERİNİN TASARIM SÜRECİNE KATILMASI İLE
KARŞILIKLI ÇERÇEVE STRÜKTÜRLERİNİN
HESAPLAMALI TASARIMI**

YÜKSEK LİSANS TEZİ

**Hanım Gülsüm KARAHAAN
(523211009)**

Bilişim Anabilim Dalı

Mimari Tasarımda Bilişim Programı

Tez Danışmanı: Doç. Dr. Sevil YAZICI

HAZİRAN 2024

Hanım Gülsüm Karahan, a M.Sc. student of İTÜ Graduate School student ID 523211009 successfully defended the thesis/dissertation entitled “COMPUTATIONAL DESIGN OF RECIPROCAL FRAME STRUCTURES: INCORPORATING FORCE VARIABLES INTO DESIGN PROCESS”, which he/she prepared after fulfilling the requirements specified in the associated legislations, before the jury whose signatures are below.

Thesis Advisor : **Assoc. Prof. Dr. Sevil YAZICI**
Istanbul Technical University

Jury Members : **Prof. Dr. Mine ÖZKAR**
Istanbul Technical University

Assoc. Prof. Dr. Fulya AKIPEK
Istanbul Bilgi University

Date of Submission : 23 May 2024
Date of Defense : 26 June 2024





To my academic career,



FOREWORD

First and foremost, I would like to express my heartfelt gratitude to my advisor Assoc. Prof. Dr. Sevil Yazıcı for her guidance and patience throughout my thesis. I deeply appreciate her generosity in sharing her expert knowledge, experience, and time. She supported me through my fixation on certain aspects of my research and taught me how to be a good and productive researcher without compromising meticulousness. I am grateful for her constant support, stimulating discussions, and inspiring mentorship.

I am sincerely thankful to Prof. Dr. Mine Özkar for sharing her deep understanding in computational design and her thoughtful feedback on my thesis. I feel privileged to have taken lectures from her where I had the opportunity to learn seminal works in the field with intellectual wonderings. I cannot overstate their importance for my academic development. Similarly, I would like to extend my thanks to Prof. Dr. Birgül Çolakoğlu for teaching me the importance of critical thinking in academia and supporting my academic enthusiasm. I would like to thank my jury member Assoc. Prof. Dr. Fulya Akıpek for her insightful comments and careful consideration on my research.

My special thanks go to Müge Halıcı, Fatih Uzun, and İnanç Şencan for their generous help during the digital fabrication process of my research. They both gave a hand with technical challenges and did their best to provide me with space and time in the lab for the physical experiments. I also would like to thank Begüm Aktaş for her encouragement in my academic research and for sharing her experiences with me in academia.

My friend Başak Bozkurt, thanks to the universe for bringing us together at Rami library. You have been a wonderful friend and colleague with whom I have had fruitful and enjoyable academic and personal conversations. Thanks for informing me what lies ahead of my academic journey.

Another thanks go to streamers on YouTube for studying long hours with rain sounds. I spent countless times studying with you. Knowing that there are people all around the world, striving to stay focused in our heavily distracted society, always keeps me motivated.

Last but not least, my lifetime gratitude is for my family who are always there for me during my highs and lows. Thank you for giving me the strength to not give up, not be a quitter but at the same time reminding me there is always another path to take and a brighter side to consider in life.

July 2024

Hanım Gülsüm KARAHAN
(Architect)

TABLE OF CONTENTS

	<u>Page</u>
FOREWORD	ix
TABLE OF CONTENT	xi
ABBREVIATIONS	xiii
SYMBOLS	xv
LIST OF TABLES	xvii
LIST OF FIGURES	xix
SUMMARY	xxiii
ÖZET	xxv
1. INTRODUCTION	1
1.1 Aim and Scope of Thesis.....	2
1.2 Methodology.....	3
2. RECIPROCAL FRAME STRUCTURES	5
2.1 Historical Context.....	5
2.2 Morphology and Geometry.....	11
2.3 Structural Behaviour.....	19
3. COMPUTATIONAL DESIGN AND MAKING	23
3.1 Computational Design Thinking.....	23
3.2 Computational Making.....	25
4. RELATIONSHIP BETWEEN COMPUTATIONAL GEOMETRY, MATERIAL AND STRUCTURE	29
4.1 Computational Geometry: NURBS and Polyhedra.....	29
4.1.1 Polyhedra.....	29
4.1.2 Non-uniform rational B-splines (NURBS).....	34
4.2 Form-finding in Architectural and Structural Design.....	37
4.2.1 Physical form-finding processes.....	38
4.2.2 Digital form-finding processes.....	41
4.3 The Role of Material Behaviour and Digital Fabrication in Design Process...44	
4.4 3-Dimensional Graphic Statics (3DGS).....	47
5. METHODOLOGY	51
5.1 Geometric Analysis.....	52
5.1.1 RF structures based on polyhedra.....	52
5.1.2 Creating RF structures from NURBS surfaces	54
5.2 Physical Experiments.....	57
5.2.1 Volumetric frame unit (VFU) exploration.....	57
5.2.2 Physical modelling of RF configurations.....	59
5.3 Digital Form-finding.....	62
5.3.1 Reciprocal structure generation.....	66
5.3.2 Structural analysis.....	67
6. RESULTS AND DISCUSSION	69
7. CONCLUSION	75

REFERENCES.....79
CURRICULUM VITAE.....87



ABBREVIATIONS

AEC	: Architecture, Engineering, and Construction
CAD	: Computer-aided design
CAAD	: Computer-aided architectural design
NURBS	: Non-Uniform Rational B-Splines
ICD/ ITKE	: Institute for Computational Design and Construction/ Institute of Building Structures and Structural Design at the University of Stuttgart.
KÇ	: Karşılıklı Çerçeve
CITA-SIAL	: Centre for Information Technology and Architecture at the Royal Danish Academy and the Spatial Information Architecture Laboratory
RF	: Reciprocal Frame
VFU	: Volumetric Frame Unit
3B	: 3 Boyut
3BGS	: 3 Boyutlu Grafik Statik
3DGS	: 3-Dimensional Graphic Statics
3D	: 3-Dimensional



SYMBOLS

$A_{1,2,3}, B_{1,2,3}, C_{1,2,3}$: translated force polyhedrons

Ba : Barye

C_i : The rotation axis

d : Diameter

e : Eccentricity

l : Engagement length of an element

L : Total length of an element

M_i : Midpoints of the element axis

N : Newton

n : Normal vector

I_i : Element axis

O_i : Center points of circles

Pa : Pascal

r : Radius

U, V : Surface directions

X : Triangular prism force polyhedron

Θ : Rotation angle



LIST OF TABLES

	<u>Page</u>
Table 4.1: Polyhedron examples.....	30
Table 5.1: Duality principle of RF structures based on polyhedral, L: total length of an element, Θ : rotation angle (Karahan and Yazıcı, 2024).....	54
Table 5.2: Polygon divisions and their corresponding RF configurations, L: total length of the element, Θ : rotation angle (Karahan and Yazıcı, 2024).....	56
Table 6.1: The comparison of VFU I and VFU II based on numeric values, (x) denotes the number of elements having the characteristics in question, eng. w: engagement window.....	72



LIST OF FIGURES

	<u>Page</u>
Figure 1.1 : (a) Grid structure connection (URL-1), (b) RF structure connection (URL-2)	2
Figure 1.2 : Workflow of the research.....	4
Figure 2.1 : (a) Indian tepee and (b) Hogan dwelling plan (Larsen, 2008).....	6
Figure 2.2 : (a) Honnecourt’s grillage and (b) Serlio’s grillage	7
Figure 2.3 : (a) Lincoln Cathedral Chapter house 3-dimensional reciprocal roof structure and (Chilton and Devulder, 2001), (b) plan view of the reciprocal roof structure (Larsen, 2008).....	7
Figure 2.4 : Puppet theatre complex designed by Kazuhiro Ishii (Pugnale and Sassone, 2014).....	8
Figure 2.5 : Leonardo da Vinci, Codex Atlanticus, fol.899v with reciprocal configurations (Robert, 2008).....	9
Figure 2.6 : Historical timeline of RF structure examples.....	10
Figure 2.7 : (a) Lamella construction (adapted from Petrović et al., 2022), (b) an RF structure with triangular nodes (URL-6), (c) an RF structure with quad nodes (URL-7), (d) RF node examples made of polygon.....	11
Figure 2.8 : Transformation of a converging node into a fan.....	12
Figure 2.9 : Transformation methods for polygons (Godthelp, 2019).....	12
Figure 2.10 : A triangular engagement window with l: engagement length, L: the length of an element, e: eccentricity (Karahan and Yazıcı, 2024).....	13
Figure 2.11 : (a) Single element, (b) Basic system, (c) Component.....	14
Figure 2.12 : RF form finding through iterative solver based on cell configuration (Parigi and Kirkegaard, 2014).....	14
Figure 2.13 : RF form finding through iterative solver based on cell configuration (Thönnissen, 2014).....	15
Figure 2.14 : RF joint examples varying from rigid to flexible	16
Figure 2.15 : A spheric RF structure derived from the icosahedron.....	17
Figure 2.16 : Mapping examples of RF structure, E_X : polygon number in X direction, E_Y : : polygon number in Y direction (Karahan and Yazıcı, 2024).....	18
Figure 2.17 : Force transmission difference between reciprocal and non-reciprocal structures (Pugnale and Sassone, 2014).....	19
Figure 2.18 : (a) Load-behaviour of non-reciprocal structures, (b) Emergent circular force flows in load-behaviour of reciprocal structures.....	19
Figure 2.19 : Bending force formation in RF structures.....	20
Figure 2.20 : Bending moment diagram in a statically determinate RF structure for a uniform load (Gelez et al., 2011).....	20

Figure 2.21 : (a) Double layer RF structure (Douthe and Baverel, 2014), (b) Double layer RF configuration (Wang and Akbarzadeh, 2022), (c) A shell nexorade (Mesnil et al., 2018), (d) RF structure working in tension (Widyowijatnoko et al., 2014).....	21
Figure 3.1 : Creating structurally efficient building components from the weaving pattern (Muslimin, 2010).....	26
Figure 3.2 : Woven node created by connection of cylinders (Suzuki et al., 2023).....	27
Figure 3.3 : (a) Creating kagome patterns from mesh topology, (b) Physical model of kagome patterns on the left and its simulation model on the right (Ayres et al., 2018).....	27
Figure 4.1 : Hexagon prism and hexagon antiprism.....	31
Figure 4.2 : The duality example.....	32
Figure 4.3 : Vector equilibrium or cuboctahedron, red denotes the 12 radiating lines edited by the author (Fuller, 1975).....	33
Figure 4.4 : 12 interrayed vectors of the rhombic dodecahedron.....	33
Figure 4.5 : Polyhedra under concentrated loads, A: tetrahedron, B: octahedron, C: icosahedron, D and E: the geodesic spheres (Fuller, 1975).....	34
Figure 4.6 : NURBS curve derivation from B-spline curve by the projection method (Pottmann, 2007).....	35
Figure 4.7 : Curve variations derived from the same control points but having different degrees.....	35
Figure 4.8 : Evaluation of a curve.....	36
Figure 4.9 : NURBS surface evaluation and normal vectors at parameters.....	37
Figure 4.10 : A 3D NURBS surface and its 2D parameter space for manipulating topological geometric patterns (Meng et al., 2023).....	37
Figure 4.11 : (a) Hooke’s hanging chain depicted by Poleni (1748), (b) Gaudi’s physical model consisted of catenary curves, (c) Colònia Güell Church columns (URL-9).....	39
Figure 4.12 : The German Pavilion in Montreal, 1967 (URL-10).....	39
Figure 4.13 : IL Pavilion at the University of Stuttgart (a) Soap-film model (b) The cable net construction (Burkhardt, 2020).....	40
Figure 4.14 : (a) A physical experiment of hanging membrane (Isler, 1983), (b) Wyss Garden Centre designed by Isler, 1961 (URL-11).....	40
Figure 4.15 : (a) Geodesic dome created from a sphere, (b) Node connection of the geodesic dome (URL-12).....	41
Figure 4.16 : (a) Digital simulation of hanging chain, (b) Roof membrane design based on forces in members (Killian, 2007).....	43
Figure 4.17 : (a) The initial grid configuration, (b) The final RF configuration created by dynamic relaxation method (Douthe and Baverel, 2009).....	43
Figure 4.18 : Dermoid project investigating material behaviour for the structural strength (CITA-SIAL, 2010).....	45
Figure 4.19 : ReciPly Dome made of pre-bent double-layer units (Brancart et al., 2017).....	46
Figure 4.20 : Assembling reciprocal frame structure through human-robot workflow (Mitterberger et al., 2022).....	47
Figure 4.21 : The dual diagrams of compression structure with the form diagram on the left, and the force diagram on the right (Block, 2009).....	48
Figure 4.22 : The element and its dual force polyhedron (Akbarzadeh et al., 2015).....	49

Figure 4.23 : Force polyhedral on the left and the corresponding form diagram on the right (Nejur and Akbarzadeh , 2021).....	49
Figure 5.1 : Inputs, outputs and process of the research.....	51
Figure 5.2 : the duality between dodecahedron and icosahedron RF configurations (Baverel and Nooshin, 2007).....	53
Figure 5.3 : the RF transformation of a cube following the duality principle (Karahah and Yazıcı, 2024).....	53
Figure 5.4 : NURBS surface generation steps (Karahah and Yazıcı, 2024).....	55
Figure 5.5 : undulated NURBS surface generation steps (Karahah and Yazıcı, 2024).....	56
Figure 5.6 : (a) Joint design, (b) An equilateral triangle fan, (c) An RF hexagon.....	58
Figure 5.7 : generative rules of an RF fan, s: support, g: get supported.....	58
Figure 5.8 : (a) Elements pointing up and down, (b) Creating a VFU.....	59
Figure 5.9 : (a) top view of VFU, (b) perspective view of VFU.....	59
Figure 5.10 : First physical experiment, (a) a hexagon unit (b) the physical model, (c) discretization of a hexagon RF unit.....	60
Figure 5.11 : Sequences of creating an RF structure following the rules.....	60
Figure 5.12 : An RF configuration made of hexagon units.....	60
Figure 5.13 : (a) An RF configuration, (b) Sequences of an RF configuration.....	61
Figure 5.14 : Sequences of the second RF configuration through hanging.....	61
Figure 5.15: VFU abstraction phases.....	62
Figure 5.16 : The three faces of VFU correspond to three congruent faces of rhombic dodecahedron.....	63
Figure 5.17 : Force polyhedron generation through creating normal vectors and setting its amplitude.....	63
Figure 5.18 : (a) Force polyhedron aggregation, (b) Iterative solver implementation, (c) The corresponding form diagram.....	65
Figure 5.19 : The transformation of the form diagram into an RF configuration by following geometric operations, (a,b) generation of reference geometry, (c) The rotation process, (d) The calculation of eccentricities and the lengths of the elements.....	67
Figure 5.20 : The supporting areas of the RF structure and their diameter sizes..	68
Figure 5.21 : Von Mises Stress analysis (above), Total displacement results (below).....	68
Figure 6.1 : Volumetric part of VFU I.....	69
Figure 6.2 : Volumetric part of VFU II.....	70
Figure 6.3: (a) Changes in number of elements, (b) Changes in the length sizes, (c) changes in diameter size of VFU I and VFU II.....	71
Figure 6.4: The comparison of VFU I and VFU II based on their formal configurations, (x) denotes the number of elements having the characteristics in question, eng. w: engagement window.....	73



COMPUTATIONAL DESIGN OF RECIPROCAL FRAME STRUCTURES BY INCORPORATING FORCE VARIABLES INTO DESIGN PROCESS

SUMMARY

Form-finding methods are mainly driven by forces and the state of equilibrium, terms architects do not typically engage with. Although form-finding is not a sheer creative act, it can be conceived of as more than just composing forces in a designerly way of speaking. Therefore, the way architects attempt to steer forces can encapsulate different design perspectives on form-finding methods. Architects usually use parametric design tools during the design exploration, afterward they evaluate the structural behaviour of their designs as a separate step. Even though physics-based engines allow for considering structural behaviour during the design process, they lack extended geometric space in which designers explore unexpected results that fall outside the defined design space. This thesis develops a comprehensive workflow that investigates a form through computational design and making processes while bringing structural efficiency forward. The research focuses on finding a reciprocal frame (RF) structure form at the convergence of geometry, structure, and material.

RF structure is studied due to the intrinsic dependency between its geometric configuration and structural behaviour. RF structure behaviour mostly relies on its geometric configuration, unlike other spatial structures for which the material and overall form determine the structural behaviour. Any change in the design variables resonates in the whole geometric configuration thus the structural behaviour changes accordingly. Therefore, top-down design approaches in which the final form is pre-determined have been studied extensively. Recent studies of RF structures focus on improving its structural behaviour but they were realized as a separate step from form-finding process as well. There is a gap in investigating bottom-up approaches in which the structural reciprocity of the form enhances the structural behaviour simultaneously. Therefore, the following research question is asked: How can we create RF structures where interdependent design variables of structural reciprocity inform the structural behaviour?

The research method consists of three main processes: 1) geometric analysis, 2) physical experiment, 3) digital form-finding. The workflow is predicated on the data flow of three processes provided during the research. Initially, geometric analysis is realized by developing a definition in an algorithmic design environment. The algorithm evaluates the geometrical efficiency of RF in terms of forming the same surface with the least material. The analysis results show that diamond or rhombus geometries can form an RF NURBS surface by requiring fewer linear elements. Therefore, rhombus geometry is investigated in the physical experiment process. The computational making process gives rise to the design of a Volumetric Frame Unit (VFU) which essentially increases the structural stiffness of RF. VFUs are joined together based on a rule-based design system to explore different RF configurations. The VFU's geometry provides an input for the digital form-finding process.

Digital form finding process is undertaken through 3-Dimensional Graphic Statics (3DGS) which is an intuitive structural form-finding method. The intuitive part stems from its ability to design forces of the form visually through polyhedral shapes. Therefore, the VFU geometry is abstracted as a polyhedron which is a rhombic dodecahedron. The resulting form diagram of 3DGS which works in pure compression is transformed into an RF structure. Transformation into an RF is realized by following analytical geometric operations. Finally, the outcome is evaluated using structural analysis software. The results emphasise that the way elements assemble, and compose a volumetric configuration enables the structure to work under compression forces along with bending forces.

This thesis contributes to the computational design field by developing an extended workflow incorporating the force variable into the design process, which is not prevalent for architects and designers. The research has demonstrated that the comprehensive design workflow in which geometry, structure, and material are intertwined paves the way for exploring outcomes with structural primacy. Consequently, structural primacy mostly associated with mechanical terms can be integrated into the design process which is recognized as a creative act to give rise to feasible and aesthetic forms.

KUVVET DEĞİŞKENLERİNİN TASARIM SÜRECİNE KATILMASI İLE KARŞILIKLI ÇERÇEVE STRÜKTÜRLERİNİN HESAPLAMALI TASARIMI

ÖZET

Form bulma yöntemleri temel olarak kuvvetler ve dengede olma hali gibi mimarların genellikle yakından ilişkili olmadıkları terimler ile oluşturulur. Tasarımcı üslubu ile değerlendirildiğinde ise form bulma tamamen yaratıcı bir eylem olmasa da kuvvetlerin oluşumundan daha fazlasını ifade eder. Bu nedenle, mimarların kuvvetleri yönetme şekli form bulma yöntemleri üzerine farklı tasarım bakış açıları içerir. Ancak mimarlar parametrik tasarım araçlarını genellikle tasarımı oluşturma aşamasında kullanırlar, strüktürel davranış değerlendirmesini ise daha sonra ayrı bir adım olarak gerçekleştirirler. Fizik tabanlı araçlar strüktürel davranış tasarımı sürecine dâhil etmeye imkân tanısa da tasarımcının tanımlı tasarım alanının dışında kalan çıktıları keşfettiği geniş geometri uzamına sahip değildir. Bu tez, formu hesaplamalı tasarım ve yapma aracılığıyla araştırırken strüktürel verimliliği ön plana getiren kapsamlı bir iş akışı oluşturmaktadır. Araştırma geometri, strüktür ve malzemenin birleşiminde olan Karşılıklı Çerçeve (KÇ) strüktür formlarını bulmaya odaklanmaktadır.

KÇ strüktürler, geometrik konfigürasyonlarının ve strüktürel davranışlarının birbirine doğal olarak bağlı olması nedeniyle seçilmiştir. Malzemenin ve genel formun strüktürel davranışı belirlediği diğer mekânsal strüktürlerin aksine KÇ strüktürlerinin davranışları daha çok geometrik konfigürasyona dayanır. Tasarım parametrelerindeki herhangi bir değişim tüm geometrik konfigürasyonu bunun sonucunda da strüktürel davranış etkiler. Form, tasarımı oluşturan geometri, strüktür ve malzeme değişkenlerinin uzlaşımında ortaya çıkar. Bu nedenle formun önceden belirlendiği yukarıdan aşağı (top-down) tasarım yaklaşımları etraflıca çalışılmıştır. Yakın zamanda yapılan çalışmalar, KÇ strüktürlerin yapısal davranışını geliştirmek üzerinedir ancak onlar da bu işlemi form bulma sürecinden sonra ayrı bir adım olarak gerçekleştirirler. Strüktürel olarak karşılıklı olmanın strüktürel davranışı eş zamanlı olarak geliştirdiği aşağıdan yukarı (bottom-up) çalışmalar oldukça sınırlıdır. Bu nedenle araştırma sorusu şu şekilde sorulmuştur: Bağımlı tasarım değişkenlerinin strüktürel davranışı etkilediği KÇ strüktürleri nasıl tasarlayabiliriz?

KÇ strüktür elemanlarının birbirini desteklemesi strüktüre kendiliğinden dengede olma hali kazandırır. Elemanların uç noktalarında birleşen diğer strüktürlerden farklı olarak, bu strüktürler ikili olarak birbirleriyle elemanların gövdesi üzerinden birleşirler. Birleşme noktaları strüktürün temel geometrik nicelikleri olan bağlantı uzunluklarının (engagement length), bağlantı pencerelerinin (engagement windows) ve iki eleman aksının arasındaki en yakın uzaklığı temsil eden eksantrikliğin (eccentricity) oluşmasını sağlar. Buna ek olarak, bağlantı pencereleri aynı zamanda en basit KÇ strüktür çözümlenmesi de olarak kabul edilen “fan” terimi ile ifade edilir. En az elemanla oluşturulabilecek fan tipi üçgen fanlardır. Eleman sayısına göre fanlar dörtgen, altıgen gibi diğer çokgen tiplerinden oluşturulabilir. KÇ strüktürlerinin ikili

birleşme noktaları basit mafsalları tasarımlarıyla çözülebilir. Ayrıca, basit eklem tasarımları strüktürün hızlı ve kolay bir araya gelmesini, sökülmesini sağlar. Strüktürün hızlı ve kolay bir araya gelmesi yapım aşamasında karbon salınımını düşürürken kolay sökülmesi de malzemenin tekrar kullanılmasını mümkün kılar. Ancak, mafsalların basitliği strüktürün karmaşık geometrisi ile ters düşer. Karmaşık geometri, elemanların iç etkileşimlerinin eş zamanlı olması nedeniyle strüktür formunun buna bağlı olarak da geometrinin önceden belirlenememesinden kaynaklanır. Karmaşık geometriye ek olarak, KÇ strüktürler strüktür dayanıklılığı için dezavantaj olarak kabul edilen bükme kuvveti ile çalışır. Bu nedenle bu tez strüktürel önceliği olan karşılıklı çerçeve strüktürleri hesaplamalı geometri, yapma ve tasarım aracılığıyla oluşturmayı hedeflemektedir.

Araştırmanın metodolojisi üç temel süreçten oluşmaktadır. Bunlar sırasıyla (1) geometrik analiz, (2) fiziksel deneyler, (3) dijital form-bulma süreçleridir. Araştırmanın iş akışı bu üç temel sürecin sağladığı veri akışına dayanmaktadır. Geometrik analiz Rhino-Grasshopper modelleme ortamında bir algoritma geliştirilerek yapılmıştır. Geliştirilen algoritma karşılıklı çerçeve strüktürlerin geometrik verimliliğini aynı yüzeyi en az elemanla oluşturma anlamında değerlendirmektedir. Bu analizin sonucu eşkenar dörtgenlerin aynı NURBS (non-uniform rational B-spline) yüzeyden karşılıklı çerçeve strüktürü oluşturmak için daha az lineer elemana ihtiyaç duyduğunu göstermiştir. Bu nedenle, eşkenar dörtgen geometrisi fiziksel deneylerde daha kapsamlı araştırılmıştır. Mafsallar, Rhino geometrik modelleme ortamında, aralarında 60 derece olan iki silindir birbiriyle orta noktalarından birleşecek şekilde tasarlanmıştır. Tasarlanan mafsallar daha sonra 3 boyutlu (3B) yazıcı ile üretilerek fiziksel sürece dâhil edilmiştir. Mafsallar ve 5 mm çapa sahip olan dairesel kesitteki 50 cm'lik lineer ahşap elemanlar altıgen bir birim oluşturacak şekilde birleştirilmiştir. Bu altıgen birim karşılıklı çerçevelerin düğüm noktalarını temsil eden eşkenar üçgen fanlardan oluşmaktadır. Fiziksel deney süreçlerinde gerçekleştirilen hesaplamalı yapma eylemi strüktürel sertliği artırılmış hacimsel çerçeve birimlerinin keşfedilmesini sağlamıştır. Hacimsel çerçeve birimler ile farklı strüktür konfigürasyonları denenmiştir. Bu deneyler sonucunda keşfedilen hacimsel çerçeve birim sayısal form bulma süreçleri için girdi oluşturmuştur.

Sayısal form-bulma süreçleri, bir tür strüktürel form bulma yöntemi olan 3 Boyutlu Grafik Statik (3BGS) ile gerçekleştirilmiştir. Bu yöntem basınç ve gerilme altında çalışan en uygun formların bulunmasında kullanılır. 3BGS yöntemi diğer strüktürel form bulma araçlarından sezgisel olma özelliğiyle farklılaşır. Sezgisel olma özelliği, kuvvetleri görsel olarak çokyüzlü geometrik formlar ile temsil ederek, tasarımcının bu bilgiyle tasarlamasına olanak vermesinden kaynaklanır. Grafik statik yöntemi tasarımcıya birbiriyle ilişkili olan form ve kuvvet diyagramlarını tasarlatmayı sağlar. Bir diyagramdaki herhangi bir değişiklik eş zamanlı olarak diğer diyagramı etkiler. Bu nedenle bu ilişkili form ve kuvvet diyagramlarına “ikili diyagramlar” denilmektedir. İkili diyagramlar üç boyutlu çokyüzlüler için şu geometrik prensip ile çalışır: her çokyüzlü için yüzeylerin köşelere, köşelerin yüzeylere denk geldiği diğer bir çokyüzlü vardır. Yüzeye dik olan normal vektörleri ikili çokyüzlüdeki köşelerin yerlerini belirler. Yüzeylerin ve köşelerin arasındaki bu yer ilişkisi “karşılıklı olma” (reciprocity) terimi ile de ifade edilir. Bu duruma örnek vermek gerekirse küp sekizyüzlünün ikili formudur. Kübün sekiz köşesi sekizgenin sekiz yüzeyini oluştururken altı yüzü de sekizgenin altı köşesine denk gelmektedir.

Fiziksel deneylerde keşfedilen hacimsel çerçeve birim geometrisi soyutlanarak çok yüzlü olan eşkenar dörtgensel on iki yüzlüye dönüştürülmüştür. 3BGS yönteminden

yararlanmak için açık kaynaklı bir algoritmik tasarım eklentisi kullanılmıştır. Eşkenar dörtgenel on iki yüzünün üç yüzü, hacimsel çerçeve birimin üç yüzüne eş olduğu için kuvvet diyagram bu yüzlere göre oluşturulmuştur. Bu bağlamda, eşkenar dörtgenlerin normal vektörleri belirlenmiş ve vektörlerin başlangıç ve bitiş noktaları birbirleriyle birleştirilerek alt ve üstte üçgen formlar oluşturulmuştur. Bu üçgen formlar, tasarlanacak çokyüzlünün alt ve üst yüzünü, vektör şiddeti de kenar uzunluklarını belirlemiştir. Ortaya çıkan kuvvet diyagramı üçgen prizmadır.

3BGS, kuvvet diyagramını temsil eden çokyüzlülerin bir araya gelmesi veya çokyüzlülerin kendi içinde alt bölümlere bölünmesiyle yeni dengede olan form diyagramları üretir. Bu nedenle oluşturulan üçgen prizma en az bir yüz diğerine komşu olacak şekilde döndürülüp ötelenerek bir araya getirilmiştir. Kümeleme işlemi tasarımcının değerlendirme ölçütlerine uyan sonuç ortaya çıkıncaya kadar devam etmiştir. Değerlendirme ölçütleri ortaya çıkan formun hacimsel özellik taşıması ve yine karşılıklı çerçeveye dönüştürüleebilecek birleşim noktalarına sahip olmasını içermektedir. Ayrıca yine bu aşamada ikili diyagramların çalışma prensibi olan birbirine dik olma hali yinelemeli çözümleyici (iterative solver) kullanılarak sağlanmıştır. Ortaya çıkan form diyagramı basınç altında dengede kalabilmektedir. Bu form diğer adımda KÇ strüktürüne dönüştürülmüştür. KÇ strüktürüne dönüştürme işlemi bir dizi analitik geometri hesaplamalarıyla gerçekleştirilmiştir. Son olarak, elde edilen KÇ strüktür biriminin strüktürel davranışı incelenmiştir. Strüktür formunun basınç altında da çalışabildiği görülmüştür.

Bu tez, hesaplamalı tasarım alanına tasarım sürecine kuvvet değişkenini de ekleyerek oluşturulmuş kapsamlı bir tasarım süreci geliştirerek katkıda bulunmuştur. Kuvvet değişkenini tasarım sürecine dâhil etmek mimarlar için yaygın bir eylem değildir. Bu araştırma göstermiştir ki geometri, strüktür ve malzemenin birlikte düşünüldüğü kapsamlı bir iş akışı strüktürel verimliliğin öne çıkarıldığı formlar keşfedilmesini sağlamaktadır. Sonuç olarak, mekanik terimlerle eşleştirilen strüktür önceliği yaratıcı süreç olarak adlandırdığımız tasarım sürecine katılarak hem verimli hem estetik formların ortaya çıkmasını sağlayabilir.



1. INTRODUCTION

Carpo (2017) points out architects are now in a data-affluent environment than ever before so that the form-finding process becomes form-searching over which architects do not have much control. The more the design problems get complex, the more appealing automated design methods become to architects. Using evolutionary algorithms by determining fitness criteria or machine learning algorithms which are based on large-data sets provide fast and accurate solutions. However, they lack intuition and improvisation that architects bring about the design process. Intuition and improvisation not only trigger design creativity but endow the designer with an informed design space in which s/he is consciously aware of design parameters and their interactions. Therefore, structuring explicit formulation of a design can yield design outcomes that may remain hidden using automated design methods.

Computational design approach enables architects to create a manageable representation of design at every state rather than considering the design process as a black box in which the explanation of the outcome is not possible. Computational making enriches the computational design process by including the perception and senses of the designer so that the form is not imposed upon matter as digital design tools usually enforce. Gürsoy (2016) established two frameworks as *making for* and *making of* as the former differentiates from the latter by being a non-deterministic design process. She further emphasized “abstraction – materialization – abstraction” cycle of *making for* process that ensures the computability of design ideas (Gürsoy, 2016, p.43). Dessi-Olive (2017) extended the computational making process by incorporating force parameter to describe a structural algebra which promotes non-deterministic hence creative design process for architects. What is common in that two research is that creative act can be traced through sensorial feedback in computational making process rather than the immaterial forms of digital design tools.

Lee (2015) developed a structural grammar using graphic statics to enable designers to generate new forms which are in equilibrium yet unexpected since structural analysis software does not suggest new geometries for the form. Geometry, structure, and material are interdependent design parameters from which architects and engineers

both benefit for creating efficient and functional forms. Therefore, the relationship between geometry, structure, and material is an essential quality for the design outcome which features structural efficiency. This thesis adopts physical and digital design processes to reason with the matter and forces at play. Reciprocal Frame (RF) structure geometry which inherently provides the designer with interdependent design parameters has been studied to evaluate the process-driven design.

1.1 Aim and Scope of Thesis

This thesis investigates geometry and its influence on force variables to explore forms with structural efficiency. RF structures consisting of linear elements with circular cross-sections rather than planar elements are studied to create 3-dimensional structures with self-equilibrium. RF structures are a unique family of structures that mutually support each other along their spans, not at their extremities (Figure 1.1). RF structure geometry offers a network morphology that distributes loads and forces simultaneously. Consequently, the network morphology of RF structure makes its geometry, form, and equilibrium state interdependent providing a designer with inclusive design space to explore their relationships.

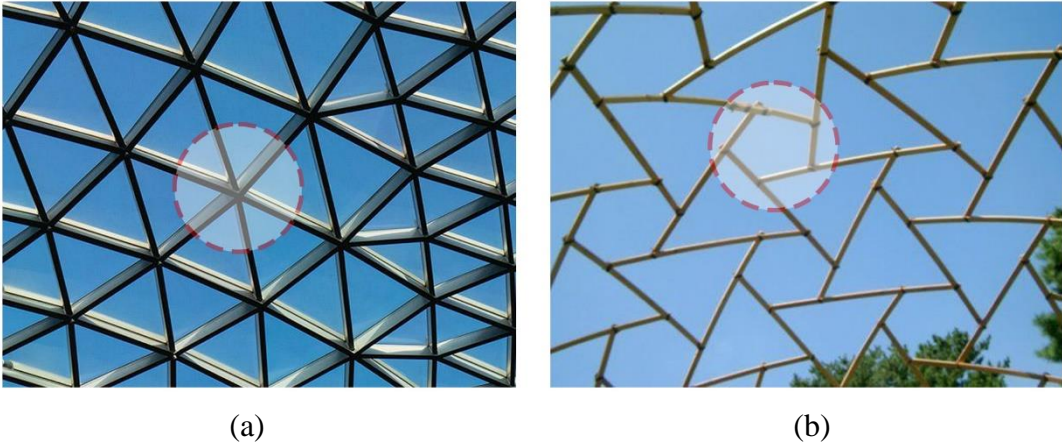


Figure 1.1: (a) Grid structure connection (URL-1), (b) RF structure connection (URL-2).

The perennial circular force flows between elements raise the geometric challenge of reciprocal structures thus making it hard to predict the final geometry of the structure. Therefore, top-down form-finding processes of RF structures in which the form is predetermined have been studied comprehensively through optimization tools and analytical investigations. Additionally, shell and spatial structures are designed to

work fully in compression or tension forces since it is the best way to transfer their dead and live loads (Adriaenssens et al., 2014). However, RF structures work mainly in bending forces (Larsen, 2004) which is regarded as a disadvantageous structural characteristic for spatial structures. There is a gap in investigating bottom-up methods to create RF structures while considering their structural efficiency through geometric investigations. Therefore, the aim is based on two viewpoints emanating from two research questions as follows:

- 1) How do geometrical shapes influence RF configurations?
- 2) How can we improve the structural efficiency of RF through a computational making and design process informed by forces?

The research focuses on developing an extensive workflow in which the designer explores RF structures employing different tool ecologies while simultaneously benefiting from geometry as a main driver of the design. The design outcome is the result of a computational design and making process in which the parameters inform each other through a continuous data flow. Therefore, the thesis aims to expand the design space of architects by including structural efficiency in the design process which is generally considered as an engineer's task or as a separate step from the design process.

1.2 Methodology

The research methodology consists of (1) geometric analysis, (2) physical experiment, and (3) digital form-finding processes respectively. Geometric analysis is undertaken in the algorithmic design modelling environment by creating definitions to examine the geometry of RF structures and how the RF geometry engages with Non-uniform rational B-spline surface parameters. After assessing the different RF geometries based on their efficiency in forming the same surface with the least material, the physical experiment is conducted with digitally fabricated joints and wooden sticks. Different RF configurations are explored from Volumetric Frame Units (VFU) through the computational making process. The VFU of the computational making process is abstracted and incorporated into the digital form-finding process to enhance its structural behaviour. Finally, the resulting form is transformed into an RF

configuration with analytical investigation steps. Structural Simulation is utilized to evaluate the structural behaviour of the design outcome.

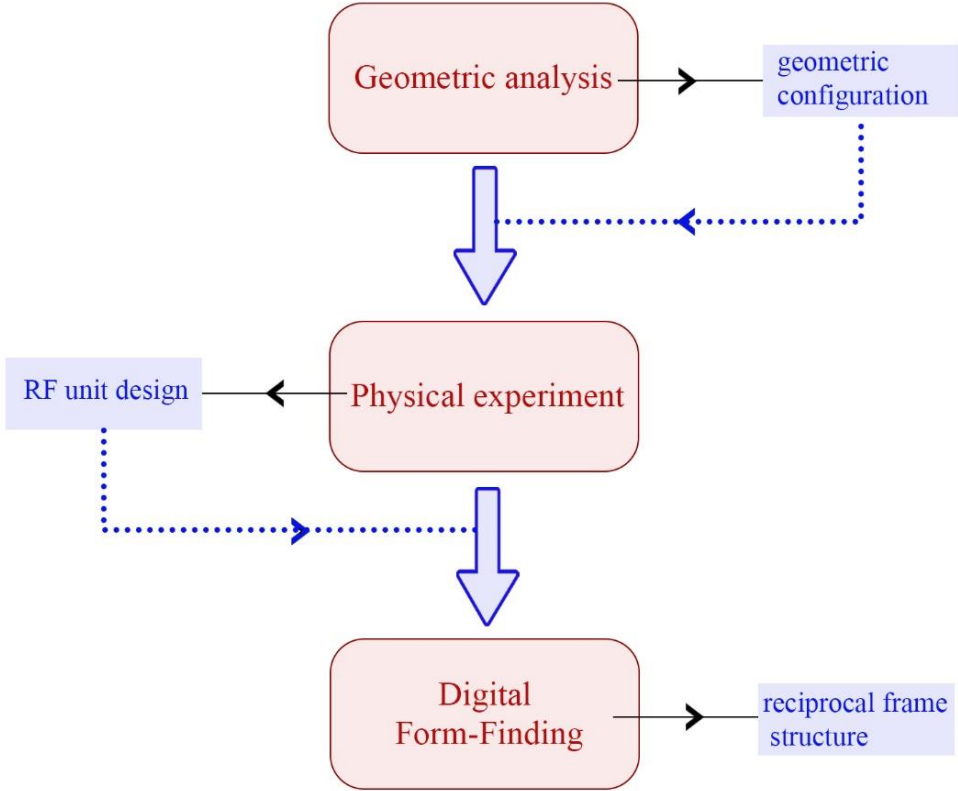


Figure 1.2: Workflow of the research.

2. RECIPROCAL FRAME STRUCTURES

In the past, the simple joints of Reciprocal Frame (RF) structures compensated the advanced construction methods to span longer distances with shorter linear elements. Beyond the structural aspect, architects and engineers have been impressed by the geometric variety that RF structures provide. Therefore, the structural reciprocity principle has not lost its significance from antiquity to today. This chapter presents 1) design and construction examples of RF in history, 2) an analysis of its morphology and geometry and a discussion of related works, and 3) structural behaviour and its implications on design.

2.1 Historical Context

As the name of the structure states, the term “reciprocal” etymologically is derived from the Latin word “reciprocus” which is the combination of recus (backward) and procus (forwards). Reciprocal is defined in the Cambridge Dictionary as below:

Adjective- operating for both, especially equally or to a similar degree.

The etymology and the definition of reciprocal comprise the fundamental principle of how the structure behaves, and explicate the way reciprocal structures differ from spatial structures. Intrinsic self-supporting structural systems were explored a long time ago because of the absence of advanced building methods. The idea of structural elements supporting each other fascinated the builders and engineers to avoid cumbersome building methods. Moreover, reciprocal structures are classified as lightweight structures which can be built with timber rather than concrete. Therefore, using timber that was the most available and ready-to-use material for construction at that time must have proliferated its construction.

The history of Reciprocal Structures dates back to ancient times such as the Neolithic pit dwelling, Indian tepee, and Hogan dwelling as documented by Larsen (2008). These are the very first examples of structural reciprocity even though most of them do not possess repetitive rules for the overall structure. Yet, they rely on the supporting relations of linear elements for the external and dead loads (Figure 2.1). In medieval

times, reciprocal structures mostly appeared to be roof and floor structures of the buildings which are called planar reciprocal frames as shown in Figure 2.2. Villard de Honnecourt's floor grillage sketches (1225-1250) which consist of short beams are one of the earliest examples of reciprocal floors (Villard de Honnecourt, 1959). Another example for planar floor design is Sebastiano Serlio's grillage design which typically represents floor plan design at that time (Serlio, 1545; Yeomans, 1997).

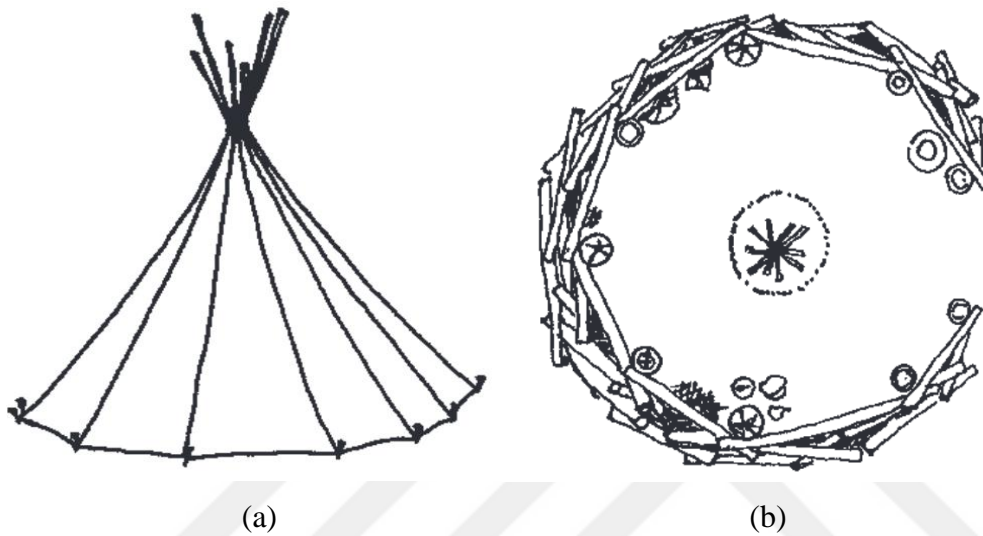
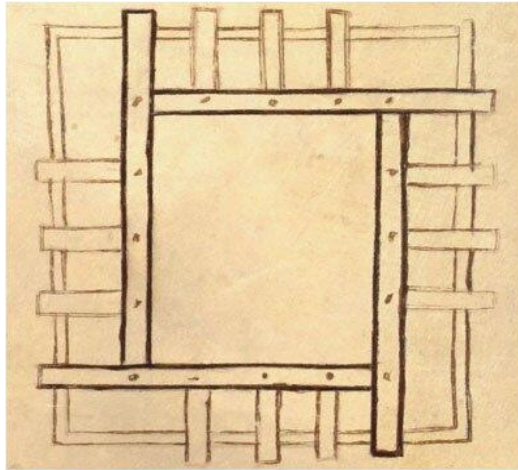


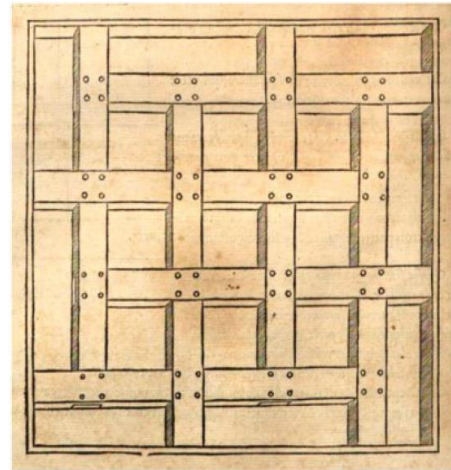
Figure 2.1: (a) Indian tepee and (b) Hogan dwelling plan (Larsen, 2008).

However, some of the roof structures do not follow planar configuration as in the case of the roof of the Lincoln Cathedral Chapter house and Puppet Theatre complex (Figure 2.3 and Figure 2.4. Chilton and Devulder (2001) investigated the structural behaviour of the roof of the Lincoln Cathedral Chapter house and reported that the reciprocal configuration of the roof was designed as a tension ring to balance axial loadings. They named the polygonal grillage which was made of reciprocal elements and placed at the base of the roof, as Reciprocal Ring Structure (Figure 2.3). Structural reciprocity must have compensated for the lack of advanced engineering in the middle Ages.

One of the main reasons that reciprocal structures emerge as roof or floor structures is that the structural reciprocity principle allows for spanning large distances with relatively short elements. It can be inferred from the note that Honnecourt (1225-1250; Villard de Honnecourt, 1859) wrote in his sketchbook about floor plan design:



(a)



(b)

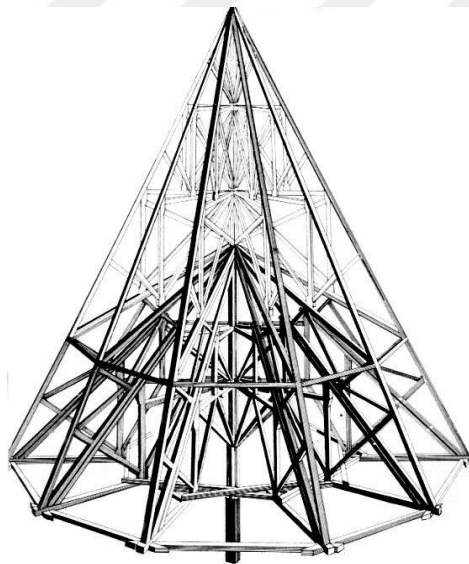
Figure 2.2: (a) Honnecourt's grillage and (b) Serlio's grillage (Zamperini, 2021).

in Italian (original):

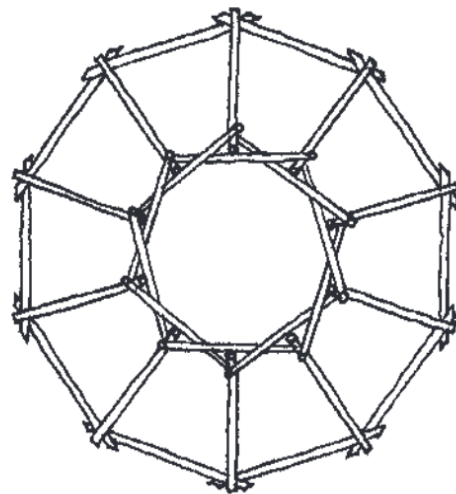
“Ensi poes over a one tor u a one maison de bas si sunt trop cor.”

Translated in English as:

“By this device, you can work at a tower or a house with timber which is too short”.



(a)



(b)

Figure 2.3: (a) Lincoln Cathedral Chapter house 3-dimensional reciprocal roof structure and (Chilton and Devulder, 2001), (b) plan view of the reciprocal roof structure (Larsen, 2008).



Figure 2.4: Puppet theatre complex designed by Kazuhiro Ishii (Pugnale and Sassone, 2014).

Leonardo Da Vinci's sketches on reciprocal structures may be the most popular historical example. As a matter of fact, reciprocal structure configuration is also named as *Leonardo grids* in literature. In Codex Atlanticus, folio 899v (Robert, 2008), Leonardo explored different configurations of reciprocally arranged elements in his sketches (Figure 2.5). Although Leonardo's first sketches show planar characteristics, he was regarded as the only person who studied complex 3-dimensional reciprocal structures in the West in this historical timeline (Pugnale and Sassone, 2014). The example justifying his reputation is the bridge he designed with segmented arched forms (Figure 2.6). The arched forms consisted of short timber elements which supported each other reciprocally. After Leonardo discovered this type of bridge for military purposes during the war (Isaacson, 2017), this type of bridges was named as temporary bridge (Anon, 1956).

John Wallis's text "Opera Mathematica"(1695) is considered the first scientific text which presents structural calculations for reciprocal floor designs (Houlsby, 2014). Wallis studied load transfer and geometry of the reciprocal structure for the first time. Even though it is not clear from the documents that the structures he designed were built on a large scale, he investigated the reciprocal planar grillage in great detail (Larsen, 2008).

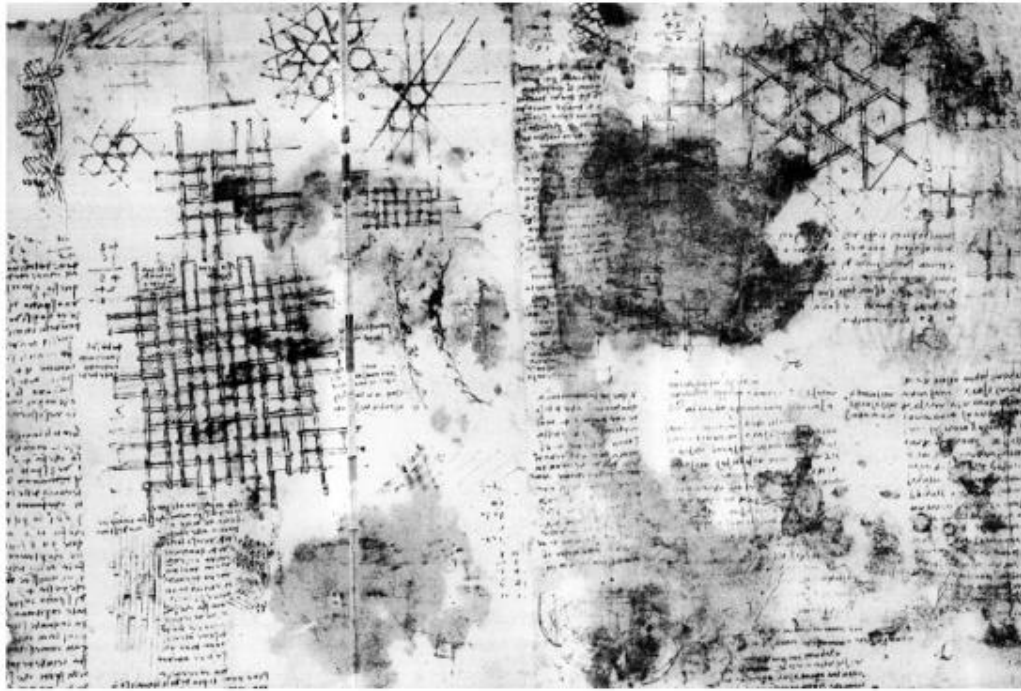


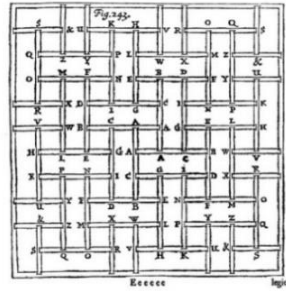
Figure 2.5: Leonardo da Vinci, Codex Atlanticus, fol.899v with reciprocal configurations (Robert, 2008).

In the 20th century, many scientific research about reciprocal structures was conducted in academia to comprehend structural reciprocity. Several patents were also registered for designing unique reciprocal configurations that have not been designed before (Pugnale and Sassone, 2014). For example, the Lamella construction with reciprocal joints for roof structures was invented by the German engineer Friedrich Zollinger (1880-1945). The reciprocal system was developed to meet the need for housing and allow for fast and cheap construction after the First World War (Larsen, 2014). Emilio Perez Pinero created a kinematic roof structure derived from reciprocal configuration and was registered in 1965 as reported by Escrig (1993).

The English designer Graham Brown was the first person who coined the term “Reciprocal Frame” based on the 3D closed circuit of sticks (Larsen, 2008). Oliver Baverel (2000) who studied reciprocal structures in his Ph.D thesis called reciprocal frame structures “nexorade” and the linear elements “nexors” which is originally derived from the Latin word nexus meaning “link” (Baverel, 2000). Although there are more connotations for reciprocal structures in literature, the terms “Nexorades” and “Reciprocal Frame” are more likely to be encountered.



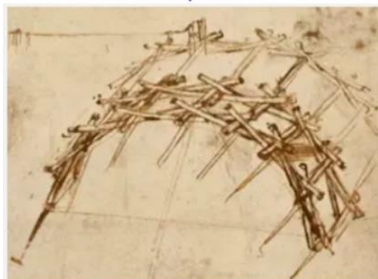
Rokko Observatory by Arup
(URL-5)



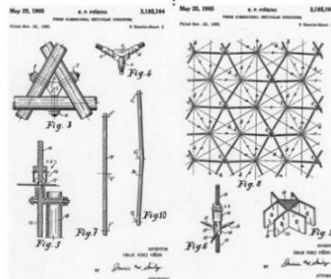
Opera Mathematica by John Wallis
(Houlsby, 2014)



KREOD Pavilion by Qing Li
(URL-4)



Da Vinci Bridge
by Leonardo Da Vinci (URL-3)



Kinematic Reciprocal Frame Structures
by Pinciro (Perez-Valcarcel, 2021)



The Lamella roof construction
by Zollinger (Tamke et al., 2010)

Figure 2.6: Historical timeline of RF structure examples.

2.2 Morphology and Geometry

RF structure elements mutually support each other, and the way they support each other comprises a node. Nodes are made of another geometric shape that occurs in the structure morphology. Thus, RF morphology needs to comprise at least two different polygons due to special node configuration. The only RF exception where the nodes do not give rise to another polygon is the RF structures consisting of planar elements instead of linear elements. RF structures with planar elements can be constructed with or without nodes. The structures made of one type of polygon inherit RF characteristics from the connection types where the one planar elements connect to the other along the span not at the end. An example of this type of RF is the Lamella vault or roof construction as shown in Figure 2.7.

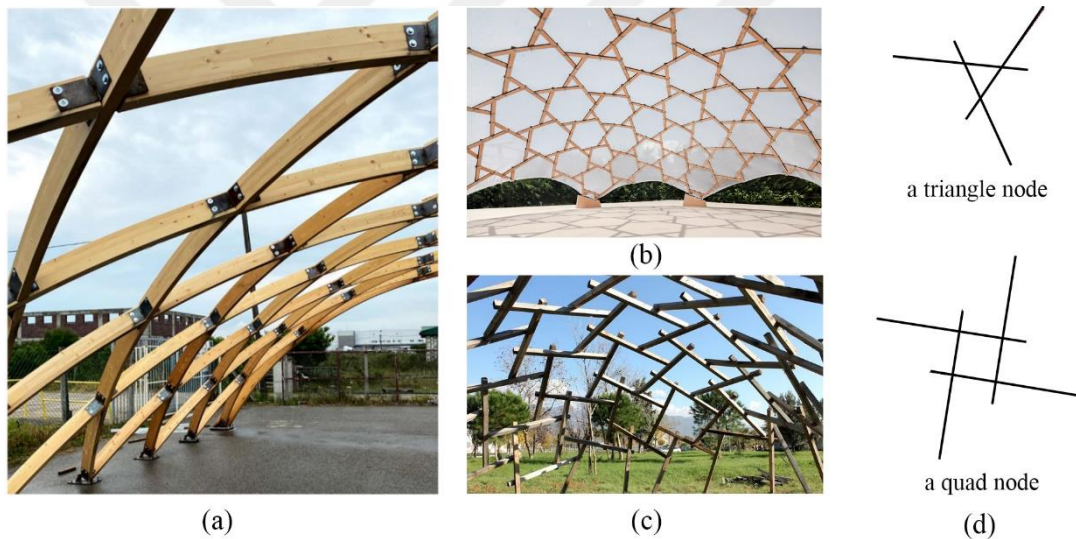


Figure 2.7: (a) Lamella construction (adapted from Petrović et al., 2022), (b) an RF structure with triangular nodes (URL-6), (c) an RF structure with quad nodes (URL-7), (d) RF node examples made of a polygon.

“Reciprocal frame” denotes the closed circuit thus its morphology can be made up by polygons. Polygons can be either regular or irregular based on the structure’s overall shape and equilibrium state. The simplest RF is called “fan” which consists of 3 elements. Fan represents the node of RF structures. Therefore, typical spatial structures start to turn into a RF structure when their nodes comprise a fan (Figure 2.8). Consequently, 3 connection points emerge each of which comprises two elements. There are three methods to transform regular polygons into an RF fan which are the rotation method, translation method, rotation-translation method, and centre-to-centre

method as shown in Figure 2.9 (Godthelp, 2019). The rotation method is realized by rotating the elements from their middle points around their normal vectors. The translation method follows the offset of the base polygon inside. However, the offset distance should not be greater than half of the element length. Rotation and translation methods can be combined but they increase complexity thus it is not common to use this method compared to rotation method. The center-to-center method is based on a scaled polygon created inside the base polygon. The middle points of the base polygon connect with the adjacent middle points of a scaled polygon one by one.

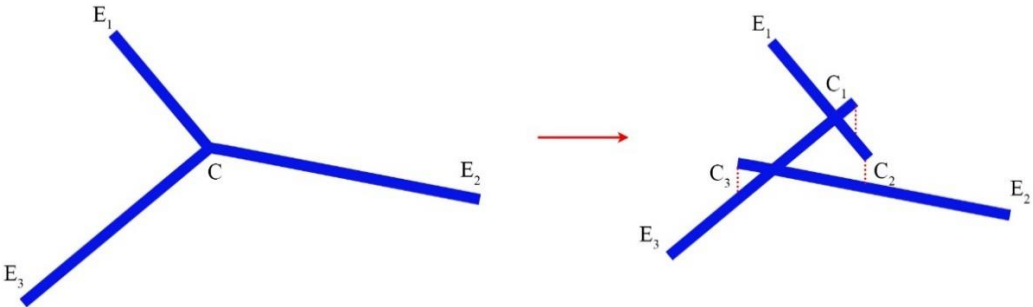


Figure 2.8 Transformation of a converging node into a fan.

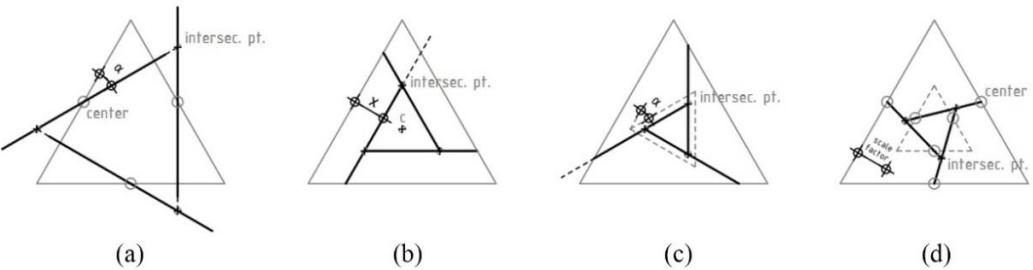


Figure 2.9 Transformation methods for polygons (Godthelp, 2019).

A fan configuration can be further examined in terms of geometrical quantities of RF structures. RF structures have three essential geometric variables that determine their final form and structural behaviour as well. These are the engagement window which is created by the displacement of several members, eccentricity which is the distance between the axes of two attached members, and engagement length which is the length of each edge of the engagement window. Following this, Figure 2.10 shows a triangular engagement window with related engagement length and eccentricity. These three geometrical quantities are interdependent variables as changing one influences the other two.

The geometric configuration of RF structures can be broken down into sub-systems in hierarchical geometric order as follows: 1) Single element: smallest system unit, 2) Basic system: decomposable into single bars, 3) Component system: decomposable into basic systems and single bars, 4) Entire system: decomposable into components systems, basic systems, and single bars (Kohlhammer and Kotnik, 2011). Figure 2.11 shows the system order described above in which the basic system corresponds to triangular fans and the component system corresponds to repetitive units. The structural morphology comprises hexagon units with triangular fans in this case.

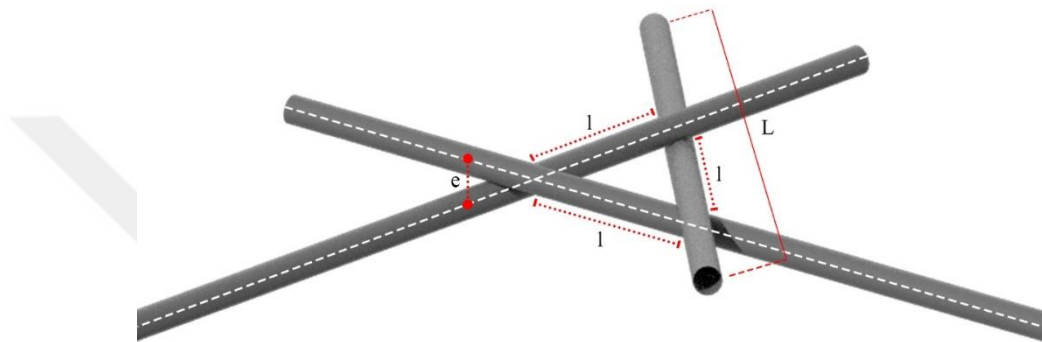


Figure 2.10: A triangular engagement window with l : engagement length, L : the length of an element, e : eccentricity (Karahana and Yazıcı, 2024).

Form-finding of RF depends on the geometrical configuration and the optimization of internal reactions between elements. Therefore, geometrical configurations are investigated through analytical operations or mapping where the latter is solved through automated optimization algorithms. Parigi and Kirkegaard (2014) created a design tool for reciprocal systems called “The Reciprocalizer” which is a Grasshopper component in Rhino software. The component takes mesh, engagement length, and eccentricity as inputs.

The tool proved its competency in building free-form RF structures as shown in Figure 2.12 (Parigi and Kirkegaard, 2014). Thönnisen (2014) devised a form-finding instrument for reciprocal structures which is based on a cell configuration allowing local manipulation of the structures over iterations. The transformation of cells into a fan was realised through geometric calculations, then the overall form reached its final form via an iterative numeric solver which simultaneously adjusted all interactions (Figure 2.13).

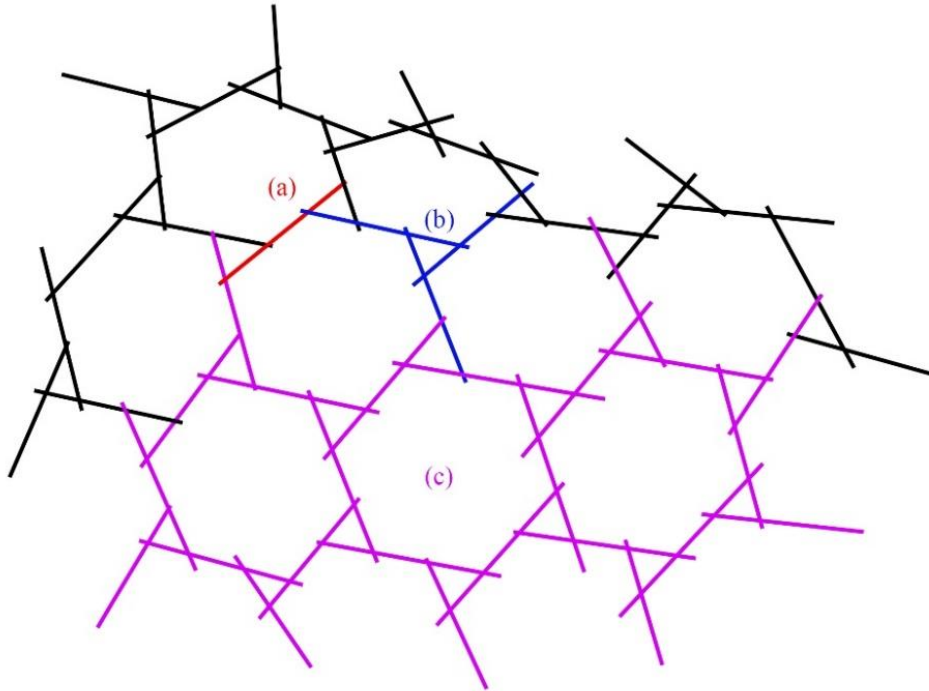


Figure 2.11: (a) Single element, (b) Basic system, (c) Component.

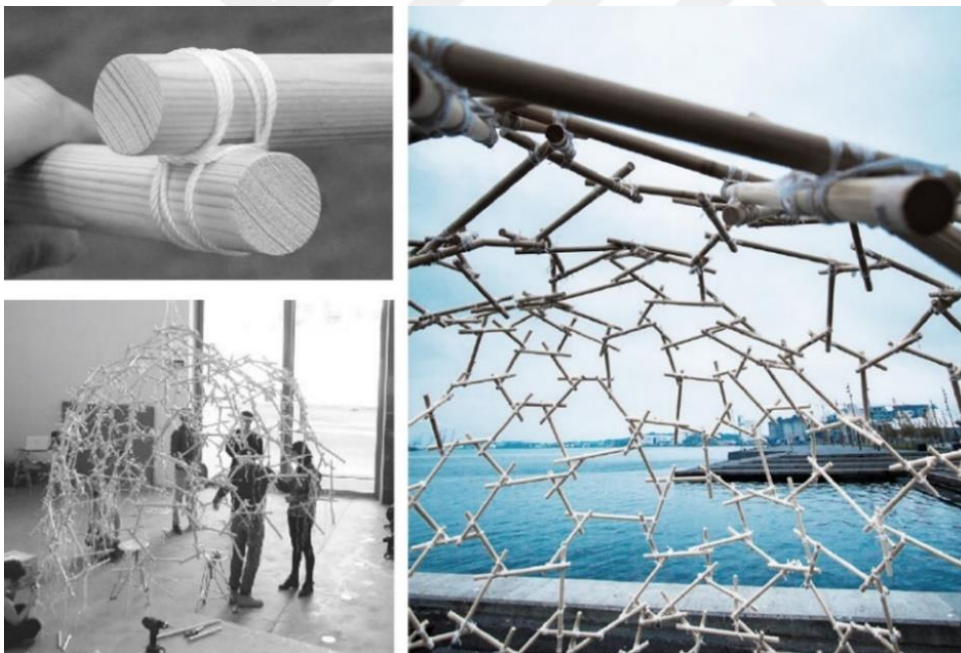


Figure 2.12: RF form finding through iterative solver based on cell configuration (Parigi and Kirkegaard, 2014).

Mesnil et al. (2018) developed a form-finding process using the translation method which focuses on geometrical transformations of RF structures resulting in the optimization of eccentricities and engagement length. Given the counterintuitive internal interactions of RF structures, their research on geometrical investigations

gains new insights into RF geometry such that the designer has control over the geometric parameters to explore efficient RF structures. Su et al. (2019) developed a numerical method for form-finding of RF structures by adding two new parameters which are contact point and contact vector to define the special placement of RF elements. Moreover, their shape optimization method was minimising strain energy under static loads.

RF structures do not require complex joints since two elements connect instead of three as typical grid structures do. These two-valent connections give rise to the internal reactions of elements. As the joint type changes from flexible to rigid, so do the internal reactions. Therefore, the joints are considered an integral part of the structure which directly affects the form thus structural behaviour (Mellado et al., 2015). RF joints vary from rope and clamp-like connectors to notchs (Figure 2.14).



Figure 2.13: RF form finding through iterative solver based on cell configuration (Thönnissen, 2014).

RF joints determine the rotation angle, translation distance of elements, and consequently the eccentricity parameter. Rope joints allow elements very high rotation angles, and they can increase the eccentricity with that much degree of freedom. Moreover, flexible joints like rope are vulnerable to quick deformation. Notch joints fix the rotation angle and they also decrease the eccentricity with the interlocking system. However, they impose the form very strictly so that they do not allow any relocation of elements after the structure is built. Therefore, notch joints may not defy additional loads which were not tested before. Clamp-like connectors allow rotation and translation along the spans of members to the extent that designers decide. They also enable bottom-up form-finding approaches while constraining the design space, unlike very flexible joints.

RF Joint types		
Clamp-like connectors	Notch	Rope
		
(Senechal et al., 2011)	(Godthelp et al., 2019)	(Mitterberger et al., 2022)

Figure 2.14: RF joint examples varying from rigid to flexible.

The way elements support and get supported causes complex reactions between elements (Parigi and Kirkegaard, 2014; Kohlhammer and Kotnik, 2011). The complex reactions arise from the non-hierarchical structural order in which every element influences the structure equally (Pugnale and Sassone, 2014). Corollary to the counterintuitive internal reactions, the final form of RF structures is not predictable. Therefore, most of the studies about RF structures adopt top-down form-finding processes in which the form is pre-determined. Even though the form is pre-determined the geometric configuration of RF requires optimization due to the simultaneous interactions of elements. The internal reactions need to reach a static equilibrium using an iterative solver, genetic algorithms, or dynamic relaxation method.

Parigi et al. (2012) developed a hybrid optimization method that includes gradient-based and genetic algorithms to create RF structures. In this study, they benefit from a gradient-based algorithm to find compatible geometric configurations yet not a topological right solution. Thus, genetic algorithms were used to search the whole design space and to find the one with topologically compatible meaning the element supports and gets supported in the right way. Baverel (2000) used dynamic relaxation for the first time since the simultaneous reactions of RF elements mimic dynamic systems until reaching the equilibrium state.

Especially for regular polyhedral forms, the geometric configuration is easier since the boundary conditions are more specific compared to free-form surfaces. Subdivision of polyhedra yields an approximation to smooth surfaces such as the subdivision of icosahedron can create a spheric RF structure. The resulting spheric RF structure is based on the polygon cells and their rotation method (Figure 2.15). Kangaroo iterative

solver is used for revealing the final placement of linear elements of a spheric RF structure.

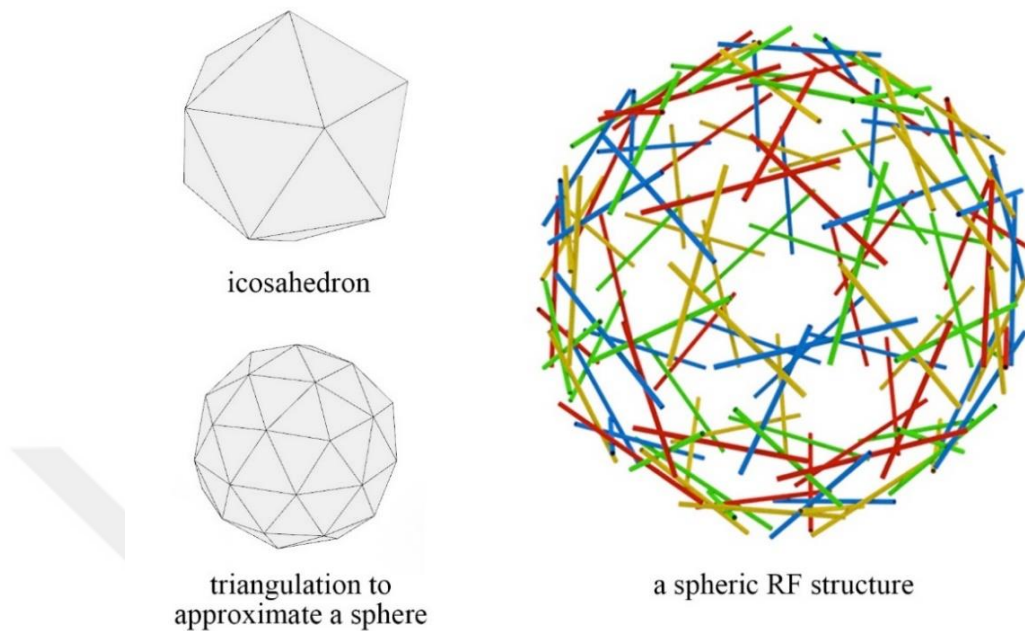


Figure 2.15: A spheric RF structure derived from the icosahedron.

Mapping is one of the ways to impose the RF units onto a pre-determined form. The pre-determined form can be either a free-form surface or a regular polyhedral. Some studies show that mapping 2D reciprocal patterns to 3D geometries has resulted in efficient structures with the condition of implementing optimization methods afterward (Song et al., 2013; Anastas et al., 2016). However, this mapping method involving post-optimization is not applicable for all kinds of free forms and discrete geometries that have double curvatures like saddle-shaped forms (Asefi and Bahremandi-Tolou, 2019).

Mapping is an advantageous method to turn free-form surfaces into an RF configuration even though the geometric configuration needs post-optimization and flexible joints. However, mapping does not benefit from structural reciprocity as it imposes geometric patterns onto a form. The reciprocal polygon units that it provides are more of a representation to create the structure. Figure 2.16 shows how the number of polygons in the X and Y directions directly affects the number of elements of RF structures. Therefore, mapping the polygons onto a surface to create RF structures with transformation does not differ from mapping polygons to create a spatial structure without transformation.

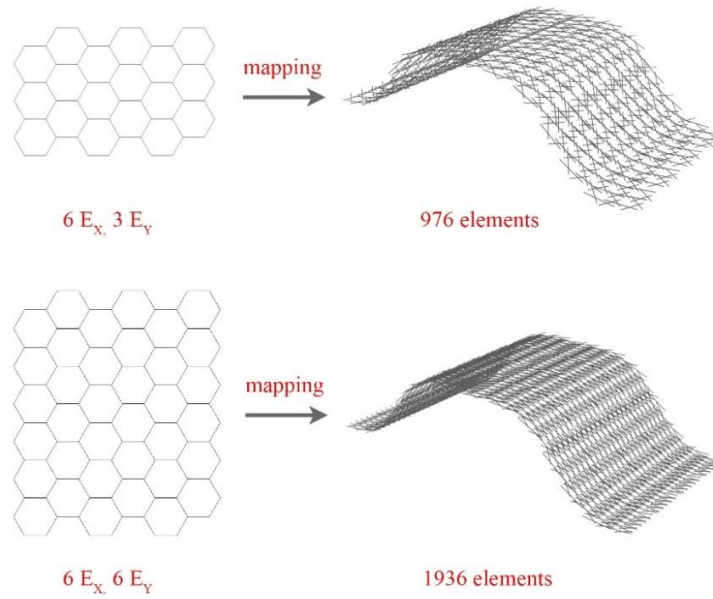


Figure 2.16: Mapping examples of RF structure, E_x : polygon number in X direction, E_y : polygon number in Y direction (Karahana and Yazıcı, 2024).

Puagnale and Sassone (2014) stated that with the aid of computation, the design process can only start from a forced top-down approach in which reciprocity does not inspire the project but just adapts to it. Following this, they emphasize the advantages of the physical modelling of reciprocal structures as designers comprehend structural reciprocity intrinsically. Therefore, to expand the geometrical space of RF structures, it is crucial to carry out a form-finding process consisting of digital and physical modelling and consider the geometrical parameters simultaneously to overcome its structural complexity.

2.3 Structural Behaviour

Elements of reciprocal structures engage in mutual reactions which create circular force flows (Pugnale and Sassone, 2014) as shown in Figure 2.17. Force flows directly influence the simultaneous interactions of elements (Figure 2.18). Even though RF structures inherently reach the equilibrium state with the circular force flows, they are not good at conveying axial loads. Brocato (2011) stated that the optimal shape of RF structures minimizes the normal forces and maximizes the bending moment which is the opposite of inverted catenary structures.

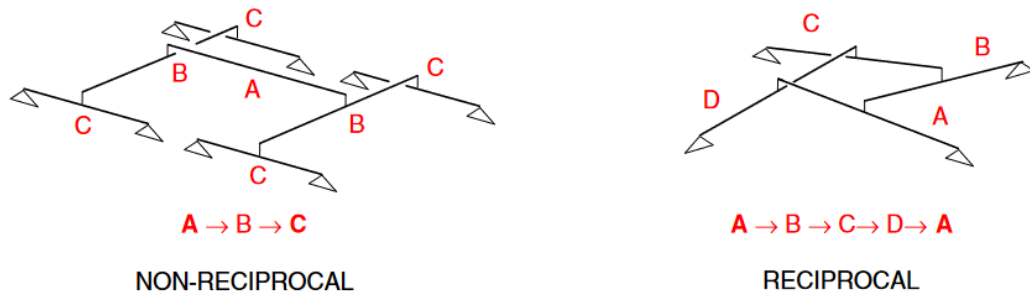


Figure 2.17: Force transmission difference between reciprocal and non-reciprocal structures (Pugnale and Sassone, 2014).

The way elements of RF structures connect each other along their spans causes bending forces which is a disadvantageous structural behaviour for the structure stability under loadings (Figure 2.19). Although circular flows decrease the structure stiffness since they give rise to movement under applied forces, they provide equal load distribution thanks to this circulation. Gelez et al. (2011) put forward that RF structures are not constrained to a few geometric configurations as flat grid RF structures are. The study showed that when the boundary conditions changed to the non-rectangular, flat RF structures did not adjust and were exposed to more bending forces whereas RF structures exhibited uniform bending load distribution as shown in Figure 2.20 (Gelez et al., 2011, p.342).

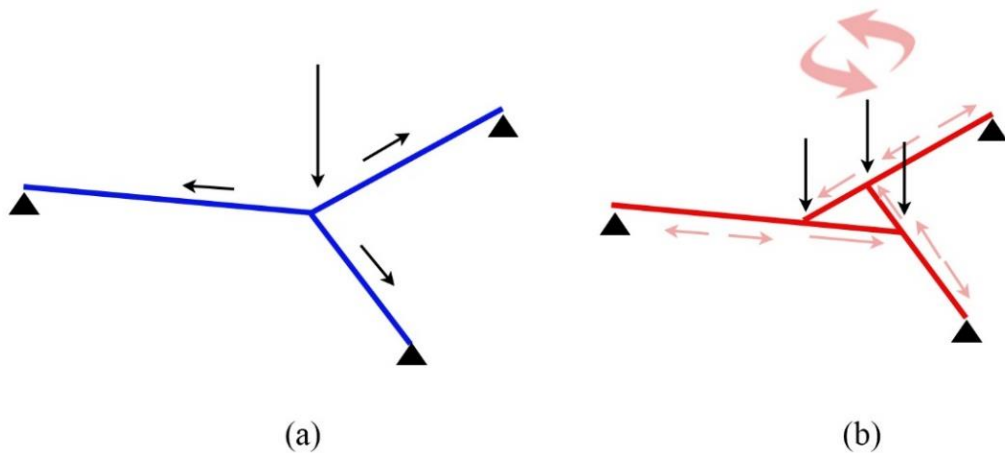


Figure 2.18: (a) Load-behaviour of non-reciprocal structures, (b) Emergent circular force flows in load-behaviour of reciprocal structures.

Double-layer RF structures prove their efficiency in resisting bending forces compared to single layer RF structures (Douthe and Baverel, 2014). Recently, some research in RF structures focuses on this issue by developing hybrid approaches such as integrating tensegrity logic into RF design (Widyowijatnoko et al., 2014), creating

bending-active double-layer RF structures (Brancart et al., 2017) and turning RF structure into compression-dominant double layer structures (Wang and Akbarzadeh, 2022) as shown in Figure 2.21. Thus, it can be inferred that double-layer RF configurations are essential to improve its resistance to bending forces compared to single layer RF configurations.

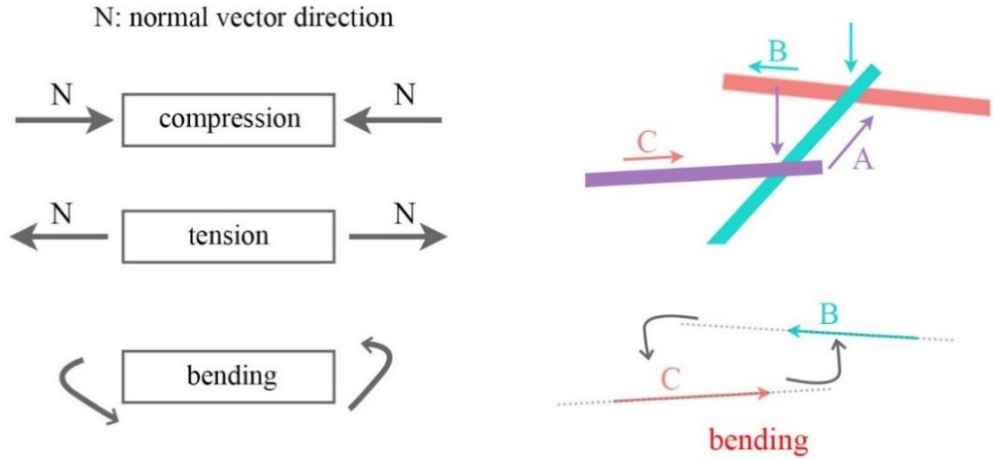


Figure 2.19: Bending force formation in RF structures.

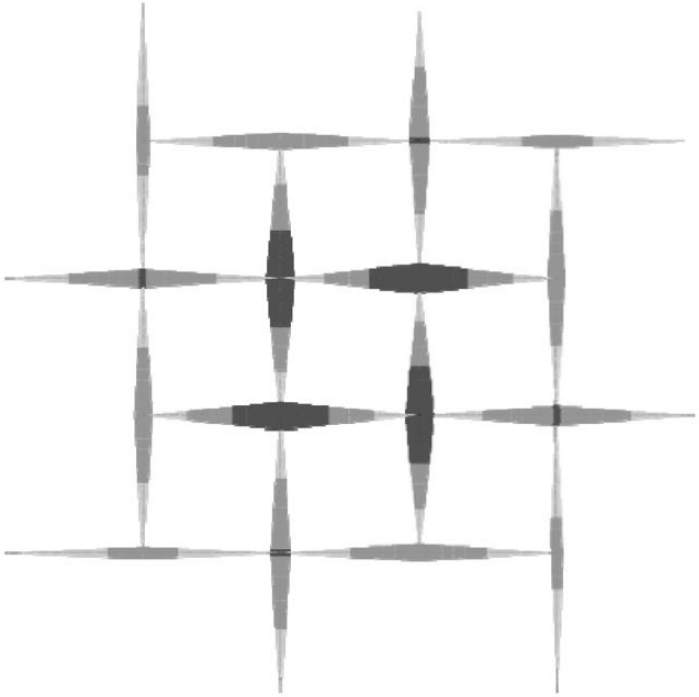


Figure 2.20: Bending moment diagram in a statically determinate RF structure for a uniform load (Gelez et al., 2011).



(a)



(b)



(c)



(d)

Figure 2.21: (a) Double layer RF structure (Douthe and Baverel, 2014), (b) Double layer RF configuration (Wang and Akbarzadeh, 2022), (c) A shell nexorade (Mesnil et al., 2018), (d) RF structure working in tension (Widyowijatnoko et al., 2014).



3. COMPUTATIONAL DESIGN AND MAKING

Computational design and digital design are two interchangeable terms that architects tend to use one for another. This issue also arose from the ever-developing digital design tools that make computational design tools more visible in the current architectural discourse. However, computational design refers to a much broader area, “a reasoning” for the design process. To affirm it is reasoning, computational design does not have to be with computers (Özkar, 2005) as digital design entails computers and software that make the design process possible. In this sense, computational design thinking has its roots before the invention of advanced digital design tools and has developed till today following a nonlinear path across different disciplines.

Computational design has engendered different terms frequently used in computational design processes such as generative, parametric, and optimization. In addition to these terms, computational making has emerged to delineate the computational design process involving material, tools, and actions. Computational making is quite a new term coined by Knight and Stiny (2015) even though it has been implicitly embedded in the computational design processes engaging with material. This chapter presents the important role of computational design and making for the creative act of architects as this thesis methodology adopts a computational making process to explore polyhedral forms of RF structures.

3.1 Computational Design Thinking

Computational design thinking discussions were sparked back in the 1960s-1970s most of which are the foundations of today’s computational design methods. Christopher Alexander was one of the earliest architects and academicians who contemplated computational design thinking in his book “A Pattern Language” (1968). He supported the use of computers in design and also suggested a formulation for architectural design problems (1968). March (1976) argued Alexander’s pattern approach as he put forward that every architectural design problem cannot be formulated in his patterns since it limits the design space of architects. Stiny and Gips

(1972) introduced shape grammars which is a rule-based formalism based on visual thinking. Shape grammars are one of the seminal computational thinking approaches as it presents visual calculation through shapes. Although shape grammars entail rules, Stiny (2006) emphasized the unpredictability of shape grammars with embedding characteristics of shapes. Stiny (2006) described “set grammars” as a more symbolic way of shape grammars since it does not allow shapes to fuse or divide. Set grammars have been widely used in architectural design for mainly plan layout generation (Stiny and Mitchell, 1978; Koning and Eizenberg, 1981; Benros et al., 2012). Mitchell (1991) developed functional grammars for structural design considering the structural performance of hut designs.

Knight and Stiny (2001) discussed the aspects of computation as *representation* and *process*, noting that it is not restricted to them, to give a useful taxonomy of computational design. They also made a distinction between *classical* and *non-classical* for the *representation* and *process aspects*. They classified the visual representation and the process with a result but having no explanation as *non-classical*. They attach *classical* to the verbal representations and the process with explanation. In this perspective, shape grammars denote a *non-classical representation / classical process* while using evolutionary algorithms or diffusion models for form generation is *non-classical representation / non-classical process*.

What makes computational design distinctive from other design perspectives is this design process in which s/he designs the inner logic of the form rather than the appearance. From this perspective, Terzidis (2006) put forward an *algorithmic form* to imply that architects can develop an algorithm and reason through that algorithm to control the design process. Frazer (1995, p.117) pointed out that the forming of material is relational; a trace or memory of the process. This approach implies a process-driven design in which the designer creates a dialogue between interdependencies which are the main design parameters.

Computational design opens up ways to think of design as a dynamic process rather than focusing on one isolated outcome. Designers can aim at different design aspects such as form, performance, and materiality simultaneously until these aspects reach the negotiation for the desired outcome (Ahlquist and Menges, 2011). Defining the relationship of design parameters not only endows architects with an integrated design

process but also several outcomes from the same process. This aspect of computational design implies its generative characteristic.

3.2 Computational Making

Making implies a set of actions to obtain a desired physical result by following predefined or improvisational steps. Ingold (2013, p.22) exemplifies *making* by creating a basket in nature where the form was not imposed on the material but rather generated in the force field of the relations between the material and maker. He goes on to state that the form emerges as a more or less transitory equilibration (Ingold, 2013, p.25). Making can be interrogated when construed as a computation approach in the design context. Knight and Stiny (2015) stated that making is doing and sensing with stuff to make things. Therefore, computational making includes perception, material, and actions in the computational design process, enriching the process with additional design parameters.

Computational making is also process-driven since the actions and material allow ambiguity during the process even though the rules are determined. Therefore, how design changes during the process gives new insight into designers about the material, geometry, and rules. Rather than focusing on input and output, the computational making process enables designers to explore something new during the process and continue with this intermediary outcome for the next design step.

Gürsoy and Ozkar (2015) developed abstract shape rules for dukta cut patterns. They materialized the pattern and presented physical actions to see the material role in the making process. Noel (2020) codifies the traditional wire-bending method utilizing making rules. Kamath (2020) creates making grammars for the thin tile vault construction and puts forward that interaction with material, tool and the environment allows the designer to make emergent design decisions that were not planned. Muslimin (2010) analysed the traditional weaving process to create structurally efficient modules derived from the weaving pattern. He created three different new geometric patterns by using these modules and following shape grammar rules as shown in Figure 3.1.

Suzuki et al. (2023) developed a computational framework for creating a grid shell structure exploiting weaving principle for units. The volumetric units are in cylindrical

shape which gives the structure the necessary structural stiffness that the deployable grid shell structure lacks. Therefore, they benefit from material behaviour while determining the geometry of the units through the computational making process as shown in Figure 3.2. Ayres et al. (2018) investigated *kagome* patterns to expand its geometric space for 3D structures through physical experiments. They point out that while digital simulation tools optimize and give the final geometric shape of the structure, physical modelling requires a compromise between the topology of the structure and the mechanical properties of the material as shown in Figure 3.3.

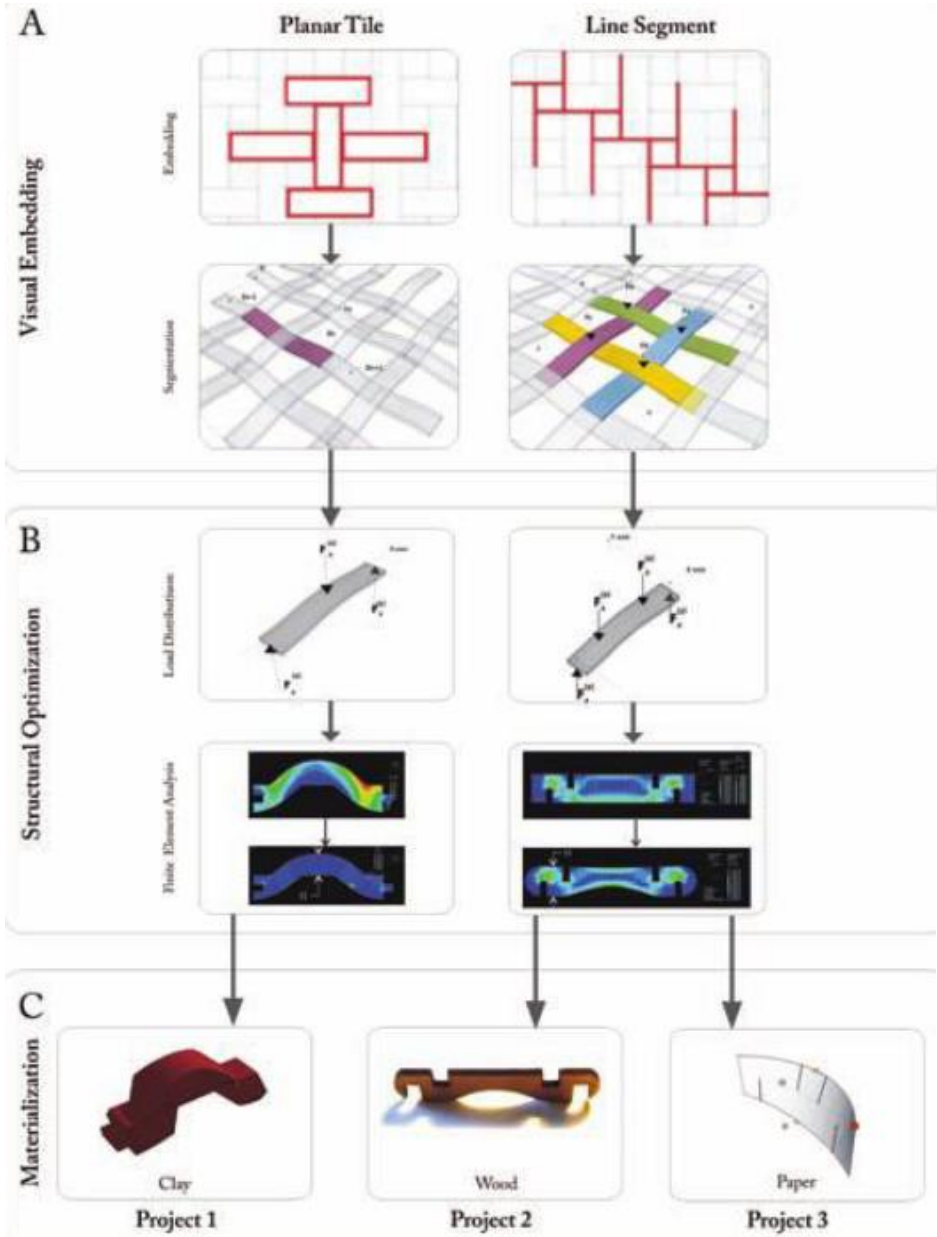


Figure 3.1: Creating structurally efficient building components from the weaving pattern (Muslimin, 2010).

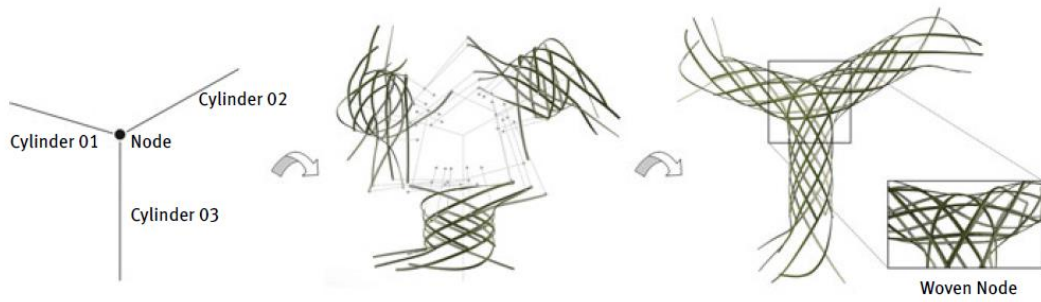
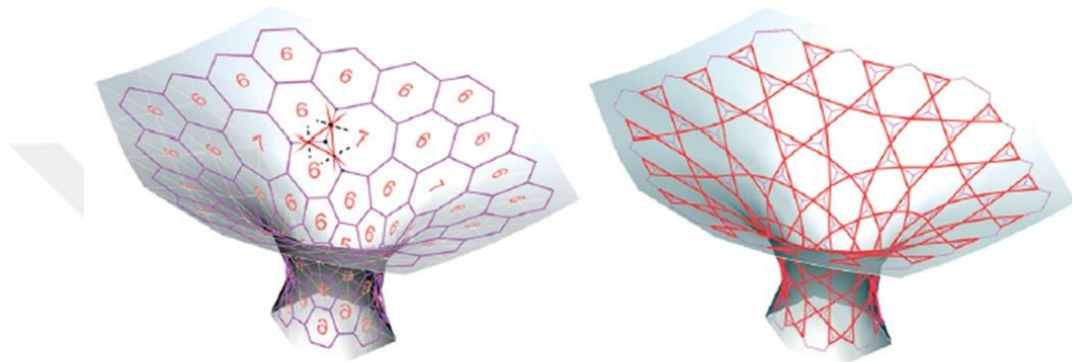
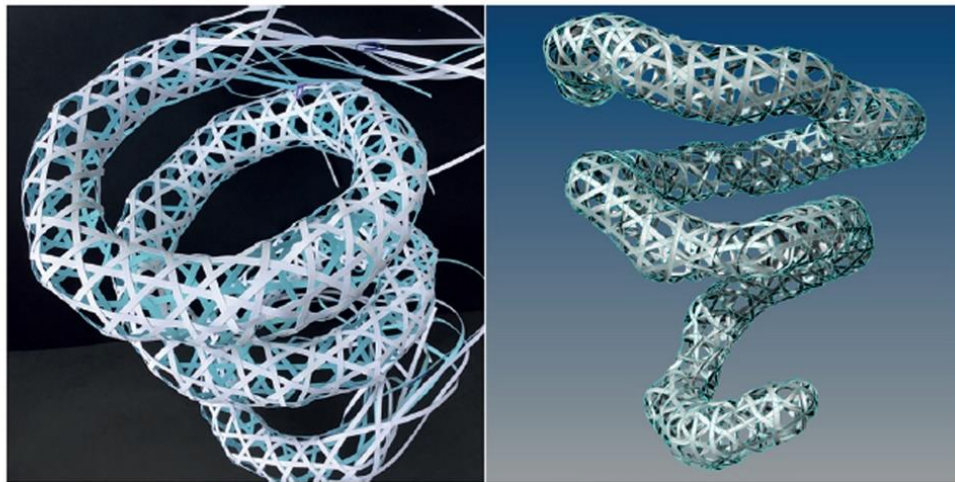


Figure 3.2: Woven node created by connection of cylinders (Suzuki et al., 2023).



(a)



(b)

Figure 3.3: (a) Creating kagome patterns from mesh topology, (b) Physical model of kagome patterns on the left and its simulation model on the right (Ayres et al., 2018).



4. RELATIONSHIP BETWEEN COMPUTATIONAL GEOMETRY, MATERIAL AND STRUCTURE

Architects define sufficient representations of design and investigate geometry, structure, and material on different levels of the design process. Exploring the relationships between geometry, material, and structure yields an architect a comprehensive design workflow, in which s/he achieves the design requirements. Exposing the relationship between geometry, material, and structure comprises the thesis workflow in which each step provides necessary input for the next step. This chapter delves into the intricate relationships of design described above to provide a framework for the workflow.

4.1 Polyhedra and NURBS Geometry

Polyhedra and NURBS are two contrasting representations of geometrical form with the former encoded in Euclidean space whereas the latter in Non-Euclidean space. In this thesis, NURBS and Polyhedra are utilized for form investigations at two different scales which are surface and unit scale. NURBS are used to determine which geometric configurations are more efficient for RF structures. Polyhedra is studied to investigate VFU geometry through 3DGS in the structural form-finding process.

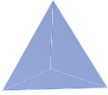
4.1.1 Polyhedra

A polyhedron is a 3-dimensional shape consisting of polygonal faces. Its polygonal faces can further be broken down into straight edges and vertices. Polyhedron geometry requires each edge to be shared by two faces and each vertex emerges where several edges and faces come together (Cromwell, 1997, p.13). Two main polyhedra classes are differentiated by their polygonal face arrangement: Platonic solids and Archimedean solids some of which are illustrated in Table 4.1. Platonic solids also known as regular polyhedra comprise congruent faces and congruent vertices at which the same number of faces meet (Pottman et al., 2007, p.81). There are five platonic solids which are tetrahedron, cube (hexahedron), octahedron, dodecahedron, and

icosahedron. Platonic solids have inscribed and circumscribed spheres as a result of their regular geometric construction.

Archimedean solids consist of two or more non-intersecting polygons thus showing variety in their face arrangement (Cromwell 1997, pp. 91-92). The angle between adjacent faces of polyhedra is called dihedral angle. Cube-octahedron, truncated octahedron, truncated cube, and rhombic-octahedron are some of the Archimedean solids which are counted as 13 in total. Seven of the 13 Archimedean solids can be obtained from Platonic solids by simple truncation and four of them can be obtained by expansion of Platonic Solids (Stott, 1910).

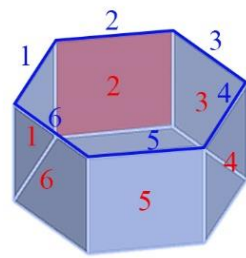
Table 4.1: Polyhedron examples.

Class and Name	ID	Faces	Vertices	Edges
 Platonic Tetrahedron	U1	4	4	6
 Platonic Octahedron	U5	8	6	12
 Archimedean Cuboctahedron	U7	14	12	24
 Concave Polyhedron Pentagrammic Crossed antiprism	none	12	10	20

Polyhedra can also be distinguished as convex and concave polyhedra based on the interior angle of faces (Cromwell, 1997). Convex polyhedron has an interior dihedral

angle of less than 180 degrees, and a line connecting two points inside the polyhedron lies entirely inside the polyhedron due to the convexity rule. A concave polyhedron has at least one dihedral angle of more than 180 degrees and as opposed to the convexity rule, a line connection lies partially or entirely outside the polyhedron. Platonic and Archimedean solids are convex polyhedra types while star polyhedron is an example of concave polyhedra.

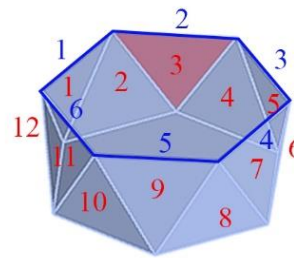
Prisms and pyramids are also sub-classes of convex polyhedra. A general prism is a polyhedron possessing two congruent polygonal faces and with all remaining faces parallelograms (Kern and Bland 1948, p. 28). Pyramids can be transformed into a prism with a cutting plane at the vertex where the side edges of a pyramid meet. Cromwell (1997, p.85) described prism and antiprism as follows: a prism contains two n-sided polygons separated by a ring of n squares whereas antiprism includes two n-sided regular polygons but separated by a ring of 2n (Figure 4.1).



hexagon prism

$$n=6$$

$$n_{\text{side}} = 6$$



hexagon antiprism

$$n=6$$

$$n_{\text{side}} = 12$$

Figure 4.1: Hexagon prism and hexagon antiprism.

Duality principle has its roots in projective geometry in which points and lines can be interchanged. It implies that geometric quantities can be derived from each other by transformation of one becoming the other. Polyhedra possesses the duality principle as well. According to the duality statement, for every polyhedron, there exists another polyhedron in which faces and polyhedron vertices occupy complementary locations (URL-8). Following this, the dual polyhedron can be obtained by connecting the midpoints of the sides around each vertex and constructing the corresponding tangential polygon (Wenninger, 1983). Figure 4.2 shows some examples of dual polyhedrons and how their face and vertex numbers interchange.

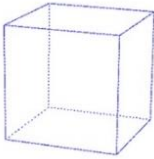
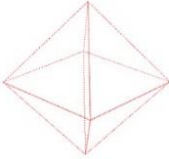
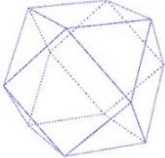
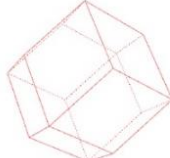
Polyhedron	Dual Polyhedron
 <p>f: 6 v: 8 e: 12</p> <p>cube</p>	 <p>f: 8 v: 6 e: 12</p> <p>octahedron</p>
 <p>f: 14 v: 12 e: 24</p> <p>cuboctahedron</p>	 <p>f: 12 v: 14 e: 24</p> <p>rhombic dodecahedron</p>

Figure 4.2: The duality example.

Polyhedral surfaces are discrete surfaces that designers make use of when they realize their free-form surfaces (Pottmann, 2007, p.103). It is based on sub-dividing the continuous surface by flat polygonal shapes. Therefore, with the thickness of a surface, polyhedral surfaces can be thought of as a concatenation of many polyhedrons. Mesh faces also inherently show this characteristic thus designers usually adopt mesh geometry to rationalise their form to be fabricated. A triangulated surface is the most popular polyhedral surface example to approximate a shape to a smooth shape.

Buckminster Fuller delved into polyhedrons for his geodesic dome which covers the largest area with the least material possible. After his geodesic dome invention, Fuller gained the term “geodesic polyhedron” to the literature. A geodesic polyhedron is the triangulation of faces of the polyhedron, and consequently, the creation of new vertices on polygonal faces to approximate a sphere. Fuller analysed the polyhedra in terms of their space-filling quality with spheres in his book “Synergetics: Explorations in the Geometry of Thinking” (1975). His aim was to distinguish the polyhedral forms which have the most volume with the least surface which he evaluated as a structural effort. The volume calculation he used was based on how many tetrahedra (1) and half octahedrons (2) the polyhedron was made of.

He famously named after cuboctahedron a “vector equilibrium” which is acknowledged as a perfectly balanced system and has many special attributes compared to other polyhedra as shown in Figure 4.3. First of all, its center-to-vertex length is identical to its edge length. Those 12 vectors radiating from vertex to centre point toward different directions with 60 degrees thus making it omnidirectional. 60

degrees angles make it a side projection view of a hexagon. The tetrahedral volume is 20 as it consists of 6 half-octahedron (2x6) and 8 tetrahedra (8x1). The dual of vector equilibrium is the rhombic dodecahedron.

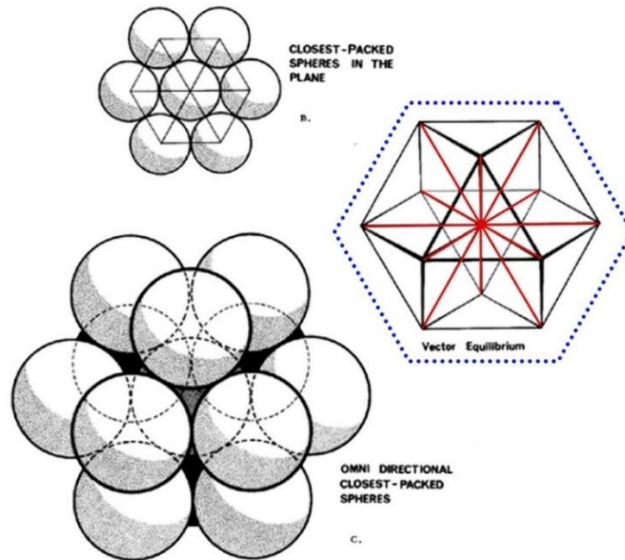


Figure 4.3: Vector equilibrium or cuboctahedron, red denotes the 12 radiating lines edited by the author (Fuller, 1975).

Corollary to his surface-to-volume ratio search, Fuller (1976) stated rhombic dodecahedron has the most tetrahedral volume which is 48 with the least surface of all space-filling geometrical forms. This makes rhombic dodecahedron the most economical all space subdividers of the universe. Furthermore, the rhombic dodecahedron shows spheric characteristics as the centres of its 12 diamond faces are symmetrically tangent at 12 interrayed points lying on the surface of any complete sphere (Figure 4.4).

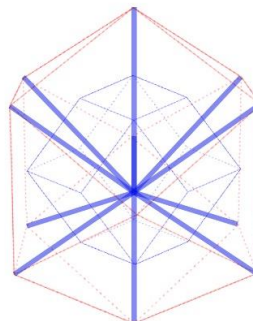


Figure 4.4: 12 interrayed vectors of the rhombic dodecahedron.

Fuller not only investigated polyhedra as geometrical representations but also how they correspond to applied forces. For instance, vector equilibrium (cuboctahedron) turns into an octahedron under compression forces. He discovered that tetrahedron would turn itself inside out under external load which makes it the most resistant structure type. The octahedron and icosahedron show dimpling under the same load but do not collapse. The geodesic spheres demonstrate very local dimpling meaning that they have less resistance to concentrated loads but very high resistance to distributed loads (Figure 4.5).

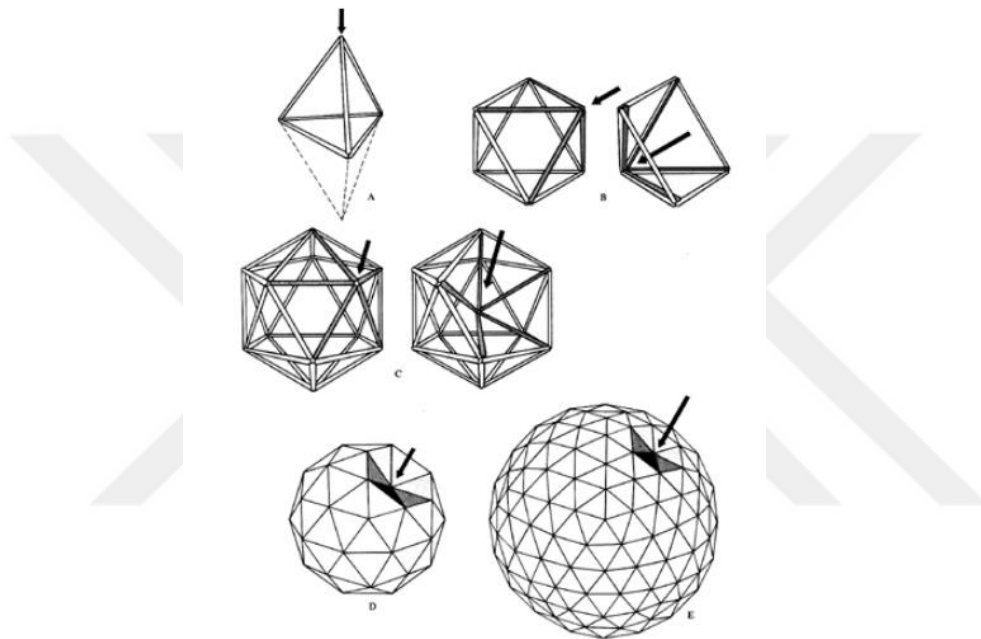


Figure 4.5: Polyhedra under concentrated loads, A: tetrahedron, B: octahedron, C: icosahedron, D and E: the geodesic spheres (Fuller, 1975).

4.1.2 Non-uniform rational B-splines (NURBS)

NURBS enables the designer to construct a wide variety of geometric forms including regular polyhedral forms, conic sections, and highly sculpted free forms. The reason NURBS have prevailed CAAD industry is that they are intuitive mathematical representations of a curve which is easy to edit in the design process. Moreover, NURBS provides an efficient data representation of geometric forms using a minimum amount of data (Kolorevic, 2009). NURBS are the abbreviation of non-uniform rational B-splines which implies that they can be derived from B-splines (Figure 4.6). NURBS curve in dimension d is essentially the central projection of the B-spline curve

in dimension $d+1$ (Pottmann, 2007). Designers did not confine themselves to B-splines because they were not able to construct conic sections except parabolas with B-splines.

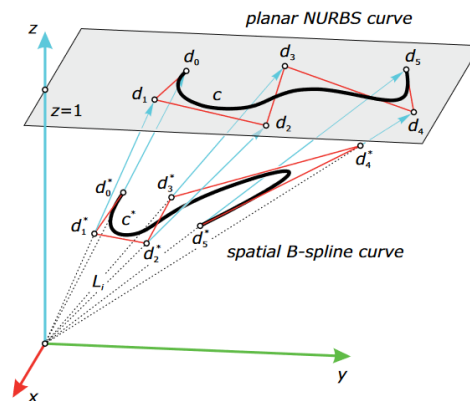


Figure 4.6: NURBS curve derivation from B-spline curve by the projection method (Pottmann, 2007).

The degree of the NURBS curve defines the type of curve or curviness of the line. The degree (d) also states the number of control points ($d+1$) which accounts for at least one more than the degree number (Figure 4.7). The algorithmic modelling environment as Rhino allows users to attain more control points to provide a more intuitive interface. Lines and polylines are degree-1, circles and ellipses are degree-2, and free-form curves are degree-3 or 5. NURBS differentiate from other curve types with their control points and weight parameters. The weight parameter directly relates to control points and how close they are placed to the curve itself. Following this, the increase in weights pulls the curve towards that control point, and the decrease moves the curve away from the control point.

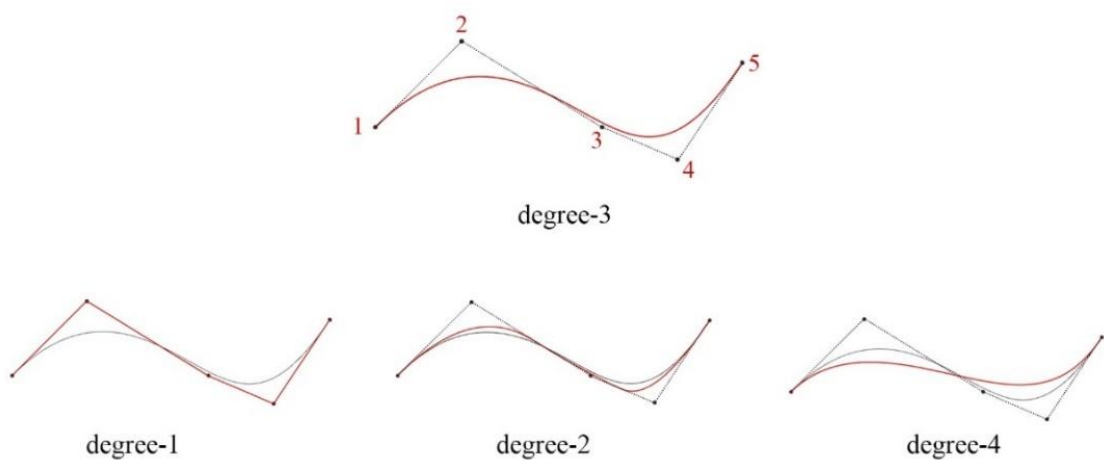


Figure 4.7: Curve variations derived from the same control points but having different degrees.

Evaluation is a method to assign a point on the NURBS curve with a numeric parameter (Issa, 2019). The parameter is the number lying in that curve domain. A curve domain denotes an interval between the minimum value where the curve starts and the maximum value where the curve ends (Figure 4.8). Changing the curve domain from arbitrary numbers to selected numbers such as 0 to 1 is called reparameterization. It should be noted that adjusting the curve domain does not change the shape of the curve in 3D space. Evaluation of the curve yields a designer more controllable design space by providing precise point construction on a curve to manipulate the form or create a new form using that point as a reference.

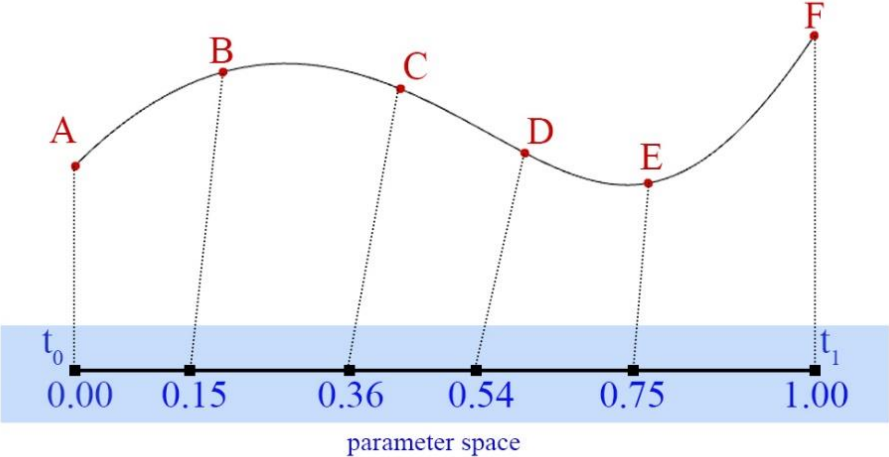


Figure 4.8: Evaluation of a curve.

Two NURBS curves, let us call them m and n , comprise a net of curves with their congruent curves m_i, n_i along each other. These translated curves (m_i, n_i) create a NURBS surface lying in two directions which are the surface parameters u and v (Figure 4.9). Correspondingly, NURBS surfaces can be controlled by a series of control points and the degrees in each direction. Therefore, NURBS surfaces store sufficient data to adjust the surface to the desired shape. For example, NURBS surfaces store x, y, z direction and normal vectors of points lying on the surface as shown in Figure 4.9. 3D NURBS surfaces have also 2D parameter space to evaluate the surface. Evaluating the parameters at equal intervals in 2D parameter space does not reflect at equal intervals in 3D space (Issa, 2019).

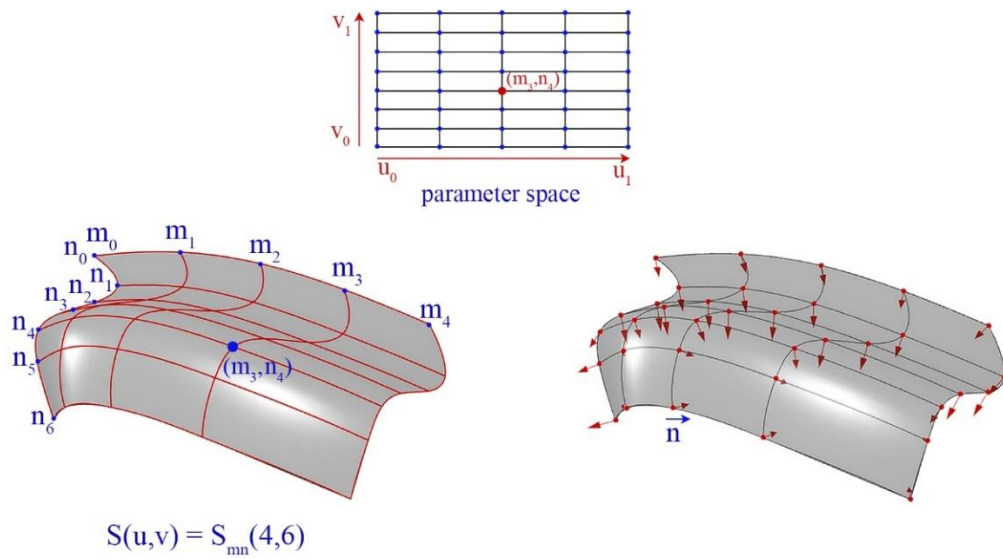


Figure 4.9: NURBS surface evaluation and normal vectors at parameters.

NURBS-based structural design has been a hot topic as designers seek efficient ways of constructing free-forms. Miki et al. (2019) introduced force diagrams represented by NURBS surfaces to manipulate shell forms while maintaining equilibrium. Meng et al. (2023) developed a direct approach to optimize free-form shells with different thicknesses. They benefit from 2D parameter space of NURBS surfaces to manipulate topological pattern of the 3D NURBS surface since it is way easier and more intuitive (Figure 4.10).

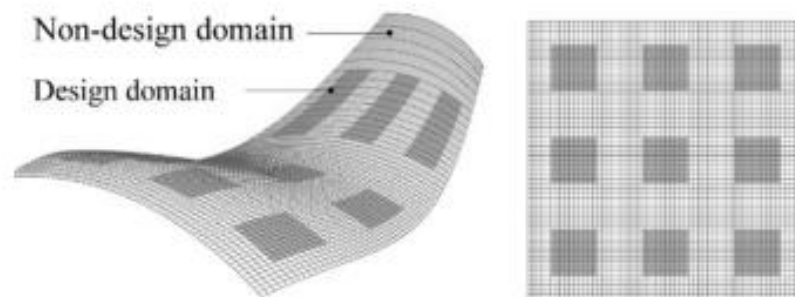


Figure 4.10: A 3D NURBS surface and its 2D parameter space for manipulating topological geometric patterns (Meng et al., 2023).

4.2 Form-Finding in Architectural and Structural Design

The expression “form follows force” indicates a process in which form is intrinsically dependent on forces rather than predetermined geometric parameters. In order to obtain a form in equilibrium, a form-finding process is a necessary operation for design

requirements. Form-finding is an interplay between structural design and architectural design as they both impose different requirements. In this sense, form-finding process can be seen as a medium that sustains an optimal form through felicitous combinations of forces, loads, and design requirements. Form-finding can also be seen as the exploration of geometry as it presents the transition from the starting geometry to the final geometry in equilibrium. The transition between initial and final form gives information about how specific shapes, materials or size of shapes/members matter for the optimal shape. Therefore, form-finding process is controlled explicitly by parameters which define the form and respond to the constraints.

The output of a form-finding process must resist the dead load which is its self-weight. The additional loadings can be included to increase its strength and, consequently safety conditions. Furthermore, the parameters to control the form-finding process are listed as follows: boundary conditions, supports, external loads, and the topology of the model, internal forces, and their relationship to the geometry (Adriaenssens et al., 2014, p.2). According to Killian (2007), form-finding can be extended as “steering of the form” which enables design discoveries that would neither be apparent in the optimized solution nor the original design intent. Thus, form-finding is a useful and fruitful process from which both architects and engineers exploit.

4.2.1 Physical form-finding processes

Even though today a form-finding process is realised in digital environments with advanced computational design and simulation tools, the form-finding method has its roots in physical experiments. The English engineer and scientist Robert Hooke (1635-1703) invented a law for an ideal form of arch which is known as Hooke’s catenary curve (Hooke, 1676). Hooke’s law presents an ideal arch form that would act in pure compression by obtaining the form of an inverted hanging chain which is in pure tension. This simple idea has set the ground for many shell structures in the past and still inspires many to come through advanced form-finding techniques. Antoni Gaudi (1852-1926) used the idea of a catenary curve and delivered a seminal work in form-finding studies with his physical model for Colònia Güell Church (Figure 4.9). Gaudi’s explorative structural form became an architectural form that was not arbitrary but was developed through a process of shaping (Graefe, 2020).

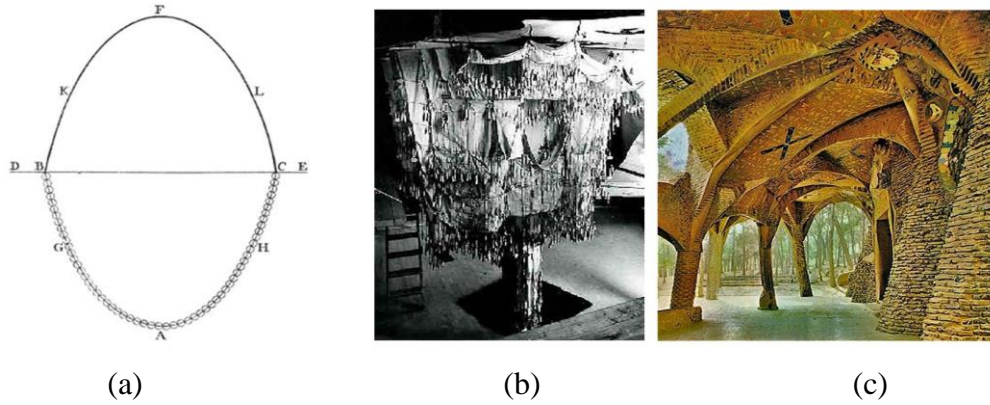


Figure 4.11: (a) Hooke's hanging chain depicted by Poleni (1748), (b) Gaudi's physical model consisted of catenary curves, (c) Colònia Güell Church columns (URL-9).

In the 1950s- 1960s, architects and engineers witnessed ground-breaking structural forms that were efficient and elegant at the same time. These new emerging forms were the result of form-finding processes which would be the method of exploring new structures in the following decades. For example, the German Pavilion (1967) in Montreal and the Olympic Stadium (1972) in Munich designed by Otto aroused interest among architects and engineers (Figure 4.12). It brought new insights into how form can be explored with pre-stressed cable nets and adapted to any shape on such a large scale while being light and floating.

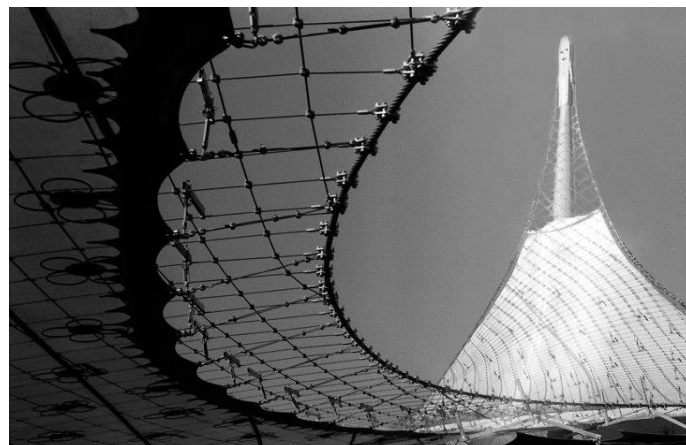


Figure 4.12: The German Pavilion in Montreal, 1967 (URL-10).

Frei Otto (1925-2015), Heinz Isler (1926-2009), Sergio Musmeci (1926-1981), and Buckminster Fuller (1895-1983) were the prominent figures that changed the way of traditional building methods. What is common in their form-finding processes is that they all were inspired by nature with different attitudes. According to Otto, the form is not primarily dependent on the designer but on the adoption processes just like in nature, and can be expressed by a combination of compressive, tensile, and bending

forces (Otto, 1971). Otto was famous for his experiments on soap films (Otto, 1969). In this experiment, he observed the physical law of minimal surface which is under constant stress and optimal distribution of material as shown in Figure 4.13 (Burkhardt, 2020; Otto, 1988).

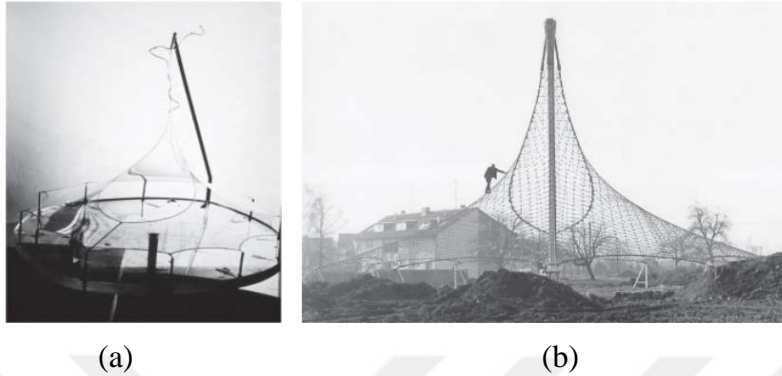


Figure 4.13: IL Pavilion at the University of Stuttgart (a) Soap-film model (b) The cable net construction (Burkhardt, 2020).

The Swiss engineer Heinz Isler is considered to be one of the greatest shell builders of 20th century. Isler saw nature as an inspiration for his natural shell shapes as optimal shapes follow natural processes (Isler, 1980). He conducted physical form-finding processes through expansion, inflation, and hanging of thin membranes. Wyss Garden Centre (1962) is one of his famous shell design examples (Figure 4.14b). Even though Otto and Isler both were inspired by nature and the evolutionary process that occurred in nature, Isler achieved a particular form thanks to his static intuition whereas Otto followed the process of evolution (Boller and D'Acunto, 2021). Therefore, their objectivity in form-finding processes differs when it comes to interfering with the final physical outcome either with static principles or relinquishing the static equilibrium to the evolutionary process completely.



Figure 4.14: (a) A physical experiment of hanging membrane (Isler, 1983), (b) Wyss Garden Centre designed by Isler, 1961 (URL-11).

Musmeci's form-finding approach is slightly different from Otto and Isler's as he was more concerned with analytical investigations on form-finding processes. He was interested in ever-changing physical and mechanical processes since he perceived nature as consisting of diverse entities that are interrelated (Boller and D'Acunto, 2021). In this sense, Musmeci sought the geometric form that is an optimal shape exposed to force flows by investigating natural processes with a mathematical perspective. Buckminster Fuller studied polyhedra forms to obtain structures that are in static equilibrium. Fuller's geometrical investigations were also based on his natural examinations. Besides his design prototypes, he also investigated how geometry directly affects the structural behaviour of the structure through mathematical calculations. Fuller (1975) points out triangle forms resist pressure more steadily compared to rectangular forms under the same applied forces. This geometric discovery paved the way for his geodesic dome. Geodesic domes are considered to be one of the strongest structures thanks to their side-by-side triangle geometric configuration as shown in Figure 4.15. With its advantageous volume-surface-area ratio of the sphere, Fuller proved the concept of a structure using less material and energy while covering extensive space (Laila et al., 2018).

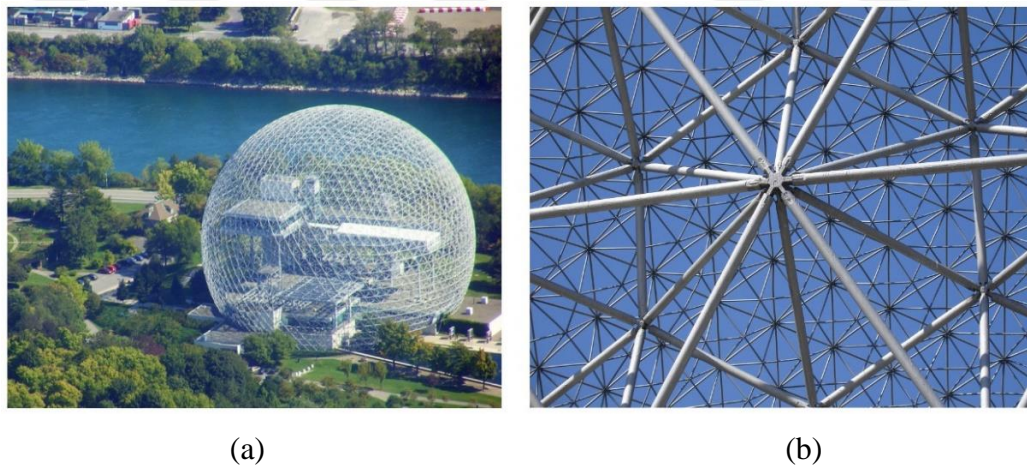


Figure 4.15: (a) Geodesic dome created from a sphere, (b) Node connection of the geodesic dome (URL-12).

4.2.2 Digital form-finding processes

As the computation power increased and led to the development of digital design tools, computer-assisted design (CAD) systems came into sight. The new digital design software has been a game-changer for architecture so computer-aided architectural design (CAAD) became a notion for designing in the late 20th century and up to the

present. Computational design approach extends the design space of architects from concept and form generation to a dynamic design space in which s/he consistently evaluates the outcome through feedback loops. The feedback loops reveal the interdependencies among form, structure and material. Therefore, architects have become capable of steering the form with its structural and material aspects which directly affect its structural efficiency.

The first digital form-finding method “Force Density Method” dates back to 1974 developed by Schek. Another commonly used digital form-finding approaches developed hitherto are Dynamic Relaxation Method (Barnes, 1999), “Particle Spring System” (Killian and Ochsendorf, 2005), “Thrust Network Analysis” (Block, 2009), “3-dimensional Graphics Statics using Polyhedral Forms” (Akbarzadeh et al., 2015), and “Combinatorial Equilibrium Modelling” (Ohlbrock and D’Acunto, 2020). Veenendaal and Block (2012) categorize the form-finding methods into three classes as follows: Stiffness matrix methods, Geometric stiffness methods, and Dynamic equilibrium methods. The stiffness matrix is among the oldest structural form finding utilizing elastic and geometric stiffness matrices. Geometric stiffness methods start with the force density method and are material-independent. Dynamic equilibrium methods find the static equilibrium solution for the structures which are in a dynamic state.

The particle spring system method is notable for providing a digital simulation of hanging chains (Figure 4.16), a well-accepted form-finding technique which was experimented with physically by Gaudi, Otto, and Isler. The static equilibrium objective is achieved by defining the topology of a particle spring network with loads on the particles, the masses of the particles, and the stiffness and lengths of the springs (Bhooshan et al., 2014). Therefore, when spring changes its location from the rest length, it implies that it is exposed to forces. Similarly, particles have a position, velocity, mass, and forces imposed on them. The system reaches a static equilibrium until springs and particles move to their equilibrium positions.

Killian (2007) put forward that through the manipulation of spring strength and/ or spring length, it is possible to direct the overall form within the limits of a given topology. By doing so, designers can diverge from finding the structurally most efficient structure to explore other structural morphologies for their design reasoning. Therefore, Killian’s bidirectional design exploration offers an intuitive investigation

of the form-finding process where designers are constantly aware of the relations between the geometric parameters of the form.

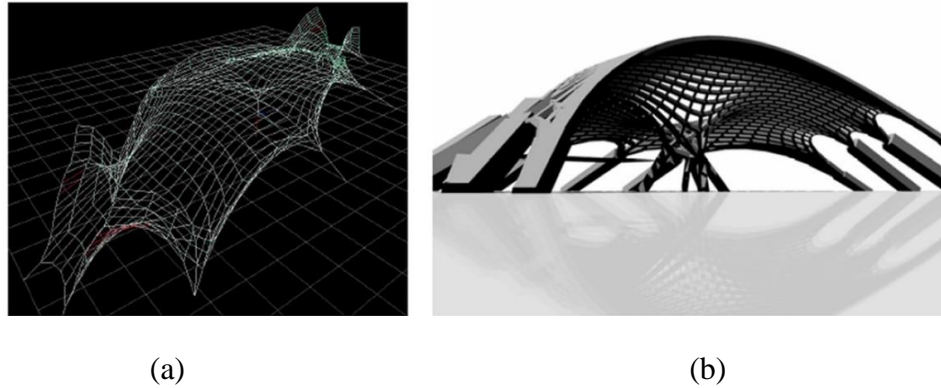


Figure 4.16: (a) digital simulation of hanging chain, (b) roof membrane design based on forces in members (Killian, 2007).

Douthe and Baverel (2009) used the dynamic relaxation method to transform the node of a traditional structure into a fan of an RF structure. They first set the initial configuration as a hexagonal grid and then defined the end positions of elements in a way they form an RF structure. The general principles of dynamic relaxation involve applying an oscillating process to the structure until the kinetic energy of beams resulting from inner stress dissipates. Only then, does the structure arrive at static equilibrium. Therefore, the movement of beams for RF transformation was modelled considering the rotational directions of fans, axial forces, bending forces, eccentricities, and stability to achieve an RF form in equilibrium (Figure 4.17).

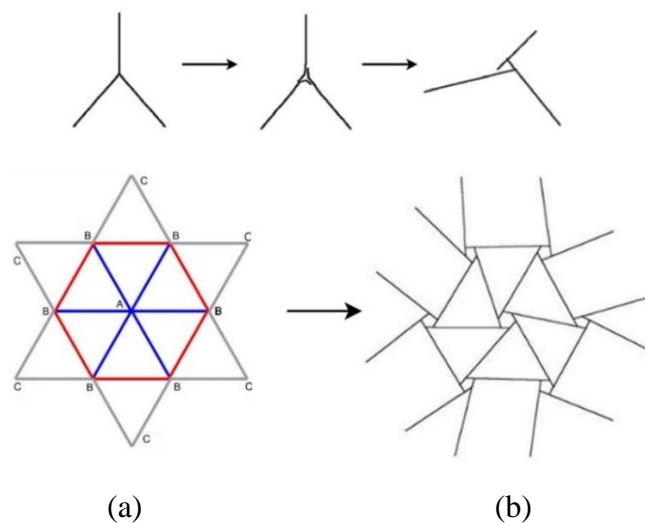


Figure 4.17: (a) The initial grid configuration, (b) The final RF configuration created by the dynamic relaxation method (Douthe and Baverel, 2009).

4.3 The Role of Material Behaviour and Digital Fabrication in Design Process

“It is a question of surrendering to the wood, then following where it leads by connecting operations to a materiality, instead of imposing a form upon matter: what one addresses is less a matter submitted to laws than a materiality possessing a nomos. One addresses less a form capable of imposing properties upon a matter than material traits of expression constituting affects.”

(Deleuze and Guattari, 1987, p.408)

Recent developments in computational design and simulation tools have extended form-finding processes in terms of practice and theory. Digital tools that allow assigning material attributes to the digital form link the geometric representation to the physical world. In this sense, material-based computational design offers a novel way to create structures by considering the material properties in the early design phase. Within this perspective, material is the main driver of the design which reacts to applied forces by changing its shape or resisting the forces in the desired shape. In both ways, material behaviour informs the designer about the efficient way of using material, avoiding excessive use. Material-based design can be evaluated as a form-finding process since material behaviour is not always predictable under different loadings and conditions, and so is the form made of it (Menges et al., 2012).

A Material-based Integrated Computational Design Model (Yazıcı, 2013) emphasises the role of material with performance and optimization parameters which ultimately increase the efficiency of the design process. ICD/ITKE Research Pavilion (2010) is a pioneering example to demonstrate how material behaviour rules drive the form. The idiosyncrasies of material affect the mechanical behaviour of the structure thus challenging the geometrical representation of the form. Oxman and Rosenberg (2012) attempted to develop a digital design tool that simulates the material behaviour of resin explored in physical experiments to promote the material integrated design process.

Dermoid is one of the early design studies that integrates material performance into the RF structure design process via computational design tools. In the Dermoid research project, the structural behaviour of every element resulting from material manipulation was scripted in design software to get real-time feedback (Burry, 2011). The individual elements were made out of plywood which shows flexibility to enable bending behaviour. The individual bent elements were tested under loads through physical experiments to provide feedback for the digital scripting process. The units

were created by bending plywood elements and connected reciprocally with zipper joints. The reciprocal frame structure was designed by joining bent plywood units which became 3D units after bending (Figure 4.18). The flexibility of plywood met the structural load and performance criteria of the structure. In this way, the material behaviour was coded as an active design parameter in the simulation tool which affects the structural strength of the structure.

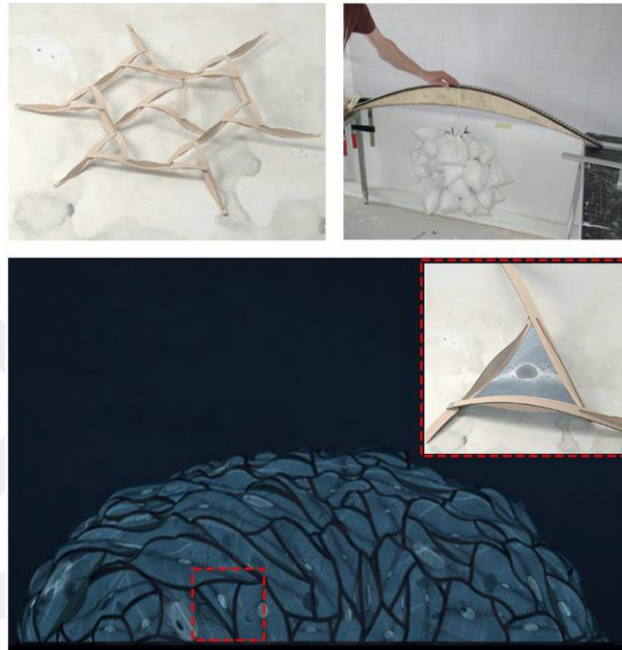


Figure 4.18: Dermoid project investigating material behaviour for the structural strength (Burry, 2011).

Another project that the reciprocal frame structure benefits from material behaviour is the ReciPlydome designed by Brancart et al. (2017). RF structures work in bending moment due to their connections along the span of an element. This results in an undesired structural property since the structure becomes weak under axial forces. Brancart et al. (2017) succeed to turn the undesired bending moment into a favourable structural property which gives stiffness to the units of reciprocal frame as shown in Figure 4.19. The spherical dome shape was used as a form to map reciprocal frame units. The results show that bending-active reciprocal frame structure made of double layer elastically curved units exhibit better loading behaviour compared to single layer reciprocal configuration.

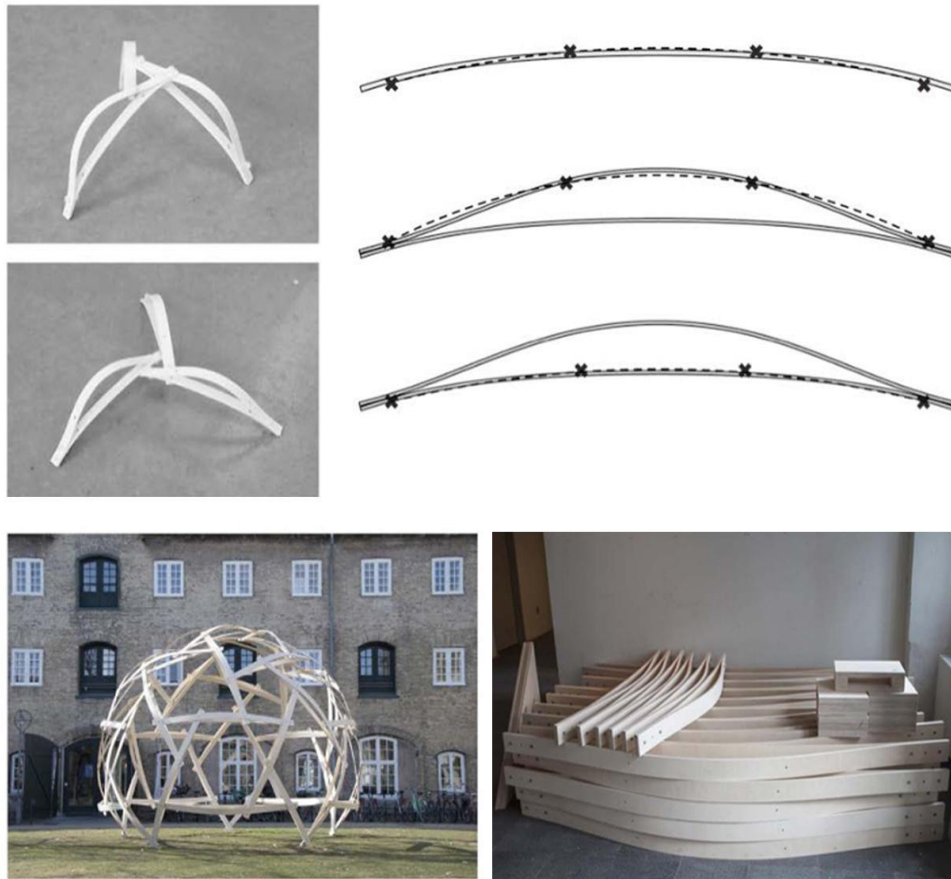


Figure 4.19: RecipiPly Dome made of pre-bent double-layer units (Brancart et al., 2017).

Digital fabrication methods currently innovate the design process by triggering new approaches to developing a better workflow between material and computational design tools. Advanced digital fabrication methods not only provide precision and rapidness for construction but also reduce significant amounts of waste. Consequently, carbon emissions decrease compared to traditional construction methods which makes it more preferable for the AEC industry. When we think of today's digital fabrication processes, robotic fabrication comes to the scene with its active system and know-how. Material-based design can be reinforced with the tool agency which can behave both as an enabler and inhibitor of ambiguity in the design process. Thus, one has to develop a communication with it regarding its affordances and constraints. The feedback loop between material behaviour, structural performance and force flows can encapsulate the fabrication constraints to enhance the holistic design approach.

Reciprocal frame structures are of particular interest in conjunction with digital fabrication since they reach optimal form depending on the internal force flows of many timber elements (Kohlhammer and Kotnik, 2011). Due to their simple

connections, reciprocal frame structures are a viable option when digital fabrication methods come forward in the research project. Mitterberger et al. (2022) introduced a cooperative design workflow between humans and robots to create reciprocal frame structure with rope joints. The study shows that mobile robots are able to follow a digital workflow from where humans left and continue to tie a knot to join the linear elements (Figure 4.20). Helm et al. (2016) adapted reciprocal frame structure to advance robot-based timber construction methods. In this research, they designed a material-driven digital design workflow for robotic assembly to provide seamless fabrication of the structure. They also stressed on the necessity of use of digital design and fabrication for the construction components with mutual dependencies.



Figure 4.20: Assembling reciprocal frame structure through human-robot workflow (Mitterberger et al., 2022).

4.4 3-Dimensional Graphic Statics (3DGS)

Even though the structural solution of the form is considered an engineer's job where architects are responsible for the concept and form, advanced computational design tools have started to blur the line between architects and engineers. Today, architects have digital design tools at their disposal by which they can inform the design process with data flow to ensure their design is also structurally efficient. Graphic statics is one of the structural form finding methods derived from geometric principles. It does not consider material during the form-finding process, however, it ensures that the emergent structure does not rely on the material strength but mainly on geometric

strength. Maximising structural strength through geometry can prioritise the efficient use of material. Therefore, without increasing the weight of the structure to resist bending forces, structural forms require rigorous design of geometry.

Graphic statics is a method that finds structural equilibrium through form and force diagrams. The theory dates back to the 19th century originally developed by Maxwell (1864). The form and force diagrams are dual diagrams which means that they are geometrically interrelated (Figure 4.21). It indicates that every change in one diagram affects the other diagram correspondingly. Moreover, the equilibrium of a node is represented by a closed polygon (Cremona [20]). 2D graphic statics method has been extended to 3-dimensional graphic statics method to explore 3-dimensional forms without converting them into 2D diagrams (Akbarzadeh et al.).

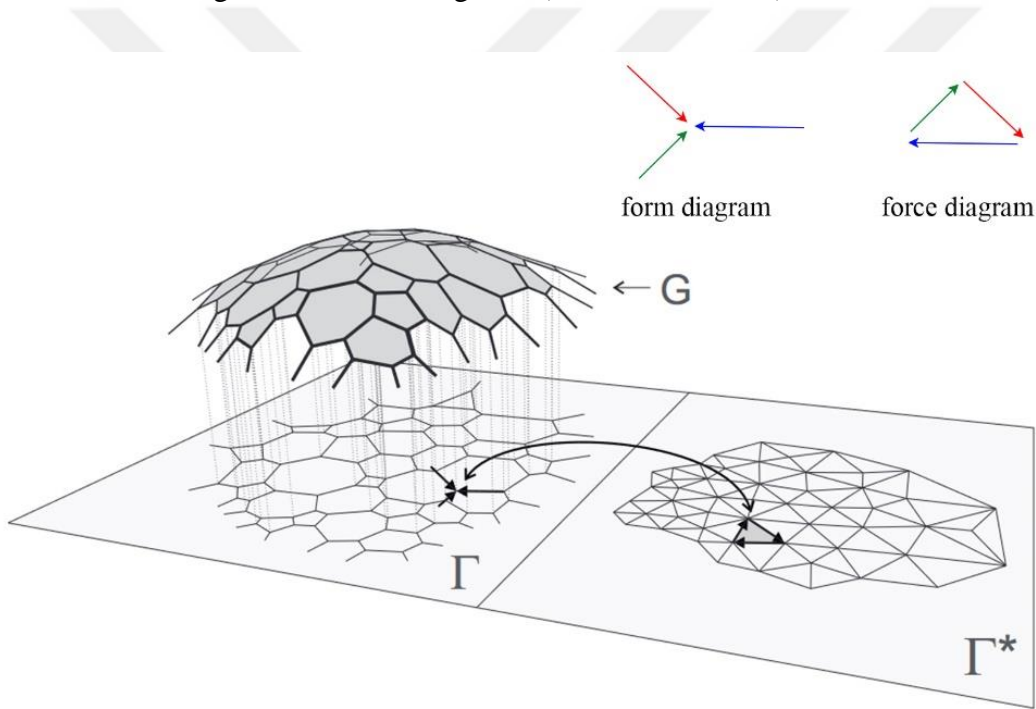


Figure 4.21: The dual diagrams of compression structure with the form diagram on the left, and the force diagram on the right (Block, 2009).

In 3DGS, polygons correspond to polyhedrons indicating that every node in equilibrium is represented by a closed polyhedron in the force diagram. The interactive design environment that 3DGS provides enables designers to create compression or tension-only structures from polyhedral force diagrams. What distinguishes 3DGS from traditional form-finding methods that also yield static equilibrium is that it allows designers to start designing with force diagrams and explore the structural forms intuitively by adjusting duality diagrams. Following the duality principle, each edge

and vertex of the form diagram corresponds to a face and cell of the force diagram respectively. If all faces are planar and all edges are perpendicular to their dual faces, the diagrams are reciprocal thus the force diagram represents the structural equilibrium (Akbarzadeh et al., 2015).

The area of the face is equivalent to the magnitude of the applied force which is perpendicular to it as shown in Figure 4.22. Therefore, for every node which is in equilibrium, there exist a polyhedron of which faces is perpendicular to one of the member of that node. Aggregation of different force polyhedra or the subdivision of polyhedra creates structural forms which is in equilibrium and work in compression or tension. 3DGS method demonstrates its competency in exploring new types of structural topologies as shown in Figure 4.23 (Nejur and Akbarzadeh , 2021; Lee et al., 2018). Furthermore, the fact that it is driven by purely geometric principles makes 3DGS convenient to explore the relation between geometry and other design parameters.

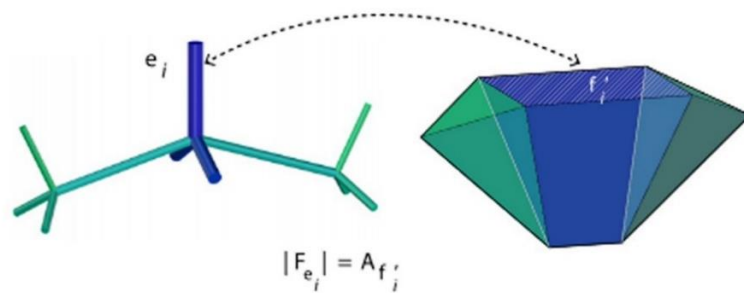


Figure 4.22: The element and its dual force polyhedron (Akbarzadeh et al., 2015).

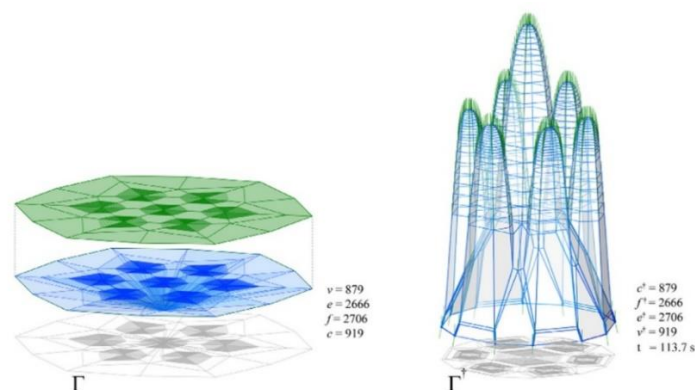


Figure 4.23: Force polyhedral on the left and the corresponding form diagram on the right (Nejur and Akbarzadeh , 2021).



5. METHODOLOGY

The research methodology comprises three main steps as follows: 1) Geometric analysis, 2) Physical experiments, and 3) Digital form-finding. The three processes are concatenated in a way one's output becomes an input for the other process (Figure 5.1). These three steps are developed to focus on different but interrelated aspects of RF structures which are geometry, material and structural behaviour respectively.

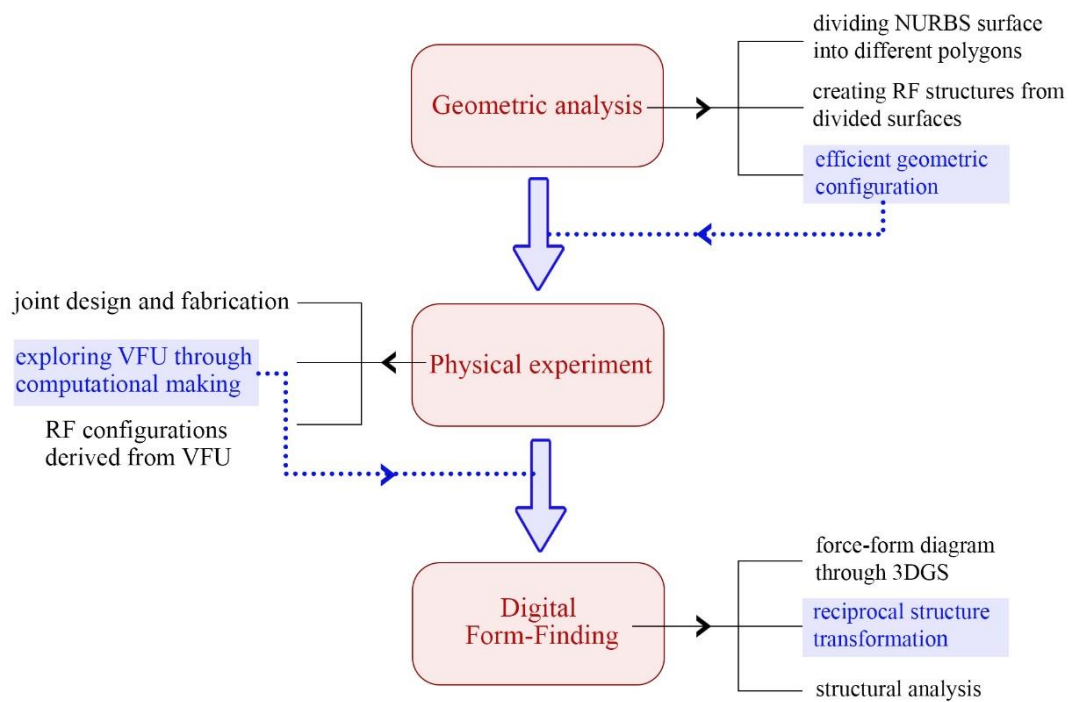


Figure 5.1: Inputs, outputs and process of the research.

Geometric analysis is realised to reveal efficient geometric RF configuration in terms of forming the same surface with smaller number of elements. The duality principle of polyhedral RF structure is used to benefit from structural reciprocity instead of imposing the polygons onto the NURBS surface. The outcome of the geometric analysis is a rhombus/ diamond geometric configuration that is further investigated through physical experiments. Digitally fabricated joints and wooden sticks are used in the physical experiments. Physical modelling process includes exploring the volumetric frame unit (VFU) which exhibits structural stiffness compared to flat RF

units and its rule-based design configurations. The digital form-finding process has three sub-steps: a) structural form-finding through 3DGS, b) RF transformation of the output of 3DGS, and c) structural analysis of RF. The form of VFU provides an input for the structural form-finding process via 3DGS which creates structural forms that work under compression. The outcome is transformed into an RF structure following analytical geometrical operations. Finally, structural analysis is undertaken to evaluate the final RF structure.

5.1 Geometric Analysis

Geometric analysis is undertaken by examining two different types of geometry which are polyhedral and NURBS surfaces. Polyhedral geometry is used for the duality principle of RF structures. NURBS surfaces are utilized to evaluate the ability of geometric shapes to form a structure.

5.1.1 Reciprocal frame structures based on polyhedra

RF structures created from polyhedra show the duality principle as shown in Figure 5.2 (Baverel and Nooshin, 2007). According to the duality principle, a polyhedral RF structure can transform into its duality polyhedral RF by changing its rotation angle. As the rotation angle changes, the engagement window expands or contracts. For instance, when the cube is transformed into an RF structure, the following changes occur: the vertex of cube become the engagement window of the RF structure. As the angle increases, the engagement windows become RF polygons and the engagement windows occur at the faces of cube (Figure 5.3). When the cube is given as an initial shape for “Reciprocal” component of “Kangaroo” plug-in in the Grasshopper environment, an RF octahedron can be obtained with the angle adjustments. The vertex of the polyhedron becomes an engagement window of an RF polyhedron as shown in Table 5.1. The duality principle is utilized for the geometric analysis of RF structures to create structural reciprocity instead of representing it as in the case of mapping. Since the polyhedral forms can turn into another RF polyhedron, the surface is conceived of as the combination of many polyhedrons as its thickness corresponds to the height of polyhedrons.

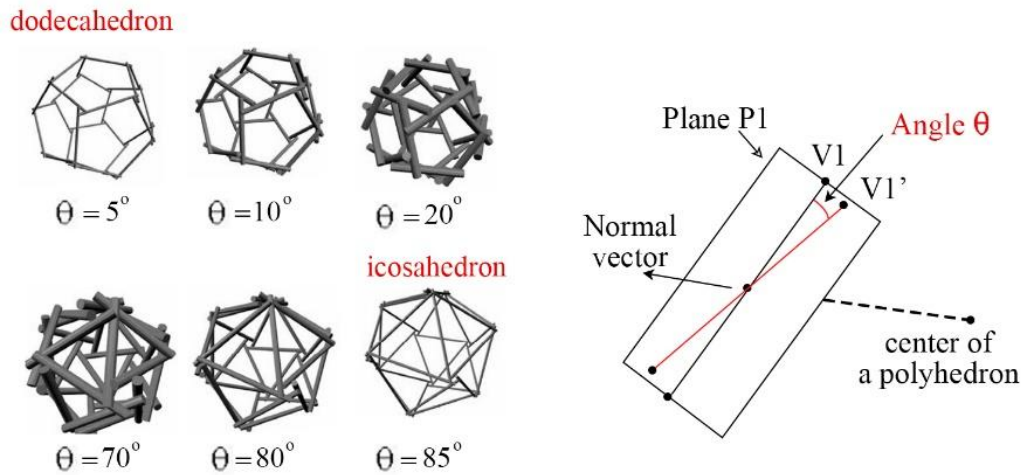


Figure 5.2: The duality between dodecahedron and icosahedron RF configurations (readapted from Baverel and Nooshin, 2007).

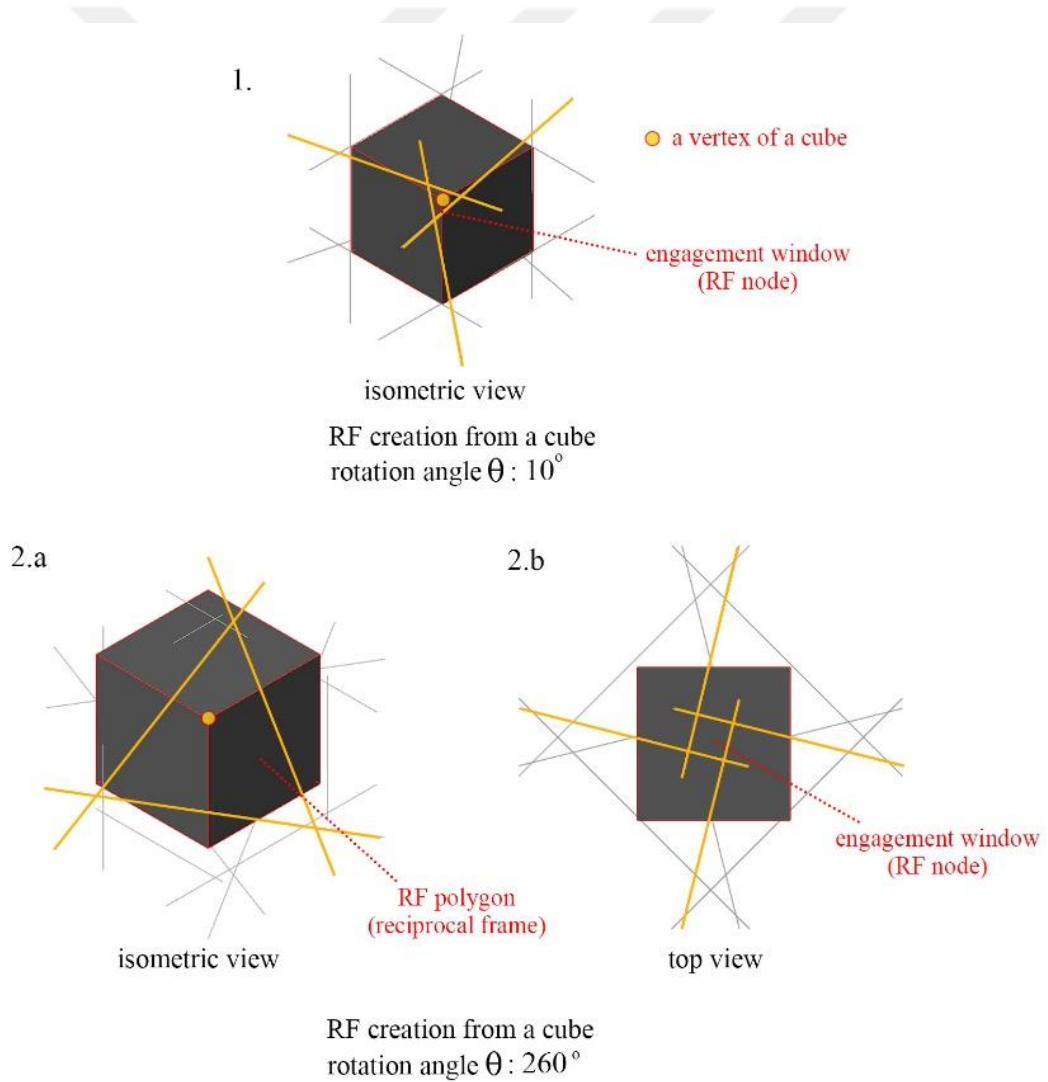
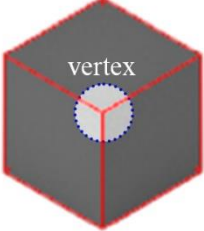
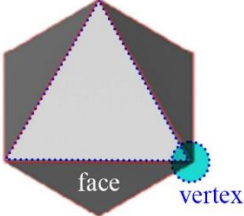
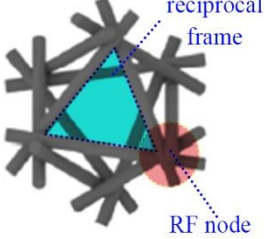
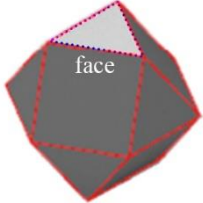
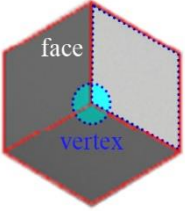
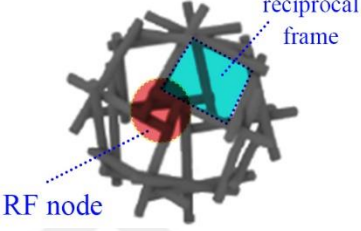


Figure 5.3: The RF transformation of a cube following the duality principle (Karahana and Yazıcı, 2024).

Table 5.1: Duality principle of RF structures based on polyhedral, L: total length of an element, Θ : rotation angle (Karahan and Yazıcı, 2024).

Polyhedron	Dual Polyhedron	Reciprocal Structure
 <p>cube</p>	 <p>octahedron</p>	 <p>L: 50, Θ: 260, radius: 1.65 cm</p>
 <p>octahedron</p>	 <p>rhombic dodecahedron</p>	 <p>L: 50, Θ: 70, radius: 2 cm</p>

5.1.2 Creating RF structures from NURBS surfaces

The surface with divisions yields the polyhedral volumes which is necessary for the duality principle. Therefore, the design algorithm is developed in the Rhino-Grasshopper algorithmic environment as follows: 1) Creating NURBS surfaces parametrically to adjust them in the U-V directions, 2) Dividing the surface into different polygons with the same U-V numbers, 3) Using Kangaroo Physics to determine the final form of RF configurations.

A NURBS surface is generated to analyse the geometric relations of RF patterns, and whether there is a correlation between the surface and the polygon parameters. A rectangular base which has 400 cm width in the X direction and 300 cm length in the Y direction is created to generate a parametric surface in the Rhino-Grasshopper environment.

Subsequently, the base is divided into five segments in the U-V direction which means it consists of six-point branches (Figure 5.4). The second and fifth branches are

elevated 100 cm, and the third and fourth branches are elevated 220 cm in the Z direction to give a scale for the surface. The thickness is set as 2 cm through extrusion. Rhombus, hexagon, and quad polygons are used to divide the created surface with the same U-V count which is 6 in both directions (Table 5.2). Depending on the shape of the polygons and the surface, polygons divide the surface into different sizes. Division parts are planarized using the “NGon” component to correspond to the flat polygons. The divided and planarized parts are joined as one mesh. The outcome mesh surface is given to the “Reciprocal Structure” of the Kangaroo plug-in component to create an RF configuration utilizing the duality principle. The RF geometric configuration is optimized through line-to-line force optimization which means the interaction is created between linear elements to stay in their specific positions. The “Reciprocal Structure” component allows for changing the rotation angle of the elements, and the line-to-line force optimization provides adjustments for the length and thickness of the elements. The rotation angles and radius of linear elements are set manually to create RF configurations.

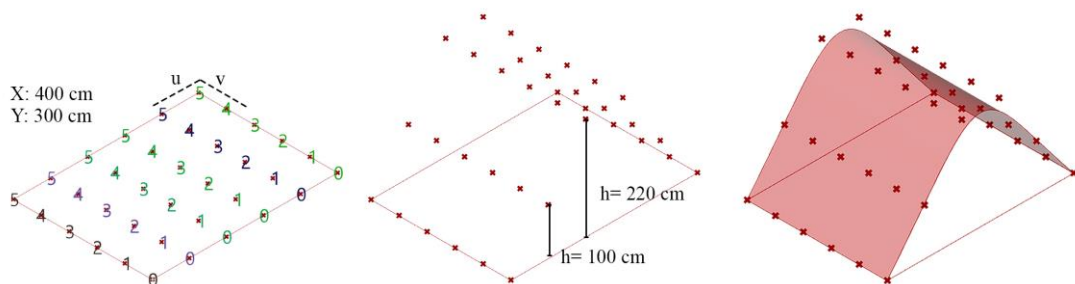


Figure 5.4: NURBS surface generation steps (Karahan and Yazıcı, 2024).

The undulating NURBS surface is created to test the developed algorithm whether it is viable for different free-form surfaces. The second and third items of the first and sixth branches are translated (+/-) 50 cm in the X direction, fourth and fifth items are translated (+/-) 100 in the X direction to create another curve for the surface. The points of the second- and fifth-point branches are moved 140 cm, and the points of the third and fourth branches are moved 100 cm in the Z direction to create undulation on the NURBS surface in Figure 5.5.

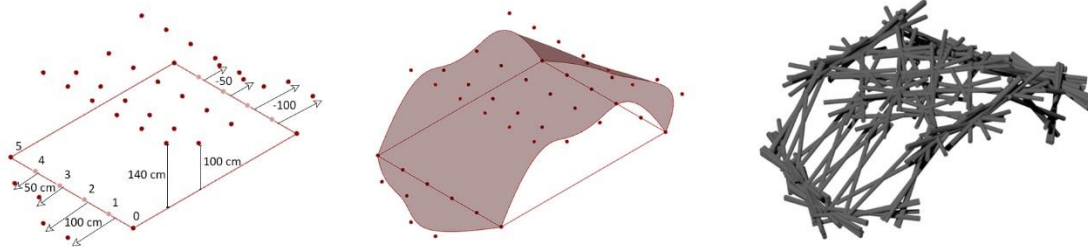


Figure 5.5: Undulated NURBS surface generation steps (Karahana and Yazıcı, 2024).

Table 5.2: Polygon divisions and their corresponding RF configurations, L: total length of the element, Θ : rotation angle (Karahana and Yazıcı, 2024).

Division type U/V count	Surface	Reciprocal Structure	Element Properties
None			Angle Θ : 210 degree L: 200 cm Radius: 4.5 cm Number: 6748
Quad U6, V6			Angle Θ : 135 degree L: 200 cm Radius: 4.5 cm Number: 432
Rhombus U6, v6			Angle Θ : 190 degree L: 200 cm Radius: 4.5 cm Number: 216
Hexagon U6, V6			Angle Θ : 60 degree L: 200 cm Radius: 4.5 cm Number: 1096

5.2 Physical Experiments

The physical experiment interrogates the material role in the interdependent design parameters. It should be noted that structural reciprocity does not work as modular structures even though it consists of repetitive units. The main difference between modular structures and RF structures is that the former allows for joining the modules together whereas in the latter, elements are added to the structure one by one due to their special placements. Every inserted element creates a reaction that influences the other, as a result overall structure can change. The outcome of the physical experiment provides an input for the digital form-finding process.

5.2.1 Volumetric frame unit (VFU) exploration

The rigid joints are designed and digitally fabricated using PLA material. The joints are designed with two cylinders connecting each other at a 60-degree angle at their midpoints (Figure 5.6a). The aim of setting a 60-degree angle is to create a rhombus whose dihedral angles are 120 and 60 degrees. The cylinders are 24 mm in height and 5.8 mm in diameter. 50 cm and 100 cm sticks with 5 mm diameter are used for the linear elements. The joints fix the eccentricities to a maximum of 5.8 mm while allowing the slight translation of engagement length.

Considering structural reciprocity, each element must follow a rule of supporting and getting supported in order when they unite. Rule-1 and Rule-2 are created to meet this requirement as shown in Figure 5.7. The triangular fans are created by following Rule 1 and Rule 2 in order (Figure 5.6b). Subsequently, a hexagon is created with the consecutive rules of Rule 1-2 with 12 sticks as shown in Figure 5.6c. Flat RF configurations are vulnerable to bending as one unit can move in one direction, and the other moves to another, creating a bending moment. The double-layer RF configurations proved their ability to improve the structural behaviour of RF structures as detailed in the 2.3 Morphology and Geometry section. Therefore, the possible double-layer or volumetric RF configurations were evaluated.

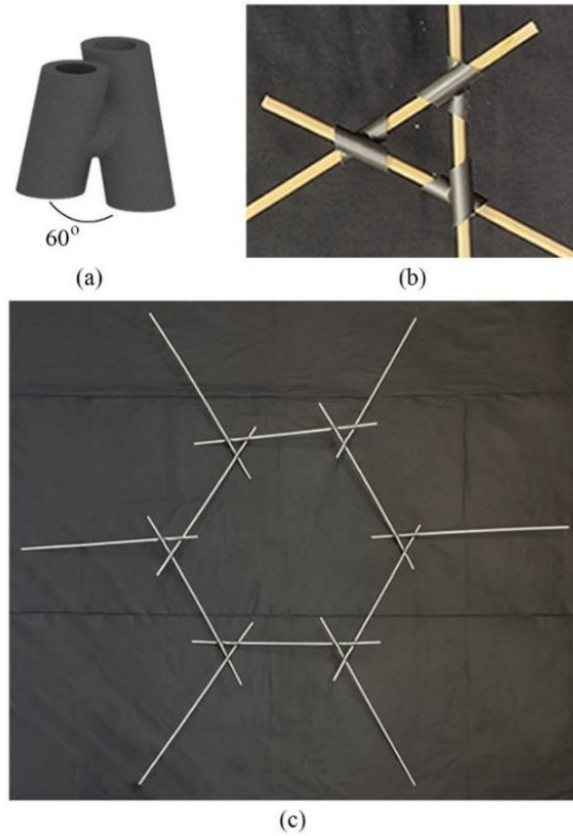
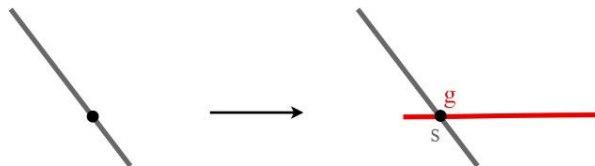


Figure 5.6: (a) Joint design, (b) An equilateral triangle fan, (c) An RF hexagon.

Rule 1:



Rule 2:

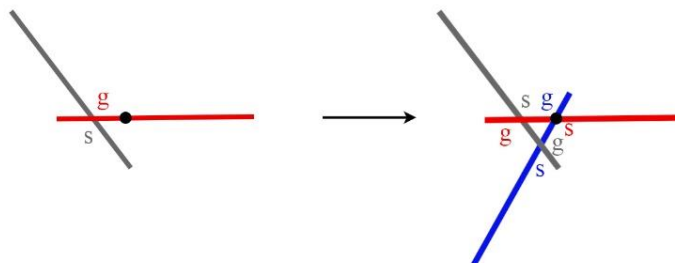


Figure 5.7: Generative rules of an RF fan, s: support, g: get supported.

The output of geometric analysis demonstrated that the rhombus polygons allow for creating RF configurations with fewer elements. The rhombus polygons are created out of hexagons by following the material behaviour. When the hexagon unit is

examined, it can be seen that the different support positions and internal reactions of elements give different axes for linear elements (Figure 5.8a). Therefore, the linear elements tend to follow upward and downward directions inherently. The 3 sticks pointing upward are pulled in and a new fan is created on top (Figure 5.8b). The resulting volumetric frame unit (VFU) has 3 rhombus faces, 7 triangle fans, and 3 sticks pointing outwards for possible connections (Figure 5.9). VFU has the structural stiffness compared to flat hexagon units.

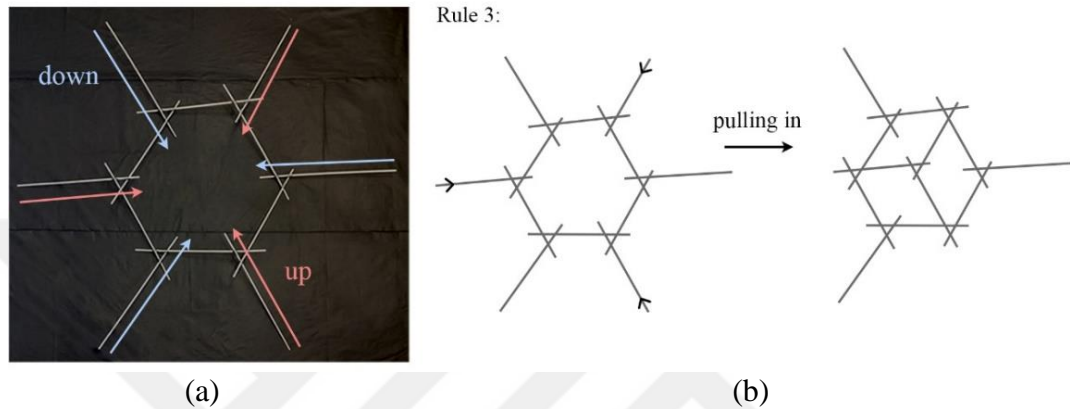


Figure 5.8: (a) Elements pointing up and down, (b) Creating a VFU.



Figure 5.9: (a) Top view of VFU, (b) Perspective view of VFU.

5.2.2 Physical Modelling of RF configurations

Flexible rubber joints were utilized with 24 cm wooden sticks. The triangular fans were created by following Rules 1-2. Fans form a hexagon by applying the same rules in order, and another hexagon is created to build up the structure (Figure 5.10). An RF configuration is created by adding linear elements to hexagons one after another following Rules 1-2 respectively (Figure 5.11). The first RF configuration is created with flat hexagon units with the same rules as shown in Figure 5.12. After that, VFU

is combined with other units by adding linear elements to the 3 elements at the perimeter with Rule 1-2. In these configurations, the mid fan of VFU was placed downward or upward due to the reactions. Furthermore, another hexagon is created around the middle VFU to reinforce the connection and also make up a possible connection as shown in Figure 5.13b.

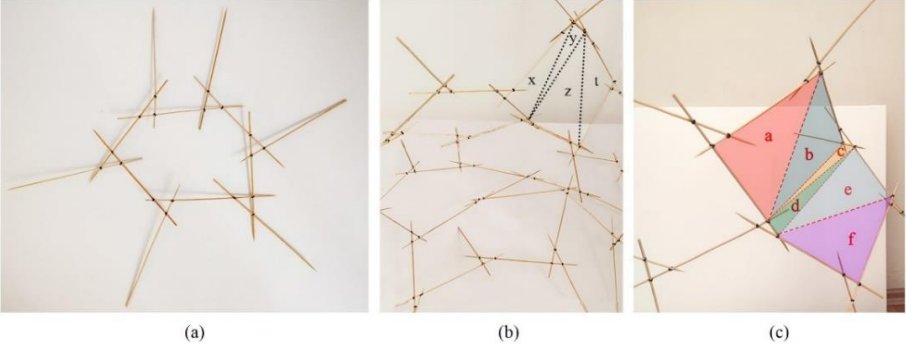


Figure 5.10: First physical experiment, (a) a hexagon unit (b) the physical model, (c) discretization of a hexagon RF unit.

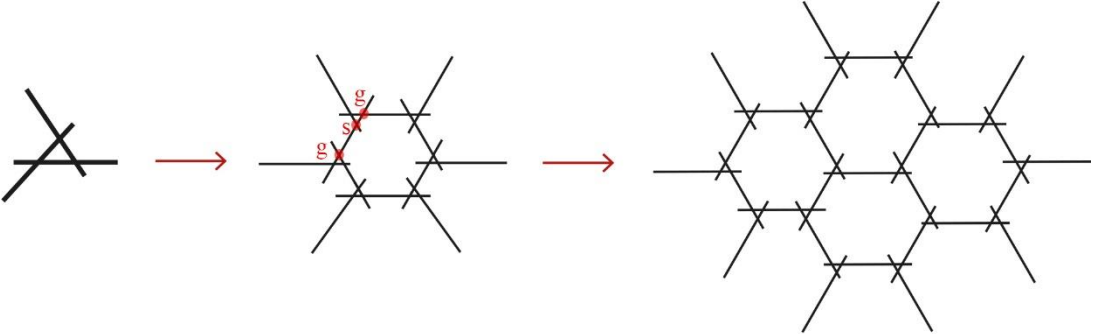


Figure 5.11: Sequences of creating an RF structure following the rules.

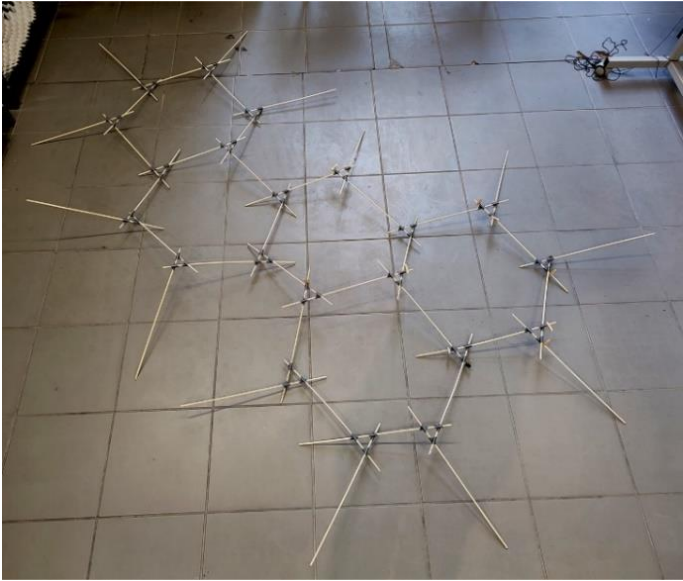


Figure 5.12: An RF configuration made of hexagon units.

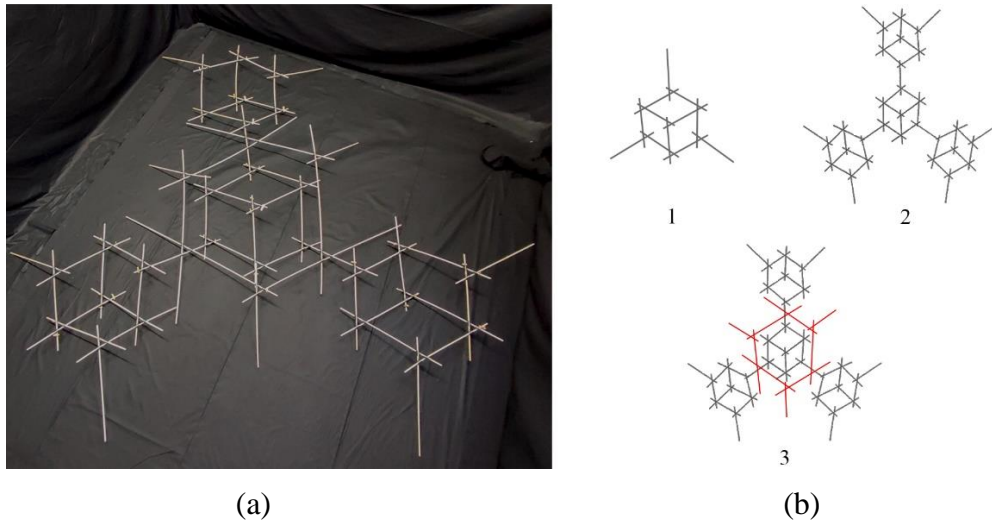


Figure 5.13: (a) An RF configuration, (b) sequences of an RF configuration.

The second RF configuration is created by hanging VFU units by rope on a vertical plane to get support (Figure 5.14). First, two sticks of VFU were hung to a vertical plane, the other stick was used to add another stick. Two more VFUs were hung to give a volume to the structure and other VFUs were added through the free sticks.

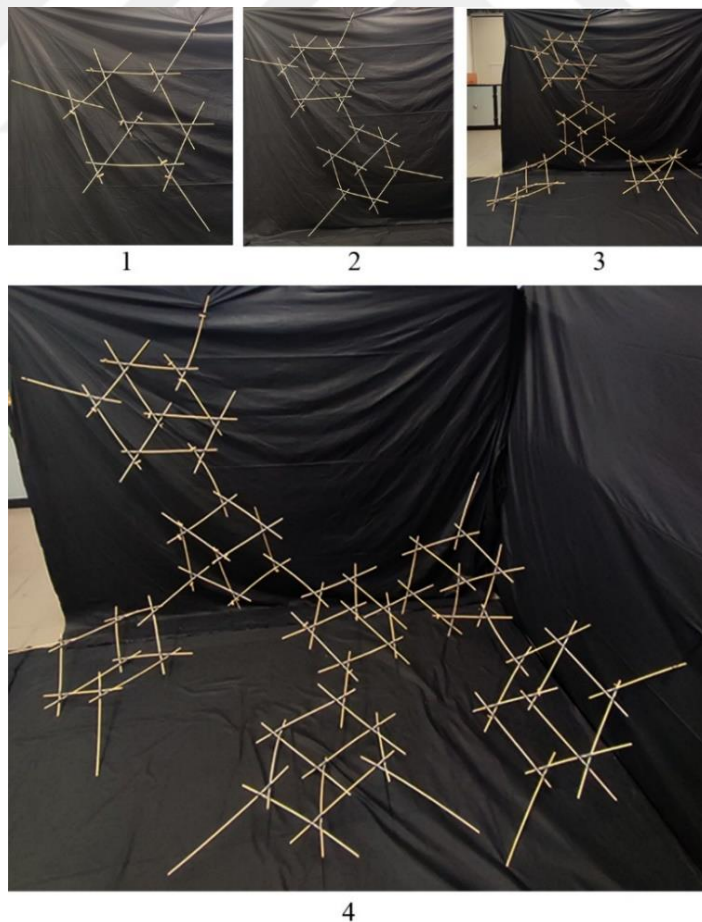


Figure 5.14: Sequences of the second RF configuration through hanging.

5.3 Digital Form-finding

VFU exhibits structural stiffness compared to flat RF units. However, it still has dominant bending forces due to RF configuration which creates circular force flows. The digital form-finding process investigates the volumetric frame unit (VFU) variations through 3DGS which resist compression forces and are also in static equilibrium with its nodes. 3DGS is used for the structural form-finding method in which the form is visually guided by polyhedrons representing the forces. However, 3DGS performs through polyhedra of which there are an infinite number. Therefore, the geometric form of VFU constrains the design space of 3DGS as it sets a goal of creating a volumetric form to gain structural stiffness.

VFU is provided as the form diagram of 3DGS. The dual force diagram is generated based on the VFU geometry. VFU geometry is abstracted in two phases by examining its geometry in two and three dimensions. First, the top view of VFU is abstracted as three rhombuses (Figure 5.15). Then, the perspective view of VFU is assessed in terms of the element directions in the Z-axis. By considering these geometric characteristics, VFU abstracted geometry corresponds to three faces of a rhombic dodecahedron with its rhombus faces and the way rhombus faces congregate in 3D space as shown in Figure 5.16.

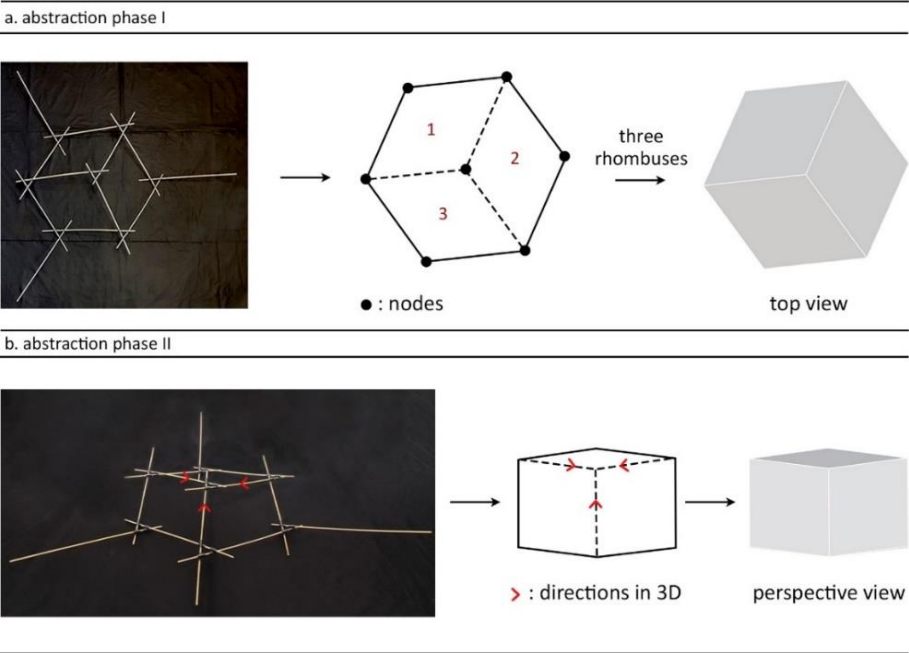


Figure 5.15: VFU abstraction phases.

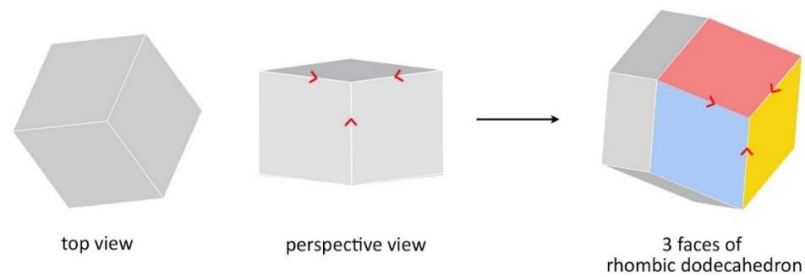


Figure 5.16: The three faces of VFU correspond to three congruent faces of rhombic dodecahedron.

To create a force polyhedron for 3DGS, the following steps are realized respectively. The edges of the force polyhedron are created by drawing normal vectors of rhombus faces as shown in Figure 5.17. The length of normal vectors is defined by an amplitude range that is between 0-100 to be able to adjust the force polyhedron. The area of faces of the force polyhedron corresponds to the magnitude of the applied force. Therefore, the larger areas meaning bigger magnitude result in proportionally shorter edges in the form diagram. The amplitude value of the normal vector is set as 60. An equilateral triangle is created by drawing a polyline between the starting and end points of normal vectors. The resulting two polygons are united through normal vectors and are lofted. The force polyhedron becomes a triangular prism as shown in Figure 5.17.

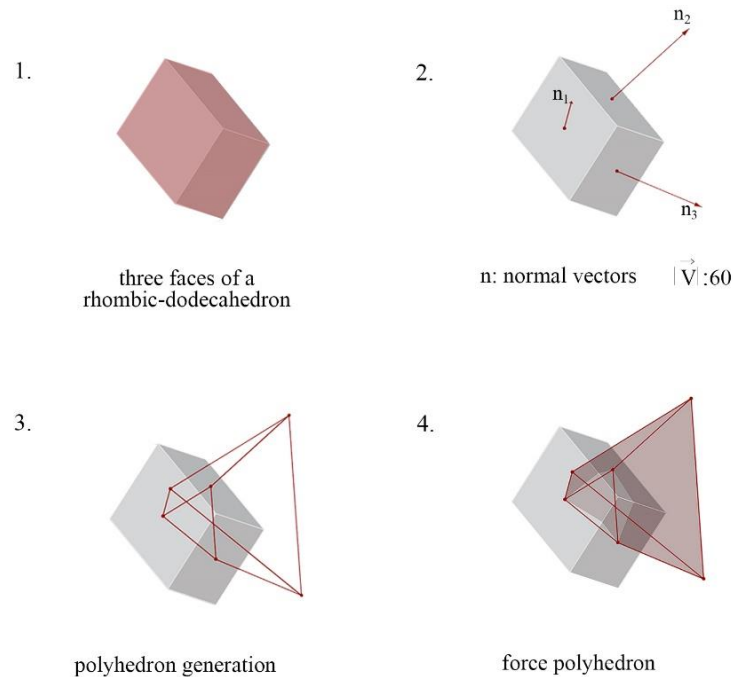


Figure 5.17: Force polyhedron generation through creating normal vectors and setting its amplitude.

“Polyframe 2” plug-in is used to exploit the 3DGS method in the Rhino-Grasshopper environment. The total ten force polyhedrons are aggregated through the translations and rotations of the same polyhedron to obtain a form diagram. The polyhedrons are aggregated in a way at least one face would be adjacent to the other polyhedron. First, three force polyhedrons ($A_{1,2,3}$) are placed on the quadrilateral faces of the triangle prism (X) by aligning its face direction (Figure 5.18a). Three more polyhedrons ($B_{1,2,3}$) are aligned to the quadrilateral faces of $A_{1,2,3}$. The last three polyhedrons ($C_{1,2,3}$) are placed on the remaining quadrilateral faces $A_{1,2,3}$ to make the elements converge to the same node. The aggregated force polyhedral consists of ten identical polyhedra representing the applied external forces of the form diagram (Figure 5.18b).

The “PFPerp” component is used as the iterative solver which attempts to make every edge perpendicular to its dual. The minimum edge length is set as 50 cm, which is the length of the VFU physical model, for the iterative solver. The output form diagram that is in equilibrium and resists compression forces is obtained as shown in Figure 5.18.

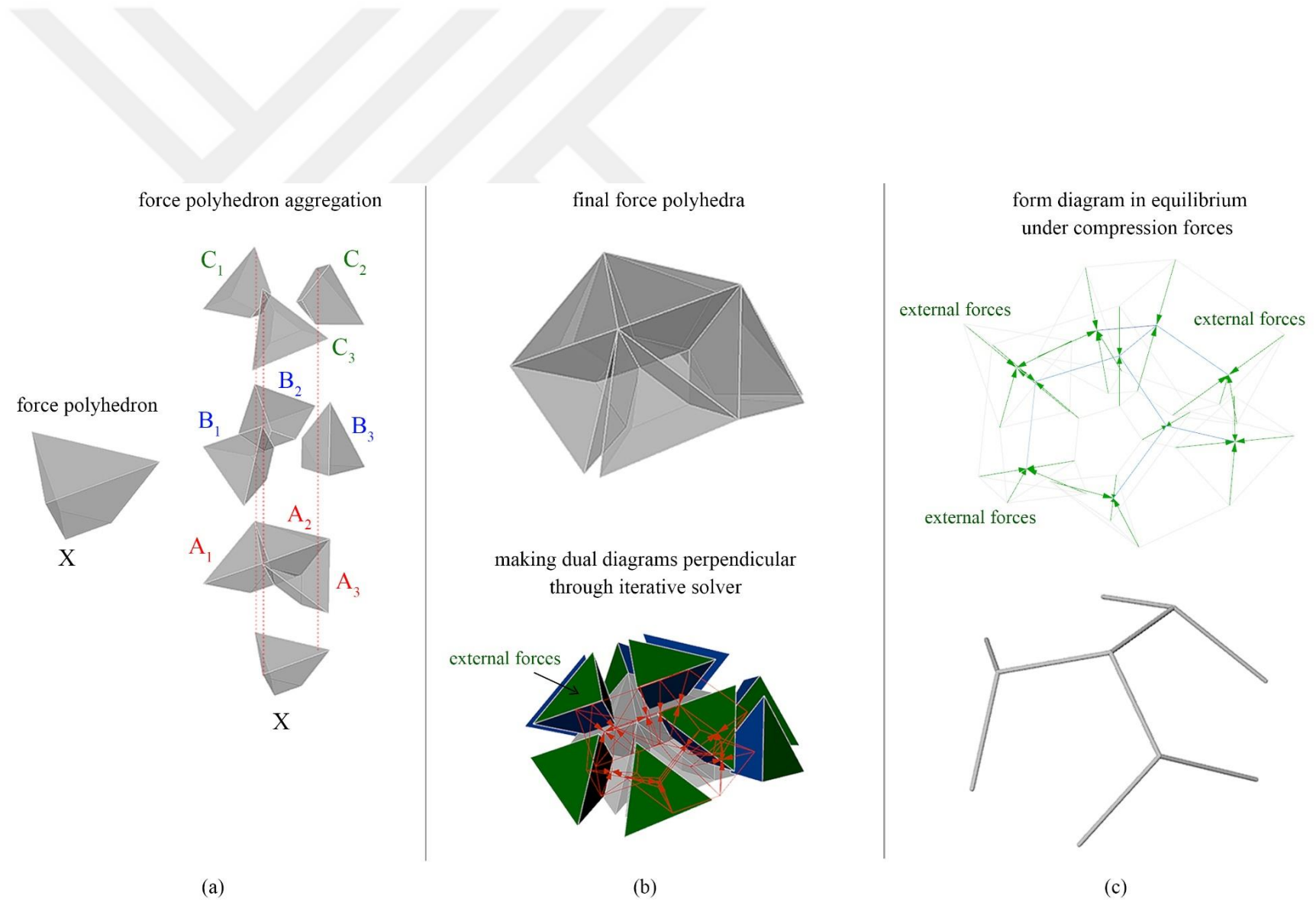


Figure 5.18: (a) Force polyhedron aggregation, (b) Iterative solver implementation, (c) The corresponding form diagram.

5.3.1 Reciprocal structure generation

The geometrical transformation of the form diagram is realised by following analytical geometric operations as suggested by Sénéchal et al. (2011). The three steps comprise the geometrical transformation as follows: (1) creating necessary reference geometries which lead to the RF transformation, (2) the rotation of elements, (3) calculation of eccentricities and the final lengths of the elements.

In the first step, the circles (O_i) are created from three midpoints (M_i) of the corresponding element axis (I_i) as shown in Figure 5.19a. The axis of rotation (C_i) starts from M_i and goes in a direction that is perpendicular to the element axis for every element. The tangent vectors of the circles and the perpendicular frames at M_i are generated to create C_i . The perpendicular frames are aligned to the tangent vectors to make the angle between I_i and C_i straight. Then the perpendicular frames are deconstructed to provide a Y direction value for C_i (Figure 5.19b).

In the second step, the rotation process is executed. The rotation planes are created by creating normal planes of C_i at M_i and are aligned to the direction of each I_i . The rotation angle is set as 10 degrees for every element axis. The element axis is rotated at M_i around C_iM_i as shown in Figure 5.19c.

The calculation of eccentricities and the extension of lengths are undertaken in the last step. The eccentricities are determined as the minimum distance of two element axes which must be perpendicular to each axis. Therefore, the cross product of two element axes creates the direction of eccentricity. The closest points between two element axes are obtained and joined as a line. This line represents the diameter of the circular-cross section of linear elements. Half of its length is the radius of the circular cross section which equals 2.14 cm as detailed in Figure 5.19d. I_1 , I_2 , I_3 are extended as 8 cm both from their end and starting points. The other elements are extended as 8 cm only from the starting points of their axes. The extension from the end points is determined based on the supporting points of elements on the ground. Following this, the elements located at the perimeter having a smaller angle with the ground, are extended 22 cm from their endpoints to level the supporting points of the RF structure (Figure 5.19d).

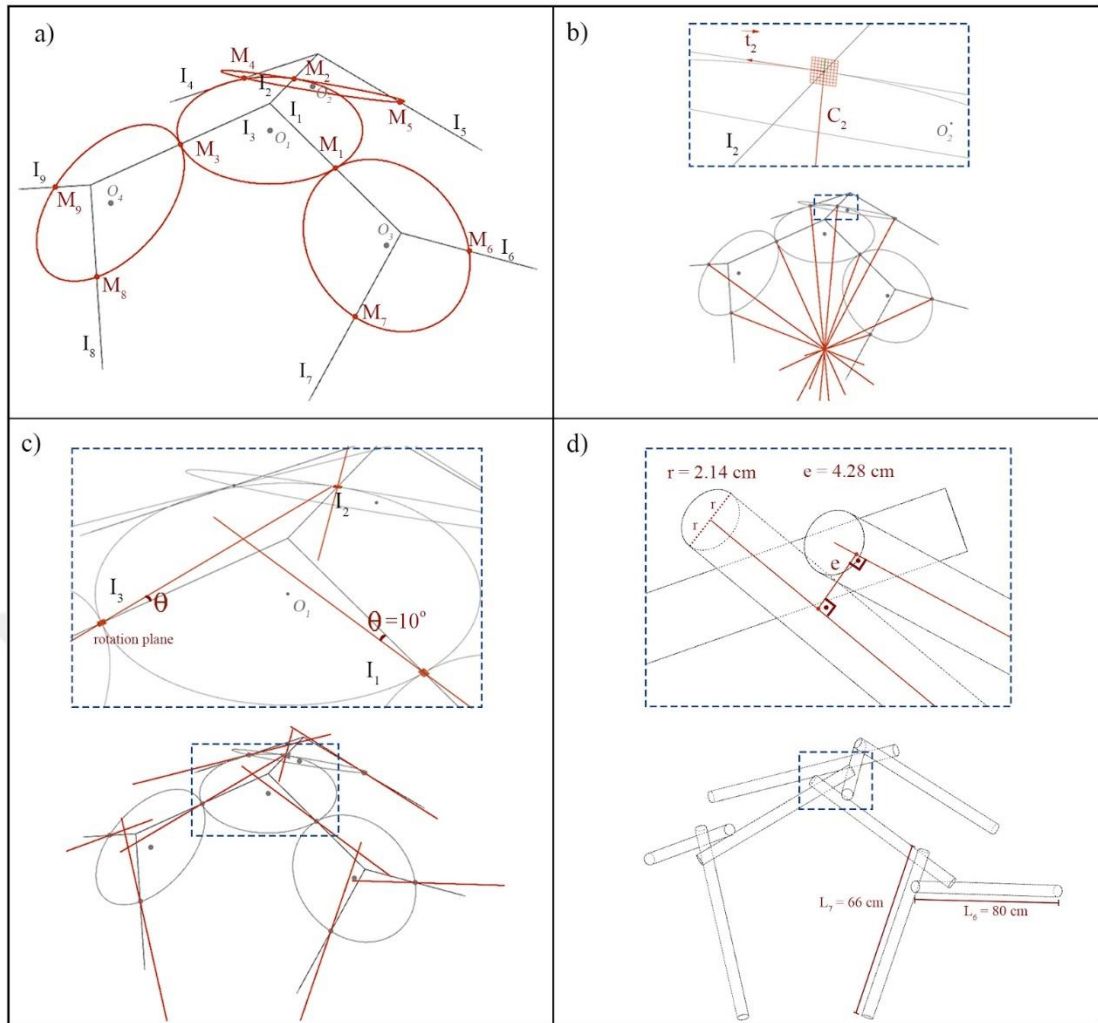


Figure 5.19: The transformation of the form diagram into an RF configuration by following geometric operations, (a,b) generation of reference geometry, (c) the rotation process, (d) the calculation of eccentricities and the lengths of the elements.

5.3.2 Structural analysis

The structural analysis is undertaken through Scan and Solve Pro: Structural Simulation software in the Rhino modelling software. The length of the elements are extended as the supporting points touch the ground through the elliptical faces (Figure 5.20). The elliptical supporting areas vary in diameter as 9.3 cm and 6.5 cm based on the elements leaning angle. The material is defined as bald cypress which has 0.46 g/cm^3 density. Additional to its self-weight, 10^{-4} Newton (N) load is applied in the negative Z direction for every element. Von Mises Stress and Displacement tests are executed from the software (Figure 5.21).

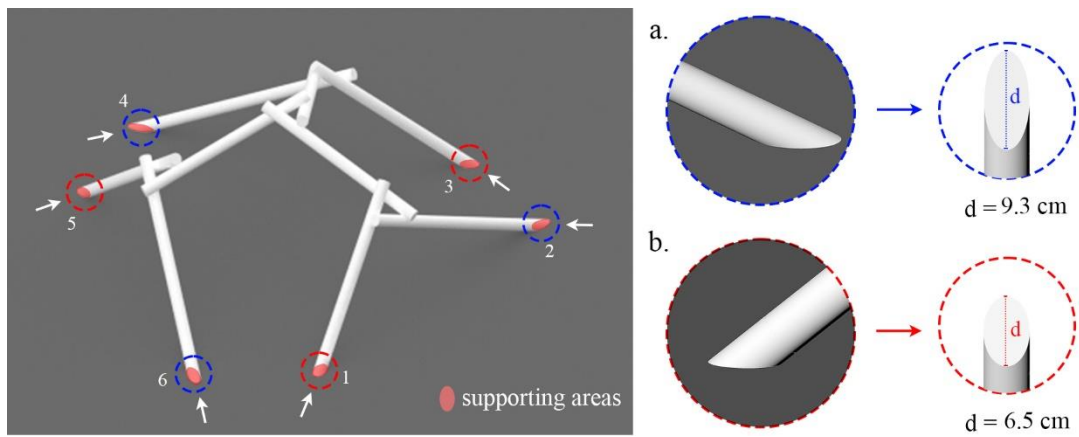


Figure 5.20: The supporting areas of the RF structure and their diameter sizes.

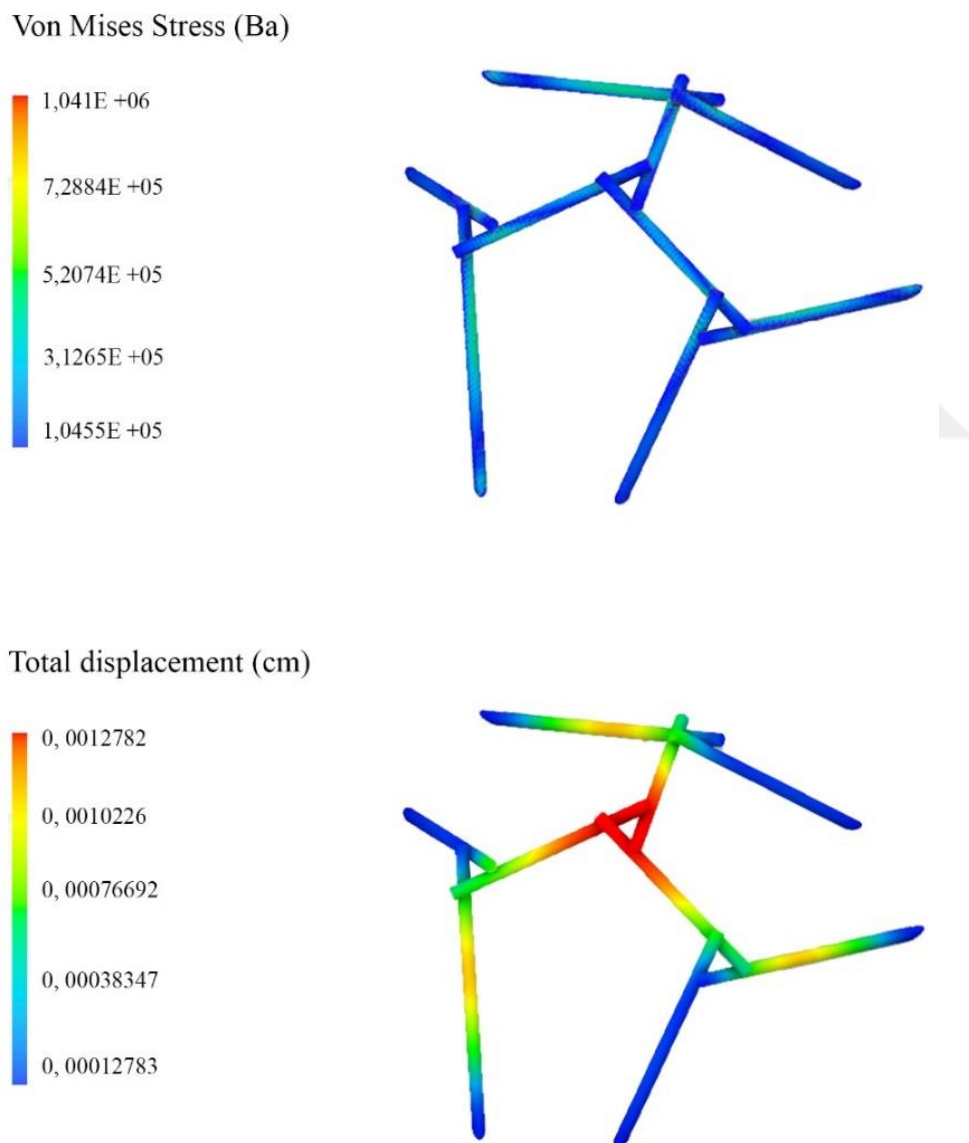


Figure 5.21: Von Mises Stress analysis (above), Total displacement results (below).

6. RESULTS AND DISCUSSION

VFU I as the outcome of the physical modelling and working mainly in bending forces, is transformed into VFU II which is the outcome of the digital form-finding process to create a compression-dominant RF structure. The findings of the research have been classified as numeric values, formal descriptions of volumetric frame units and the structural analysis results. VFU I and VFU II show the same volumetric characteristics with three elements converging to form an equilateral angle as shown in Figure 6.1 and 6.2. The elements differ in engagement lengths. VFU I makes up a triangle engagement window with a 4.5 cm engagement length while VFU II does it with a 7.5 cm engagement length.

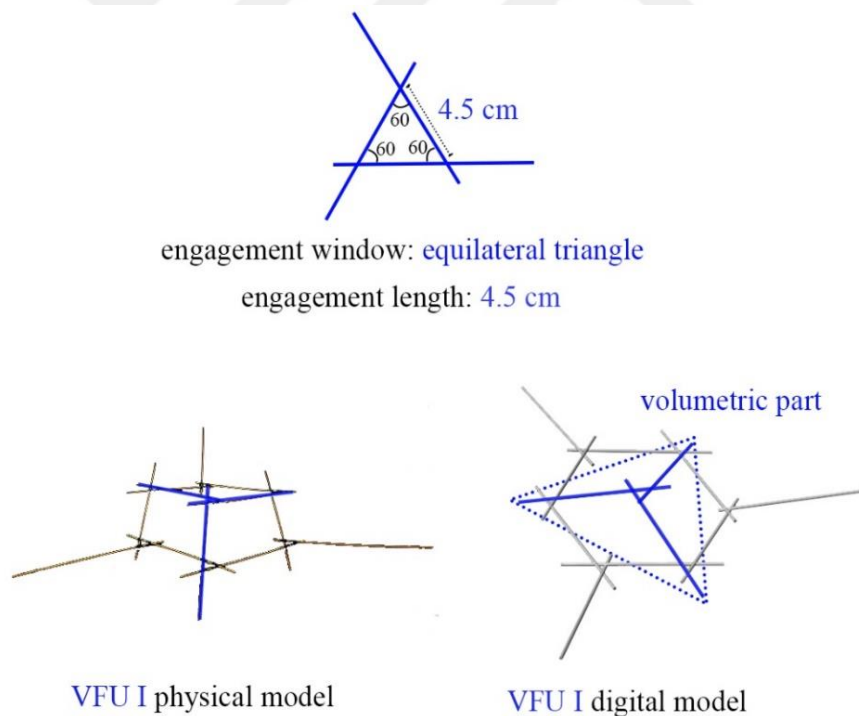


Figure 6.1: Volumetric part of VFU I.

The number of elements decrease in VFU II configuration, however three elements pointing outwards in VFU I were excluded in the geometric abstraction of three rhombuses since they only help creating RF fans. Therefore, VFU II shows the same number of elements (9) as driven from three rhombuses (Figure 6.3). VFU II has four

engagement windows whereas VFU I has 7. The bending forces arise from engagement windows since elements support each other along their spans. Therefore, for a compression-dominant RF structure, the fewer engagement windows indicate less bending moment. The numeric increases and decreases are visualized in Figure 6.3. The fan type of VFU II varies as an equilateral and isosceles triangle thus angle between elements changes accordingly. An equilateral triangle fan of VFU I is the one giving the volumetric form as shown in Figure 6.1 while the other three fans are in an isosceles triangle shape (Table 6.1). VFU I has equilateral triangles for its fan type hence keeping 60 degrees for every engagement window.

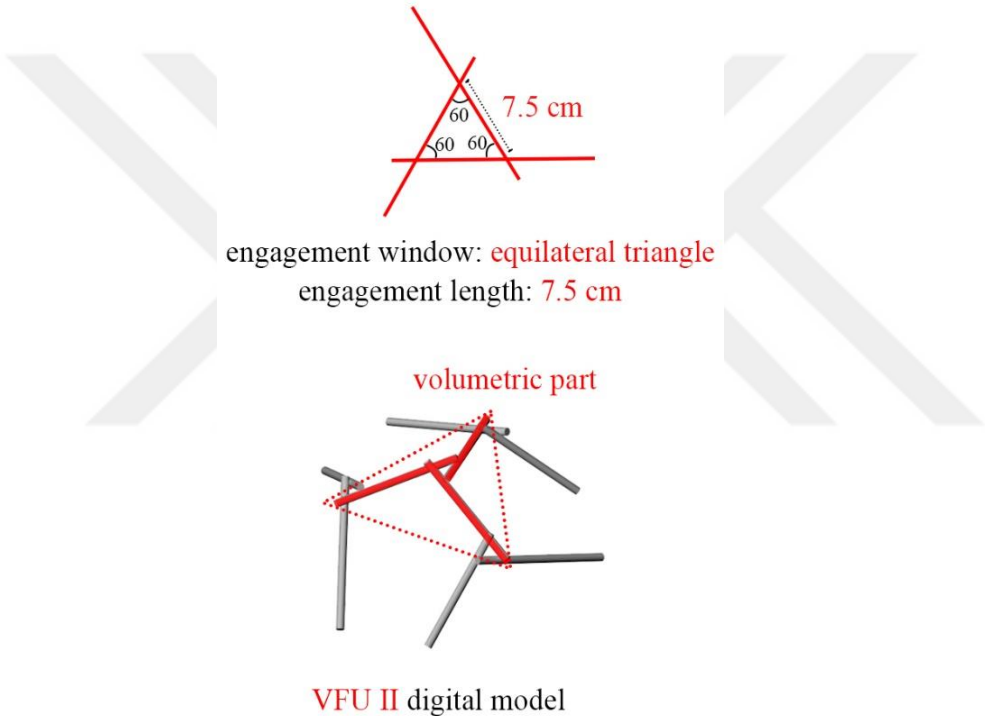


Figure 6.2: Volumetric part of VFU II.

Both VFU I and VFU II have linear elements which have circular cross-sections. The length and diameter of elements in VFU I is 50 cm, 0.5 cm respectively. The lengths of elements in VFU II increase due to RF structure transformation. Moreover, lengths vary due to different leaning angles. The elements leaning more to the ground result in having 88 cm total length, and the rest has 66 cm. The thickness of linear elements dramatically increases to resist compression forces. The diameter size is 0.5 cm for elements of VFU I whereas this value climbs to 4.28 cm which is almost 8.5 times greater as shown in Figure 6.3.

Table 6.1: The comparison of VFU I and VFU II based on numeric values, (x) denotes the number of elements having the characteristics in question, eng.w: engagement window.

Numeric changes	Angle of eng.w (degree)	Length (cm)	Diameter (cm)
VFU I	60	50	0.5
VFU II	Fan I: 60 Fan II: 20 80 80	66 (6) 80(3)	4.28

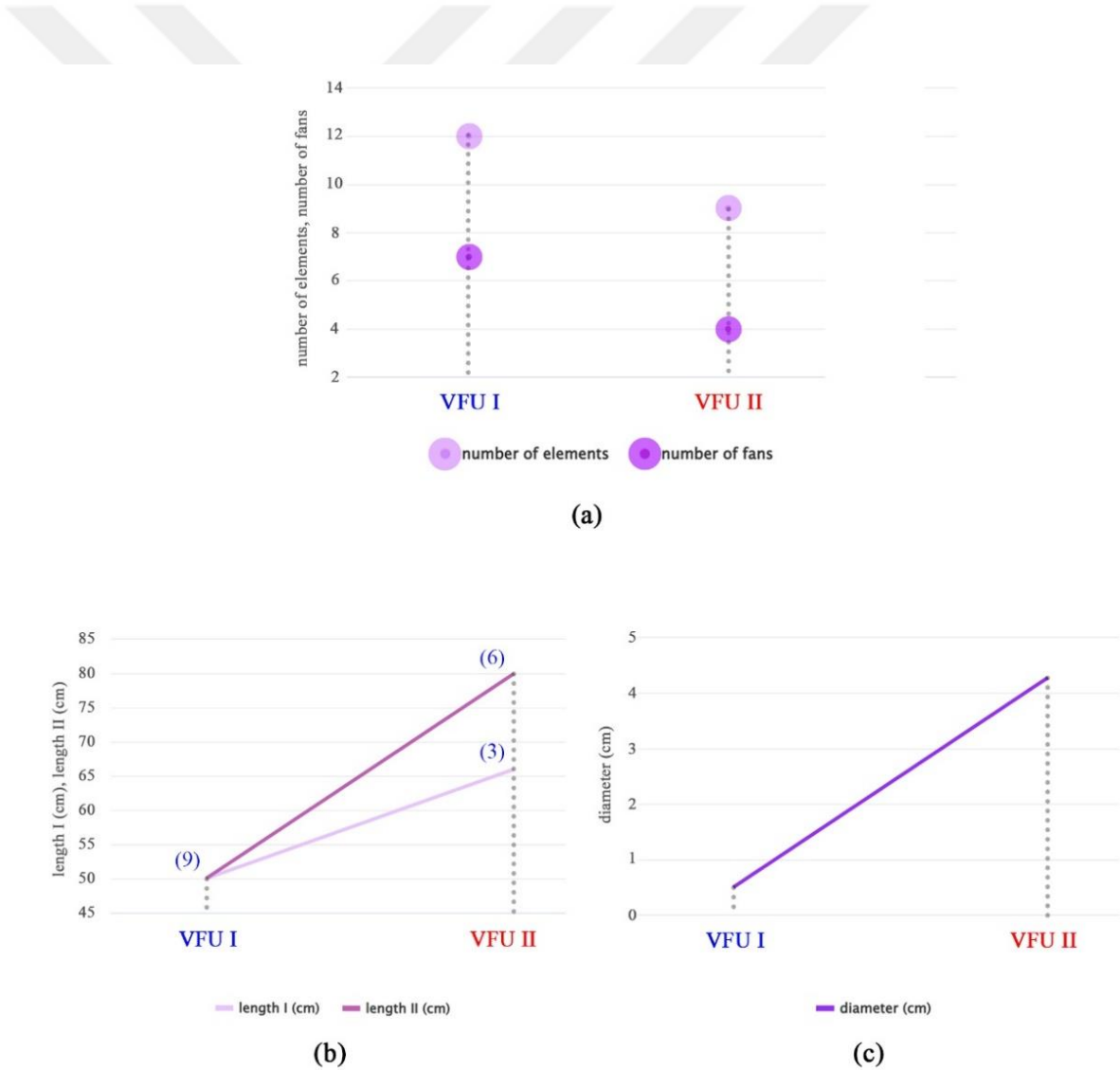


Figure 6.3: (a) Changes in number of elements, (b) Changes in the length sizes, (c) Changes in diameter size of VFU I and VFU II.

VFU I-II geometric configuration is assessed based on their formal features as shown in Figure 6.4. Volumetric parts are the same for both RF units with the 120-degree dihedral angle. Base polygons which are created by uniting the points where the elements meet the ground are in hexagon shape. VFU I has three rhombuses as RF polygons, and VFU exhibits pentagon polygons as shown in Figure 6.4.

The results of Geometric Analysis section show that RF configurations directly relate to the polygonal faces from which the engagement windows emerge based on the duality principle. Table 5.2 shows the numeric results of the analysis in which the rhombus division yields the most efficient RF configuration with 216 linear elements in terms of material saving compared to hexagon and quad shapes. The first physical experiment shows how the RF hexagon units get easily discretized because of the very light elements and flexible joints. The discretization arises from the different axes of elements thus creating different normal vectors on the same polygonal face. The first RF configuration made of hexagon units resulted in an almost flat configuration since the hexagon units were flat. When VFU was used to create a structure, the challenge was to have a fragile connection between VFUs. The final RF structure did not allow for building up in the Z direction. In the hanging physical model, the RF structure follows a linear path because of the one-stick connection thus limiting the volumetric behaviour. Given that RF configurations do not work well when exposed to axial forces, hanging resulted in an unstable RF configuration under loadings.

The output of 3DGS is a form which works in pure compression. When the structure is transformed into an RF configuration, the structure becomes a compression-dominant structure due to emerging engagement windows and the element's position. The structural analysis shows that VFU II experiences Von Mises Stress which is 104,1 Pascal (Pa) at maximum. The maximum displacement of VFU under its self-weight and 10^{-4} N additional load is 0.0012782 cm.

VFU I-II both are investigated on a unit scale which directly affects the structural behaviour. VFU II configuration can also be evaluated as a self-standing spatial structure since it provides solid supporting points. Furthermore, the joints are an integral part of the structural behaviour. Even though the joints are designed and used for physical modeling which contributes to exploring VFU I, VFU II is evaluated as

their final element position is fixed to each other. The main reason of that is the challenge of defining the relation between the joints and the structure in digital environment. Further research may include joint design for VFU II and their effect on overall design.

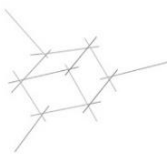
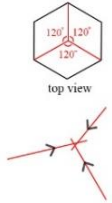
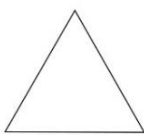
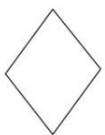
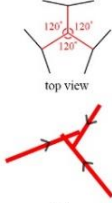
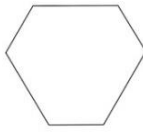
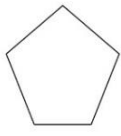
Formal changes	volumetric	base polygon	eng.w type	RF polygon
 VFU I	 Yes	 regular hexagon	 (7) equilateral triangle	 (3) rhombus
 VFU II	 Yes	 irregular hexagon	 (1) equilateral triangle  (3) isosceles triangle	 (3) pentagon

Figure 6.4: The comparison of VFU I and VFU II based on their formal configurations, (x) denotes the number of elements having the characteristics in question, eng.w: engagement window.



7. CONCLUSION

Structural behaviour and form are often considered separately by architects inasmuch as when formal concerns dominate the design, architects enhance their design with material and additional load-bearing elements. However, a post-optimization strategy for design is not only time and energy-consuming but also inefficient for material consumption as the form relies on it. To evaluate structure and form together, RF structures have been investigated due to their interdependent design parameters which are geometry, material and structure. The research has demonstrated that developing an extensive workflow in which designers engage in geometry, material and structure yields an outcome where structural primacy and formal descriptions are designed and calculated together.

Geometry lies at the intersection of architectural and structural design expressing the design whether in digital or physical environment. Although geometry is at the core of structure, architects do not necessarily develop an intuitive understanding of geometry. As a result, most of the digital design tools are used as black boxes without questioning the underlying relations of the form. RF structures are geometrically rich as they intrinsically have fan and RF polygons. The way fans comprise RF polygons not only informs the structural morphology but also gives insight into how the geometrical shapes influence structural primacy and equilibrium. This research benefits from computational geometry to understand the relationship between RF configuration and its geometrical shapes. In this way, the subsequent processes are informed with geometric information instead of arbitrary geometric shape choices.

RF morphology allows for creating curved surfaces without having to bend linear elements. These linear elements comprise flat faces of polygons varying as RF units and engagement windows and how they are connected to each other determine the overall form. Therefore, the fact that flat elements create the curved forms brings forward two opposite geometrical design space which are Euclidean and non-Euclidean space. From this point of view, the research has investigated RF geometrical configurations in polyhedral forms (Euclidean) and forming NURBS surfaces (non-

Euclidean). The geometrical analysis highlights the rhombus shape, which has fewer elements to form a curved surface with flat polygons that is the RF structure's inherent characteristic. A 2D rhombus polygon is transformed into a 3D polyhedral following structural reciprocity to improve its structural behaviour. Therefore, the present research exploits geometry at its finest, both as an inspiration and a logical explanation of the sub-processes of the workflow.

Structural reciprocity is deeply experimented with in the physical modelling process. Physical experiments play an intermediary role between geometric analysis and the digital form-finding process. Geometric analysis and digital form-finding are purely driven by geometry without material. Therefore, computational making allows for exploring RF configurations with rules by experiencing the constraints and facilities of the material. Volumetric Frame Unit (VFU), which is the original contribution of this thesis, is explored through the reactions between matter and forces to create a structure showing structural stiffness. The wooden material and the joints inform the polyhedral shape in the research so that linear elements under different force vectors are detected. The polyhedral form is created through visual feedback of geometry and the forces at play. It can be inferred that different types of materials and joint types may give rise to different force fields in which the maker adjusts accordingly.

VFUs are also united with the same designed joints to create an RF structure on a bigger scale. Although VFU has three elements pointing outwards for possible connections, the connection of units did not result in an RF structure which has enough height to erect from the ground for a bigger scale. The same joints giving the stiffness for VFU end up with pressing the structure downwards on a bigger scale experiments. Therefore, the results suggest that the joints for unit connection is crucial to determine the final form. Furthermore, using hybrid joints have the potential to create new geometrical shapes which do not fall inside the designer's geometric space.

3DGS informs the design process by visually guiding how force and form evolve together. This interactive design space helps the designer to understand the relationship between the form and its static equilibrium state. Moreover, 3DGS enables designing with forces in geometric forms which is polyhedral. Conceiving forces as polyhedra is a more convenient way for architects who tend to design with shapes rather than numbers. Furthermore, it also helps designer to understand how the specific placement of elements for desired forces create new geometrical shapes for the structure. In this

sense, 3DGS is adopted to upgrade VFU to make it work in compression forces which are considered more advantageous for structure durability and stability. 3DGS method relies on the equilibrium of a point or in other words “node” which means that it is not restricted to any prior shape. Therefore, the resulting RF structure geometry sheds light on which geometrical shapes provide compression forces for RF configurations. The way rhombus faces of RF polyhedrons turn into a pentagon contributes to geometrical information of RFs which is essential to understand the relation between their structural behaviour and geometry.

The research incorporates the outputs of the physical making process into an immaterial environment to inform the process. Therefore, computational making has defined the structural form-finding process where there are infinite numbers of polyhedrons to start designing with. VFU geometry provides a necessary form diagram from which the force diagram is derived. Even though the force polyhedron is derived from a specific form, aggregation of force polyhedrons allows designers to create newly designed alternatives. This research shows that the form-finding process can be achieved in an unrestricted environment without becoming a form-searching process, as restrictive design parameters and the designer's intuition ultimately guide the design process.

Force variables can be one of the main drivers of design that triggers unexpected results in contrast to the restrained mechanical act it implies. Therefore, architects can integrate force variables into the design process to have functional yet structurally feasible outcomes while exploring unconventional results. This thesis aims to bridge the gap in RF literature where geometrically rich RFs working mainly in bending can also be turned into structurally efficient RF structures. The research expands geometrical design space of RF structures with structural primacy by calculating forces and geometry together unlike conventional design process where structural primacy is evaluated separately. Fusing force variables into the formal design process can broaden the computable part of design knowledge.



REFERENCES

- Ahlquist, S., Menges, A.** (2011). *Computational Design Thinking*. John&Wiley Press.
- Akbarzadeh, M., Van Mele, T., & Block, P.** (2015). On the equilibrium of funicular polyhedral frames and convex polyhedral force diagrams. *Computer-Aided Design*, 63, 118–128. <https://doi.org/10.1016/j.cad.2015.01.006>
- Alexander, C.** (1968). *A Pattern Language*. Center for Environmental Structure.
- Anastas, Y., Rhode-Barbarigos, L., & Adriaenssens, S.** (2016). Design-to-Construction Workflow for Cell-Based Pattern Reciprocal Free-Form Structures. *Journal of the International Association for Shell and Spatial Structures*, 57(2), 159–176.
- Anon.** (1956). *Leonardo Da Vinci*, memorial edition based on the Leonardo Exposition held in Milan in 1939. Reynal& Company, New York.
- Adriaenssens, S., Block, P., Veenendaal, D., & Williams, C.** (Eds.). (2014). *Shell structures for architecture: Form finding and optimization*. Routledge/ Taylor & Francis Group.
- Asefi, M., Bahremandi-Tolou, M.** (2019). Design challenges of reciprocal frame structures in architecture. *Journal of Building Engineering*, 26, 100867.
- Ayres, P., Martin, A. G., & Zwierzycki, M.** (2018). *Beyond the basket case: A principled approach to the modelling of kagome weave patterns for the fabrication of interlaced lattice structures using straight strips*. In: Dörfler, K., Knippers, J., Menges, A., Parascho, S., Pottmann, H., & Wortmann, T. (Eds.). (2023). *Advances in Architectural Geometry 2023*. De Gruyter. <https://doi.org/10.1515/9783111162683>
- Block, P.** (2009.). Exploring Three-dimensional Equilibrium. (Ph.D thesis). Massachusetts Institute of Technology, MA USA.
- Benros, D., Duarte, J., Sean, H.** (2012). A New Palladian Shape Grammar. *International Journal of Architectural Computing*, 10(4), pp. 521-540.
- Baverel, O.** (2000). Nexorades: A family of Interwoven Space Structures. (Ph.D thesis). University of Surrey. Guildford.
- Baverel, O., & Nooshin, H.** (2007). Nexorades Based on Regular Polyhedra. *Nexus Network Journal*, 9(2), 281–298.
- Bhooshan, S., Veenendaal, D., Block, P.** (2014). Particle-spring systems: Design of a cantilevering concrete shell. In Adriaenssens, S., Block, P., Veenendaal, D., Williams, C. (Eds.), *Shell structures for architecture: Form finding and optimization*. Routledge/ Taylor & Francis Group.

- Boller, G., & D'Acunto, P.** (2021). Structural design via form finding: Comparing Frei Otto, Heinz Isler and Sergio Musmeci. In J. Mascarenhas-Mateus, A. P. Pires, M. M. Caiado, & I. Veiga, *History of Construction Cultures* (1st ed., pp. 431–438). CRC Press.
- Brocato, M.** (2011). Reciprocal Frames: Kinematical Determinacy and Limit Analysis. *International Journal of Space Structures*, 26(4), 343–358.
- Burry, M.** (2011). *Scripting Cultures: Architectural design and programming*. John Wiley&Sons Ltd.
- Carpo, M.** (2017). *The second digital turn: Design beyond intelligence*. The MIT Press.
- Chilton, J.C., Devulder, T.** (2001). Reciprocal Ring Structure of the Chapter House Roof, Lincoln Cathedral.
- Cromwell, P. R.** (1997). *Polyhedra*. New York: Cambridge University Press.
- Dessi-Olive, J.** (2017). Computing with Matter, Shapes and Forces: Toward Material and Structural Primacy in Architecture. (M.Sc. thesis). Massachusetts Institute of Technology, MA USA.
- Deleuze, G., Guattari, F., & Massumi, B.** (1989). A Thousand Plateaus: Capitalism and Schizophrenia. *Journal of Interdisciplinary History*, 19(4), 657.
- Douthe, C., & Baverel, O.** (2009). Design of nexorades or reciprocal frame systems with the dynamic relaxation method. *Computers & Structures*, 87(21–22), 1296–1307.
- Douthe, C., & Baverel, O.** (2014). Morphological and Mechanical Investigation of Double-Layer Reciprocal Structures. *Nexus Network Journal*, 16(1), 191–206.
- Escrig, F.** (1993). Las estructuras de Emilio Perez Pinero. *Arquitectura transformable*, 30-32, Sevilla.
- Ferkiss, V., Fuller, R. B., & Applewhite, E. J.** (1976). Synergetics: Explorations in the Geometry of Thinking. *Technology and Culture*, 17(1), 104.
- Fleischmann, M., Knippers, J., Lienhard, J., Menges, A., & Schleicher, S.** (2012). Material Behaviour: Embedding Physical Properties in Computational Design Processes. *Architectural Design*, 82(2), 44–51.
- Frazer, H.** (1995). *An Evolutionary Architecture*. Architectural Association, London.
- Gelez, S., Aubry, S., & Vaudeville, B.** (2011). Behavior of a Simple Nexorade or Reciprocal Frame System. *International Journal of Space Structures*, 26(4), 331–342.
- Graefe, R.** (2020). The catenary and the line of thrust as a means for shaping arches and vaults. In B. Addis (Ed.), *PHYSICAL MODELS* (1st ed., pp. 79–126). Wiley.
- Godthelp, T.S.** (2019). Timber Reciprocal Frame Structures. (M.Sc thesis). Eindhoven University of Technology, Eindhoven, The Netherlands.

- Godthelp, T. S., & Jorissen, A. J. M.** (2019). *The Timber Reciprocal Frame Designer: Free form design to production*.
- Gürsoy, B.** (2016). Formalizing Making in Design. (Ph.D thesis). Istanbul Teknik Üniversitesi, Fen Bilimleri Enstitüsü, İstanbul.
- Helm, V., Knauss, M., Kohlhammer, T., Gramazio, F., Kohler, M.** (2016). Additive robotic fabrication of complex timber structures. In A. Menges, T. Schwinn, & O. D. Krieg (Eds.), *Advancing Wood Architecture* (1st ed., pp. 1–10). Routledge.
- Houlsby, G.T.** (2014). John Wallis and the Numerical Analysis of Structures. *Nexus Netw J* 16, 207–217 <https://doi.org/10.1007/s00004-014-0179-7>
- Hooke, R.** (1676). *A Description of Helioscopes, and Some Other Instruments*. London.
- Ingold, T.** (2013). *Making: Anthropology, archaeology, art and architecture*. Routledge.
- Isaacson, W.** (2017). *Leonardo Da Vinci*. Domingo Yayinevi.
- Kamath, A. V.** (2020). Making grammars for material and tectonic complexity: An example of a thin-tile vault. *Design Studies*, 69, 100944.
- Kern, W. F., and Bland, J. R.** (1948). Prism. §13 in *Solid Mensuration with Proofs*, 2nd ed. New York: Wiley, pp. 28-32
- Kilian, A., & Ochsendorf, J.** (2005). Particle Spring Systems for Structural Form-Finding. *Journal of the International Association for Shell and Spatial Structures*, 46(147).
- Kilian, A.** (2006). *Design Exploration through Bidirectional Modeling of Constraints*. (Ph.D thesis). Massachusetts Institute of Technology.
- Kilian, A.** (2007). The Steering of Form. *Journal of the International Association for Shell and Spatial Structures*.
- Knight, T., & Stiny, G.** (2001). Classical and non-classical computation. *ARQ: Architectural Research Quarterly*, 5(4), 355-372.
- Knight, T., & Stiny, G.** (2015). Making grammars: From computing with shapes to computing with things. *Design Studies*, 41, 8–28.
- Kohlhammer, T., & Kotnik, T.** (2011). Systemic Behaviour of Plane Reciprocal Frame Structures. *Structural Engineering International*, 21(1), 80–86.
- Kolarevic, B.** (Ed.). (2009). *Architecture in the digital age: Design and manufacturing* (Repr). Taylor & Francis.
- Koning, H., Eizenberg, J.** (1981). The language of the prairie: Frank Lloyd Wright's prairie houses. *Environment and Planning B: Planning and Design* (8), 295-323.
- Laila, T., Arruda, A., Barbosa, J., & Moura, E.** (2018). The Constructive Advantages of Buckminster Fuller's Geodesic Domes and Their Relationship to the Built Environment Ergonomics. In F. Rebelo & M. Soares (Eds.), *Advances in Ergonomics in Design* (Vol. 588, pp. 357–368). Springer International Publishing.

- Larsen, O. P., Brancart, S., Temmerman, N. D., & Laet, L. D.** (2018). *ReciPlyDome and ReciPlySkin bending-active transformable lightweight shelters*.
- Larsen, O. P.** (2008). *Reciprocal frame architecture*. Elsevier.
- Larsen, O. P.** (2014). Reciprocal Frame (RF) Structures: Real and Exploratory. *Nexus Network Journal*, 16(1), 119–134.
- Lee, J.** (2015). Grammatical Design with Graphic Statics: Rule-based Generation of Diverse Equilibrium Structures. (M.Sc thesis). Massachusetts Institute of Technology, MA USA.
- Lee, J., Mele, T. V., & Block, P.** (2018). Disjointed force polyhedra. *Computer-Aided Design*, 99, 11–28. <https://doi.org/10.1016/j.cad.2018.02.004>
- Lionel, M.** (1976). *The Architecture of Form*. Cambridge: Cambridge University Press.
- Maxwell, J.** (1864). On reciprocal figures, frames and diagrams of forces. *Phil Mag*, vol. 27, pp. 250–261.
- Menges, A., Ball, P., & Turner, J. S.** (2012). *Material Computation*. John Wiley&Sons.
- Mesnil, R., Douthe, C., Baverel, O., & Gobin, T.** (2018). Form finding of nexorades using the translations method. *Automation in Construction*, 95, 142–154.
- Mitterberger, D., Atanasova, L., Dörfler, K., Gramazio, F., & Kohler, M.** (2022). Tie a knot: Human-robot cooperative workflow for assembling wooden structures using rope joints. *Construction Robotics*, 6(3–4), 277–292.
- Muslimin, R.** (2010). Learning from Weaving for Digital Fabrication in Architecture. *Leonardo*, 43(4), 340–349. https://doi.org/10.1162/LEON_a_00007
- Noel, V. A. A.** (2020). Situated Computations: Bridging Craft and Computation in the Trinidad and Tobago Carnival. *Dearq*, 27, 62–75.
- Nejur, A., & Akbarzadeh, M.** (2021). PolyFrame, Efficient Computation for 3D Graphic Statics. *Computer-Aided Design*, 134, 103003.
- Ohlbrock, O.P., D'Acunto, P.** (2020). A Computer-Aided Approach to Equilibrium Design Based on Graphic Statics and Combinatorial Variations. *Computer Aided Design* 121.
- Otto, F.** (ed.) (1969). *Minimal nets*. Stuttgart: IL1
- Otto, F.** (ed.) (1971). *Biology and Building*. Stuttgart: IL3
- Otto, F.** (ed.) (1988). *Bubbles*. Stuttgart: IL18
- Oxman, N., & Rosenberg, J. L.** (2007). Material-based Design Computation An Inquiry into Digital Simulation of Physical Material Properties as Design Generators. *International Journal of Architectural Computing*, 5(1), 25–44.
- Özkar, M.** (2005). *Lesson 1 in Design Computing Does not Have to be with Computers*. 311–318. <https://doi.org/10.52842/conf.ecaade.2005.311>

- Parigi, D., & Kirkegaard, P. H.** (2014). The Reciprocalizer: An Agile Design Tool for Reciprocal Structures. *Nexus Network Journal*, 16(1), 61–68.
- Parigi, D., & Kirkegaard, P. H.** (2014). Design and Fabrication of Free-Form Reciprocal Structures. *Nexus Network Journal*, 16(1), 69–87.
- Parigi, D., Kirkegaard, P. H., & Sassone, M.** (2012). Hybrid Optimization in the Design of Reciprocal Structures. I *IASS-APCS 2012 Proceedings: from spatial structures to spaces structures* The International Association for Shell and Spatial Structures.
- Pérez-Valcárcel, J., Muñoz-Vidal, M., Suárez-Riestra, F., López-César, I. R., & Freire-Tellado, M. J.** (2021). Deployable bundle modulus structures with reciprocal linkages for emergency buildings. *Engineering Structures*, 244, 112803.
- Petrović, M., Ilić, I., Mijatović, S., & Šekularac, N.** (2022). The Geometry of Timber Lamella Vaults: Prototype Analysis. *Buildings*, 12(10), 1653.
- Pugnale, A., & Sassone, M.** (2014). Structural Reciprocity: Critical Overview and Promising Research/Design Issues. *Nexus Network Journal*, 16(1), 9–35. <https://doi.org/10.1007/s00004-014-0174-z>
- Poleni, G.** (1748). *Memorie storiche della gran cupola del Tempio Vaticano*, Padua.
- Robert, V.P.** (2008). Perception of Order and Ambiguity in Leonardo's Design Concepts. *Nexus Netw J* 10, 101–127.
- Schek, H.J.** (1974). The Force Density Method for Form Finding and Computation of General Networks. *Computer Methods in Applied Mechanics and Engineering* 3(1), pp. 115-134.
- Sénéchal, B., Douthe, C., & Baverel, O.** (2011). Analytical Investigations on Elementary Nexorades. *International Journal of Space Structures*, 26(4), 313–320.
- Song, P., Fu, C.-W., Goswami, P., Zheng, J., Mitra, N. J., & Cohen-Or, D.** (2013). Reciprocal frame structures made easy. *ACM Transactions on Graphics*, 32(4), 1–13. <https://doi.org/10.1145/2461912.2461915>
- Su, Y., Ohsaki, M., Wu, Y., & Zhang, J.** (2019). A numerical method for form finding and shape optimization of reciprocal structures. *Engineering Structures*, 198, 109510.
- Suzuki, S., Martin, A., Ren, Y., Chen, T.-Y., Parascho, S., & Pauly, M.** (2023). BamX: Rethinking Deployability in Architecture through Weaving. In K. Dörfler, J. Knippers, A. Menges, S. Parascho, H. Pottmann, & T. Wortmann (Eds.), *Advances in Architectural Geometry 2023* (pp. 207–220). De Gruyter. <https://doi.org/10.1515/9783111162683-016>
- Stiny, G., Gips, J.** (1972). Shape Grammars and Generative Specification of Painting and Sculpture. In *Information Processing 71*, pp.1460-1465.
- Stiny, G., Mitchell, W.** (1978). The Palladian grammar. *Environment and Planning B*, 5(1), 5-18.

- Stiny, G.** (2006). *Shape: Talking about Seeing and Doing*. Cambridge, MA: MIT Press.
- Stott, A. B.** (1910). Geometrical Deduction of Semiregular from Regular Polytopes and Space Fillings. *Verhandelingen der Koninklijke Akad. Wetenschappen Amsterdam* 11, pp. 3-24.
- Tamke, M., Riiber, J., & Jungjohann, H.** (2010). Generated Lamella. 340–347. <https://doi.org/10.52842/conf.acadia.2010.340>
- Terzidis, K.** (2006). *Algorithmic architecture* (1st ed). Architectural Press.
- Thönnissen, U.** (2014). A Form-Finding Instrument for Reciprocal Structures. *Nexus Network Journal*, 16(1), 89–107.
- Veenendaal, D., & Block, P.** (2012). An overview and comparison of structural form finding methods for general networks. *International Journal of Solids and Structures*, 49(26), 3741–3753.
- Honnecourt, V.D.** (13th century). *Album de dessins et croquis [Livre de portraiture]*, ms.fr.19093. Departement des Manuscrits, Bibliotheque nationale de France, Paris. <https://archive.org/details/facsimileofsketc00vill/page/n11/mode/2up>
- Houlsby, G.T.** John Wallis and the Numerical Analysis of Structures. *Nexus Netw J* 16, 207–217 (2014). <https://doi.org/10.1007/s00004-014-0179-7>
- Wang, Z., & Akbarzadeh, M.** (2022). A polyhedral approach for the design of a compression-dominant, double-layered, reciprocal frame, multi-species timber shell. In Proceedings of the IASS Annual Symposium affiliated with APCS 2022 conference, Beijing, China, 2022, pp. 1-12(12).
- Wenninger, M. J.** *Dual Models*. Cambridge, England: Cambridge University Press, 1983.
- Widyowijatnoko, A.** (2019). Rection as a Synthesis of Reciprocal and Tensegrity Structure. *Nexus Netw J*. vol. 21, no. 1, pp. 465-478.
- William, M.** (1991). Functional Grammars: An Introduction. In Reality and Virtual Reality (ACADIA 1991), pp. 167-176. Troy, NY: ACADIA.
- Yazıcı, S.** (2013). A Material-based Integrated Computational Design Model in Architecture. (Ph.D thesis). Istanbul Teknik Üniversitesi, Fen Bilimleri Enstitüsü, İstanbul.
- Yeomans, D.** (1997). The Serlio floor and its derivations. *Architectural Research Quarterly*, 2: 74-83.
- Zamperini, E.** (2021). Timber floors made with elements shorter than the span covered in treatises and technical literature. In J. Mascarenhas-Mateus, A. P. Pires, M. M. Caiado, & I. Veiga, *History of Construction Cultures* (1st ed., pp. 193–200). CRC Press.
- Url-1** <<https://www.litcoindustries.ae/structural-steel/grid-shell/>>, date retrieved 09.05.2024.
- Url-2** <https://www.leonardodavincis inventions.com/civil-engineering-inventions/da-vinci-bridge/#google_vignette>, date retrieved 09.05.2024.

- Url-3** <https://www.leonardodavincisinventions.com/civil-engineering-inventions/da-vinci-bridge/#google_vignette>, date retrieved 09.05.2024.
- Url-4** <https://www.archdaily.com/275460/kroed-chun-qing-li-of-pavilion-architecture/kreod_pavilions_0004?next_project=no>, date retrieved 09.05.2024.
- Url-5** <<https://www.arup.com/projects/rokko-shidare-observatory>>, date retrieved 09.05.2024.
- Url-6** <<https://www.behance.net/gallery/101285765/Reciprocal-Dome-%28Nexorades%29/modules/583751495>>, date retrieved 09.05.2024.
- Url-7** <<https://parametrichouse.com/architecture-design-2/>>, date retrieved 09.05.2024.
- Url-8**
<<https://mathworld.wolfram.com/DualPolyhedron.html#:~:text=By%20the%20duality%20principle%2C%20for,called%20reciprocation%2C%20or%20polar%20reciprocation.>>, date retrieved 29.04.2024.
- Url-9** <<https://www.gaudidesigner.com/uk/colonia-guell.html>>, date retrieved 12.05.2024.
- Url-10** <<https://www.metalocus.es/en/news/frei-otto-german-pavilion-expo-1967>>, date retrieved 12.05.2024.
- Url-11** <<https://structurae.net/en/structures/wyss-garden-center>>, date retrieved 12.05.2024.
- Url-12** <https://www.archdaily.com/572135/ad-classics-montreal-biosphere-buckminster-fuller/546a753be58ecea75a00002f-abdallahh-jpg?next_project=no>, date retrieved 12.05.2024.



CURRICULUM VITAE

Name Surname : Hanım Gülsüm Karahan

EDUCATION :

- **B.Sc.** : 2020, Izmir Institute of Technology, Faculty of Architectures, Department of Architecture

PUBLICATIONS, PRESENTATIONS AND PATENTS ON THE THESIS:

- **Karahan H.G, Yazıcı S.** (2024). Expanding Geometric Design Space of Reciprocal Frame Structures through Surface Panelization. Digital Design in Architecture XV. National Symposium (MSTAS), July 1-2, 2024, Balıkesir, Turkey.

OTHER PUBLICATIONS, PRESENTATIONS AND PATENTS:

- **Karahan, H.G., Aktaş, B., Bingöl, C.K.** (2023). Use of Language to Generate Architectural Scenery with AI-Powered Tools. In: Turrin, M., Andriotis, C., Rafiee, A. (eds) Computer-Aided Architectural Design. INTERCONNECTIONS: Co-computing Beyond Boundaries. CAAD Futures 2023. Communications in Computer and Information Science, vol 1819. Springer, Cham.